Aus der

Klinik und Poliklinik für Psychiatrie und Psychotherapie

Klinikum der Ludwig-Maximilians-Universität München

Multi-scale, multi-modal stratification and comorbidity analysis of patients with psychotic disorders

Dissertation

zum Erwerb des Doctor of Philosophy (Ph.D.)

an der Medizinischen Fakultät

der Ludwig-Maximilians-Universität München

vorgelegt von

Adyasha Tejaswi Khuntia

aus

Patrapada / Indien

Jahr

2025

Mit Genehmigung der Medizinischen Fakultät der
Ludwig-Maximilians-Universität München

Erstes Gutachten:	Prof. Dr. Nikolaos Koutsouleris
Zweites Gutachten:	Prof. Dr. Bertram Müller-Myhsok
Drittes Gutachten:	Priv. Doz. Dr. Annette Schaub
Viertes Gutachten:	Prof. Dr. Michael Landgrebe

Dekan: Prof. Dr. med. Thomas Gudermann

Tag der mündlichen Prüfung: 09.01.2025

Table of Contents

Abstract (English):

The prevalence of somatic comorbidities in psychiatric disorders is a well-established phenomenon. Incidences of somatic comorbidities such as cardiovascular diseases significantly contribute to the high mortality rate observed in psychiatric populations, thereby impacting the global health burden. Metabolic syndromes, defined as the key risk factors for cardiovascular disease, have been widely studied, with obesity being a predominant factor. Notably, obesity is also a common comorbid condition in psychiatric disorders. Moreover, overweight and obese individuals are at higher risk of developing psychiatric disorders, while patients with psychiatric disorders are susceptible to becoming overweight and obese. However, the interaction between obesity and psychiatric disorders remains elusive, and there is a lack of brain-derived measures to study obesity specifically in psychiatric patients. Moreover, age is a significant metabolic risk factor that contributes to the occurrence of metabolic syndromes and appears to influence psychiatric groups as well, yet this relationship remains poorly understood.

Against this background, the current dissertation aims to unravel the association between obesity and psychiatric disorders as well as develop a novel tool to capture obesity related brain changes by using multi-site large cohort neuroimaging datasets and the machine learning (ML) methods. Furthermore, we aim to shed light on the already established brain-ageing phenomena in psychiatric disorders. In this regard we will develop brain-age predicting models by using multiple modality neuroimaging data sets in two analyses. Furthermore, by using the newly developed tool to quantify the measures of obesity, we will understand the association between obesity, brain-ageing and clinically relevant variables in psychiatric group.

In the first study, we developed a ML based body mass index (BMI) predictor by using voxelized whole brain structural images to study the intricate relationship between gray matter volume (GMV) and BMI in a selected healthy control (HC) sample including 770 participants. To assess the model generalizability, we applied this model to a separate HC sample including 734 individuals. Next, we computed a brain-based BMI gap score (BMIgap) for each individual quantifying the difference between brain-estimated and measured BMI. Similarly, we obtained the BMIgap scores in clinical samples comprising individuals with schizophrenia (SCZ, N=146), clinical high-risk states for psychosis (CHR, N=213) and recent-onset depression (ROD, N=200). Finally, we explored associations between BMIgap scores and clinically relevant variables specifically for SCZ patients.

In the second study, we addressed the complexities of brain-ageing at multiple levels. Initially, we developed a ML based age-predictor using region-of-interest (ROI) GMV data. ROIs were extracted using multiple brain atlases from a cohort of 1170 HC individuals. Subsequently, we created a second ML age-predictor using voxelized whole-brain GMV data derived from an independent HC sample obtained from multi-site studies (N=770). We computed the brain age estimation (BrainAGE) score by subtracting the model predicted age and chronological age. Both models were independently applied to separate HC samples to assess their generalizability and

subsequently to various patient groups. The first model was applied to patients with SCZ (N=503) and major depressive disorder (MDD, N=519). The second model was applied to patients with SCZ (N=146), CHR (N=213) and ROD (N=200) individuals. To understand the association between brain-ageing and obesity as well as their association with psychiatric disorders, we leveraged the utility of the established BMIgap scores and associated them with the computed BrainAGE scores as well as other clinically relevant variables.

In the first study, we established an efficient BMI-predictor robustly predicting BMI (R^2=0.28, MAE=2.75) in the HC sample. The BMIgap scores of SCZ and CHR individuals were higher, while the BMIgap scores of ROD individuals were lower compared to HC individuals. Brain patterns associating diagnostic separability and BMI-predictiveness were associated with longer illness-duration, later disease onset and higher hospitalization frequency.

The brain-age predictor using ROI data performed with an MAE of 6.35 years and successfully generalized to the independent HC sample showing no significant differences. The second BrainAGE model developed using voxelized whole brain GMV images demonstrated robust performance, achieving a MAE of 4.73 years surpassing the performance of the model using ROI data, even though a similar methodology was applied. In both cases, the application of the brain-age models to psychiatric patients, particularly those with SCZ, revealed a positive BrainAGE deviation compared to HC samples. When the ROI-based model was applied to the MDD group, a positive BrainAGE deviation was observed, but this was limited to specific atlases. The voxelized BrainAGE model was also applied to CHR and ROD individuals. The CHR group exhibited a positive deviation, whereas the ROD individuals did not show significant differences compared to HC individuals. We found that the brain regions predictive of both BMI and BrainAGE overlapped, potentially suggesting that somatic conditions may share similar brain signatures, particularly in frontal areas and the control network. However, other regions did not overlap, indicating that while the two conditions may share common neurobiological pathways leading to shared brain alterations, they also possess independent pathways. The clinical variables showed associations at distinct levels, with signatures displaying patterns of comorbidity between obesity, brain-ageing and SCZ expression, as well as a pattern independent of brain-ageing.

We introduce the concept of 'BMIgap' as a potential tool to disentangle the personalized risk of obesity-related brain alterations in individuals with psychiatric disorders and further used it as a brain-obesity estimate to identify shared commonalities between obesity, brain-ageing and psychiatric condition.

List of figures

List of tables

List of abbreviations

AAL3 Automated anatomical labeling (Version 3)

BAC Balanced accuracy

BDI-II Beck depression inventory-II

BMI Body mass index

BMIgap Body mass index gap

BrainAGE Brain age gap estimation

BSR Bootstrap ratio

CAT12 Computational anatomy toolbox (Version 12)

CHR Clinical high-risk

CPZ Chlorpromazine equivalents

CV Cross validation

CV1 Inner cross-validation cycle

CV2 Outer cross-validation cycle

CVR Cross-validation ratio

DMN Default mode network

ECNP-NNADR European college of neuropsychopharmacology neuroimaging network accessible data repository

FWHM Full-width-at-half maximum

GAF Global assessment of functioning

GMV Gray matter volume

HOMA-IR Homeostatic model assessment for insulin resistance

HC Healthy controls

HC left-out Independent left-out healthy controls

HC normative Normative healthy controls

HDRS-17 Hamilton depression rating scale - 17 items

GMV Gray matter volume

GWAS Genome-wide association studies

HC Healthy control

HPA Hypothalamic–pituitary–adrenal axis

kg Kilograms

LV Latent variable

m^2 square of height measured in meters

MAE Mean absolute error

MDD Major depressive disorder

ML Machine learning

MRI Magnetic resonance imaging

OFC Orbitofrontal cortices

PANSS Positive and Negative Symptom Scale total score

PCA Principal component analysis

PFC Prefrontal cortex

R^2 Coefficient of determination

r Correlation coefficient

ROI Region of interest

rs-fMRI Resting-state functional magnetic resonance imaging

SCZ Schizophrenia

sMRI structural magnetic resonance imaging

SPLS Sparse partial least squares

SVM Support vector machine

VBM Voxel-based-morphometry

ViPAR Virtual pooling and analysis of research data platform

WHO World health organization

WMV White matter volume

1. Introduction

1.1 Understanding the complex relationship of psychiatric disorders and associated comorbidities

1.1.1 Mental health as a crucial health challenge

Mental disorders are considered one of the central health challenges of the 21st century (Wittchen et al., 2011). Over the past three decades, psychiatric disorders including Major depressive disorder (MDD) and Schizophrenia (SCZ) have become leading contributors to the global disease burden. Moreover, the number of individuals affected by psychiatric disorders has risen from 80.8 million in 1960 to 125.3 million, highlighting the growing impact of these conditions. This increase persists despite gradual but significant improvements in healthcare focus and treatment management compared to previous decades. Furthermore, psychiatric disorders represent approximately one-quarter of the global disability burden. For example, global statistics indicate that over one-tenth of the global population is affected by a psychiatric disorder, specifically more than one-third of the EU population are impacted annually (Patel & Saxena, 2014; Wittchen et al., 2011). Furthermore, research by the United Nations estimates that approximately 264 millions of global population is affected by depression (GBD 2017 Causes of Death Collaborators, 2018).

Identifying challenges stemming from mental health problems has been recognized as a significant societal issue, particularly in light of the psychological consequences brought about by the global COVID-19 pandemic. In fact, World Health Organization (WHO) has reported a massive surge in the global incidence of anxiety and depression as a result of the COVID-19 pandemic, estimating 53.2 million additional cases (COVID-19 Mental Disorders Collaborators, 2021). Moreover, psychiatric disorders have been identified as one of the greatest challenges that society must address in the coming decades, particularly given the psychological ramifications of the COVID-19 pandemic (COVID-19 Mental Disorders Collaborators, 2021). These findings underscore that psychiatry faces more significant challenges compared to other branches of medicine. The figures are particularly concerning, given the substantial public healthcare costs associated in tackling psychiatric disorders.

Furthermore, research has indicated that individuals with psychiatric disorders have a higher likelihood of experiencing additional diseases throughout their lifetime—a phenomenon known as comorbidity (Maj, 2005; McGrath et al., 2020). Examples of comorbid conditions frequently associated with psychiatric disorders include other psychiatric illnesses, metabolic syndromes (such as diabetes), cardiovascular diseases and risk factors for ageing-related conditions. The presence of these comorbid diseases significantly influences the global burden of psychiatric disorders (McGrath et al., 2020).

Schizophrenia

SCZ is a profound psychiatric disorder that impacts an individual's cognitive, perceptual, and emotional functioning (Anticevic et al., 2015). Though less prevalent than other psychiatric disorders, SCZ affects approximately 24 million people of the global population. The WHO estimates its prevalence approximately 1 person in 222 adults (*GBD Results*). Despite extensive research, no single cause of SCZ has been identified; it is understood that SCZ arises from a combination of genetic predispositions and various environmental factors including stressful life events or extensive drug use (Kahn et al., 2015). While SCZ is classified as a severe mental illness, early diagnosis and treatment can enable patients to lead fulfilling lives and maintain their daily routines. However, SCZ is a heterogeneous disorder, posing challenges for early diagnosis. Patients often do not present with "pure" diagnoses but rather have coexisting psychiatric and medical comorbidities (Abdullah et al., 2020). The clinical presentation of SCZ is further complicated by substantial psychiatric comorbidity, affecting both early diagnosis and understanding of the condition's etiology. Psychiatric disorders such as depression, anxiety, and substance abuse frequently co-occur with SCZ, exacerbating its clinical manifestations. Additionally, somatic diseases such as cardiovascular risk factors as well as type 2 diabetes often co-occur with SCZ, contributing significantly to the early and high mortality rates observed in these patients (Dieset et al., 2016). Furthermore, SCZ has been associated with ageing related brain structural abnormalities which further exacerbate the condition.

Clinical high-risk (CHR)

Conceptualization of the CHR state for psychosis was introduced in 1996 to facilitate the early identification of individuals with higher risk to develop a first episode of psychosis (Fusar-Poli et al., 2013; Huber & Gross, 1989). This state is characterized by the presence of mild positive psychotic symptoms which are not sufficiently severe or persistent to meet the criteria for a full-blown psychotic disorder diagnosis (Fusar-Poli et al., 2013). The simultaneous occurrence of these milder symptoms allows for the identification of vulnerable individuals before the onset of a more severe psychotic disorder (Solmi et al., 2023). Epidemiological studies indicate that CHR status exists in approximately 1.7% of the general population and notably higher prevalence at 19.2% in clinical groups (Salazar de Pablo et al., 2021). Over the past three decades, research has demonstrated that around 20-25% of individuals identified as being at high risk for psychosis develop the condition within 2 to 3 years of initial assessment, with the risk extending up to 10 years post-initial presentation (Fusar-Poli, 2017).

Depression

Worldwide MDD stands as the most common psychiatric disorder which exerts the greatest impact on the global burden of diseases amongst other psychiatric disorders (Stein et al., 2020). It is characterized by persistent lowered mood significantly affecting an individual's everyday life. It was ranked third in the global burden of disease in 2008 by WHO and has estimated that the disorder will rank first by 2030 due to the constant increase annually. Globally, approximately 280

million individuals are impacted by depression, constituting 5% of adults, with an additional 5.7% of individuals aged over 60 years. The rates are higher among women (6%) compared to men (4%) (Bains & Abdijadid, 2024). Depression is caused from a multifaceted interplay of social, psychological and biological factors, including adverse life events such as unemployment, traumatic experiences, genetic, neurochemical, hormonal and psychological dimensions (Remes et al., 2021). Similar to other psychiatric disorders, depression can arise as a symptom or consequence of another underlying condition, such as SCZ or bipolar disorder. This comorbidity complicates the clinical picture, making it challenging to discern whether depression is a primary disorder or secondary to the other psychiatric condition. Furthermore, epidemiological research indicates a significant overlap between depression and other psychiatric disorders, particularly anxiety disorders and substance use disorders (Steffen et al., 2020). Research indicates that around 50–60% of people who have dealt with depression also acknowledge having encountered at least one anxiety disorder at some point in their lives. Furthermore, depression has been identified as a contributing factor for many somatic diseases including type 2 diabetes, cardiovascular disease, hypertension (Brenes, 2007). Due to these factors, recent studies are focusing on a specific subtype of the phenomenon characterized by recent onset of depressive (ROD) episodes emerging within a relatively short timeframe (Koutsouleris et al., 2021; Lalousis et al., 2022).

1.1.2 Brain abnormalities in common psychiatric disorders

The evolution of diverse neuroimaging techniques in the past four decades has proven instrumental in examining common phenomena observed across psychiatric disorders (Yen et al., 2023). Recent advancements in various neuroimaging modalities, particularly quantitative structural imaging techniques including voxel-based morphometry (VBM) as well as functional neuroimaging have significantly contributed to this field. There has been a progressive utilization of structural neuroimaging techniques, particularly structural MRI (sMRI), in the diagnosis of psychiatric disorders (Falkai et al., 2018). The predominant focus of studies has been on assessing the clinical potential of such neuroimaging techniques to understand the aberrant structural brain changes associated with psychotic and affective disorders, as well as finding potential biomarkers.

SCZ and CHR

It has long been recognized that SCZ is characterized by clinical and cognitive changes, along with structural anomalies in the brain. This understanding dates to Kraepelin's early observations, particularly documented in 1919, where he speculated on the potential cellular damage to the cortex associated with the disorder. However, since the late 1920s, pneumoencephalographic studies have revealed that enlarged ventricles are a characteristic feature among patients with chronic SCZ, at a macroscopic level (Bleuler, 1950; “Dementia Praecox and Paraphrenia.,” 1972). Moreover, since the 1990s, SCZ has been increasingly perceived as a psychiatric disorder

characterized by “disrupted structural brain connectivity” (Friston & Frith, 1995; Pettersson-Yeo et al., 2011). These findings increased the interest in studying the brain structural changes in SCZ patients. Among all the structural brain abnormalities observed in SCZ, alterations in GMV change have been examined thoroughly, specifically using VBM (Kubicki et al., 2002; Shenton et al., 2001). A plethora of studies have shown that patients with SCZ have consistently shown GMV deficits in extensive brain regions relative to the HC individuals specifically in the frontal and temporal lobe, cingulate and insular cortex and the thalamus. Moreover, these patients exhibit enlarged lateralized ventricular structures and diminished regional brain volume, particularly in the frontal operculum and lateral temporal lobes (Fornito et al., 2009; Shenton et al., 2001) (Fornito et al., 2009; Shenton et al., 2001). Furthermore, recent review article has highlighted GMV abnormalities progressing from first episodic stages to later chronic stages in SCZ showing lower GMV relative to controls in the thalamus, bilateral insular cortex as well as left parahippocampal, anterior cingulate, middle frontal, postcentral gyri (Howes et al., 2023).

Interestingly, research has been directed towards identifying the anatomical brain changes occurring during first-episode SCZ specifically since these findings may indicate a progression of brain changes after disease onset, which may be beneficial for early disease diagnosis. These findings have revealed that CHR individuals display similar volumetric abnormalities akin to patients with SCZ, specifically cortical brain abnormalities (Borgwardt et al., 2008; Damme et al., 2020). However, whether these brain changes persist unchanged or progress throughout the disease course, remains elusive. While recent findings indicate that these brain changes are less widespread in early stages with gradual increase in the GMV deficits at later disease course. Specifically, longitudinal analysis using neuroanatomical datasets of patients with SCZ across 25 years have revealed that initially brain-functional changes are brain region-specific, while both functional and GMV-structural abnormalities occur later and affect broader brain regions, while abnormalities in structural connectivity emerge during the later stages of SCZ disease progression (Shen et al., 2023).

Depression

Meta-analyses have revealed that adult individuals displaying past experiences of depression exhibit lower GMV specifically in frontal cortical regions, specifically the prefrontal cortex (PFC) and orbitofrontal cortices (OFC) dorsal striatal areas, including the putamen and caudate nucleus as well as limbic regions such as the amygdala, anterior cingulate cortex and hippocampus compared to HC individuals without depressive episodes (Arnone et al., 2012, 2016; Vandermeer et al., 2020). Furthermore, ROD individuals exhibit GMV alterations in brain regions, including parietal-temporal regions, PFC, thalamus, insular lobe, cerebellum, basal ganglia and limbic structures (Amidfar et al., 2021).

Moreover, it has been observed that brain abnormalities observed in depression samples are not as extensive and widespread as those seen in association with SCZ. This is because SCZ is associated with GMV abnormalities in a broader set of brain regions (Bora et al., 2011). Yet, there

are considerable overlapping patterns of brain abnormalities across the 2 diagnostic categories such as in the hippocampus, PFC, and insula which are recurrent in subjects with MDD or SCZ as compared HC individuals, notably at early stages of these disorders as well (Busatto, 2013).

1.1.3 Neurobiological pathways

Kraepelin's last contribution, "The Manifestations of Insanity", towards psychiatric nosology was pivotal in delineating SCZ and depression as distinct diagnostic entities (Heckers et al., 2022; Kraepelin & Beer, 1992). This work has been both acknowledged and critiqued by numerous researchers, due to the increasing evidence indicating substantial overlap among major psychiatric disorders in terms of genetic risk factors, endocrine and metabolic markers, brain structure and function, clinical symptomatology, and cognitive impairments (Heckers et al., 2022).

Schizophrenia

The neurobiology underlying the symptoms seen in patients with SCZ has consistently been linked to neurotransmitters and their pathways (Brisch et al., 2014; Howes et al., 2023). Particularly, dysfunction in presynaptic subcortical region-specific dopamine transmission appears to play a central role in mediating psychosis in SCZ(Brisch et al., 2014; Howes et al., 2023). Therefore, changes in dopamine function have been correlated with the manifestation of delusional and psychotic-like symptoms in individuals with SCZ. Furthermore, the thalamus, recognized as a pivotal relay station for transmitting information to and from the cerebral cortex, plays a critical role in the primary circuit responsible for psychotic symptoms, which connects the thalamus, cerebral cortex and striatum. Any alteration in these brain regions has been noted to disrupt the entire network, leading to the manifestation of psychotic symptoms. In particular, dysfunction in the thalamus and cerebral cortex predominantly affects the striatum and dopamine D2 receptors causing hallucinations and delusional symptoms (Luvsannyam et al., 2022). Dopaminergic neurons release dopamine and glutamate and gamma-aminobutyric acid (GABA) which are the co-transmitters during synaptic signaling. Glutamate and GABA act in the excitatory inhibitory pathways respectively, aiding in the transmission of dopamine neuronal activity to the striatum. Furthermore, the antagonists of the key glutamate N-methyl-D-aspartate (NMDA) receptor such as ketamine and phencyclidine, have the potential to disrupt thalamic circuitry, resulting in cognitive dysfunction and psychotic symptoms (Luvsannyam et al., 2022).

In addition, significant contributions of genetic factors to the etiology of SCZ have been demonstrated. Genome-wide association studies (GWAS) have uncovered hundreds of distinct loci of genes implicated in SCZ. These findings suggest a highly pleiotropic genetic risk across major psychiatric disorders, indicating common risk variants shared between SCZ, MDD, bipolar disorder and autism spectrum disorder. Numerous suspected genetic loci predispose individuals to the neurological disruptions observed in SCZ. Notably, genes such as COMT, DISC1, RGS4, PPP3CC, ZDHHC8, AKT1, neuregulin, dysbindin, G72/G30, TRAR4, and alpha-7 nicotinic

receptor genes have been associated with SCZ, primarily through their roles in dopamine regulation, thereby contributing to the underlying pathogenesis of the disorder (Cannon, 2005).

Depression

The neurobiology of depression has been associated with alteration in levels of one or more of the monoamines, including serotonin, norepinephrine and dopamine, commonly referred to as the monoamine hypothesis. 5-HT1A, a serotonin auto-receptor existing on the soma and dendrites of 5-HT neurons is a crucial element which controls the 5-HT release all over the brain. It functions by exerting a negative feedback influence on the firing activity of these neurons (Blier et al., 1998). Dysfunctioning in this 5-HT1A receptor is vital in the pathophysiology of MDD (Kaufman et al., 2016). These studies indicate that variations in the 5-HT transporter are associated with heightened reactivity of the amygdala, potentially causing negative attentional bias and may further contribute to the development of cognitive distortions such as personalization, overgeneralization and exaggeration in patients suffering from depression. Similarly, depletion of an essential amino acid, tryptophan, a crucial element for 5-HT synthesis, has been associated with inducing depressive symptoms in such patients (Blier et al., 1998; Kaufman et al., 2016).

Depression has also been conceptualized as disorder of the mesolymbic system (Nestler & Carlezon, 2006). This system comprising dopaminergic neurons originating in the ventral tegmental area and connecting to the nucleus accumbens, plays is pivotal in mediating the reward pathway and motivation. Several lines of evidence implicate altered dopaminergic transmission and dysfunction within the mesolimbic pathway in the pathophysiology of depression (Dean & Keshavan, 2017). In this perspective, depression emerges when individuals encounter significant stress or loss, resulting in a suppression of the reward pathway, which manifests in symptoms such as anhedonia and despair. Correspondingly, studies suggest that chronic stress triggers adaptive changes within the dopaminergic mesolimbic pathway. These alterations are associated with disturbances in the regulations of brain-derived neurotrophic factor and impaired neuroplasticity (Nestler & Carlezon, 2006). Furthemore, GWAS have extracted 178 genetic risk loci and suggested more than 200 candidate genes linked to MDD. Amongst these, genes with zinc finger domains have been identified (Flint, 2023).

1.2 Somatic comorbidities associated with psychiatric disorders

1.2.1 Overview of associations and implications

Due to the multifactorial etiology of common psychiatric disorders, medical comorbidities are a common occurrence among patients with psychiatric disorders compared to general populations. Particularly, people with psychiatric disorders often have somatic comorbidities. Infact, individuals

with somatic diseases exhibit higher susceptibility towards developing psychiatric disorders. Conversely, the likelihood of having a somatic disease is approximately doubled among those with psychiatric disorders as compared to HC individuals (Weiss et al., 2020). Notably, approximately 30-50% of individuals with psychiatric disorders present somatic comorbidities, such as cardiovascular disease, type II diabetes, respiratory issues and lung diseases (Dornquast et al., 2017). For example, depression occurs in comorbidity with many somatic diseases such as patients with myocardial infarction (40–65%), patients with cancer (25%), patients with cerebrovascular diseases (25%), multiple sclerosis relative to healthy individuals (Kupfer & Frank, 2003). Additionally, among individuals with SCZ and CHR, the co-occurrence of somatic diseases, particularly associated with cardiovascular diseases, is a major contributor to the high mortality rate (Abdullah et al., 2020; De Micheli et al., 2024; Dieset et al., 2016).

Metabolic syndrome, typically characterized as a cluster of risk determinants associated with the development of cardiovascular diseases, has been observed in approximately every second patient aged above 45 years with SCZ (DE HERT et al., 2009; Wilson et al., 2005). Common features of metabolic syndrome include obesity, insulin resistance, elevated blood sugar levels, low high-density cholesterol, Type-II diabetes, dyslipidemia, and fatty liver. This clustering of health conditions in individuals with cardiovascular disease ultimately contributes to higher mortality rates observed specifically in patients with psychiatric disorders (Shen et al., 2023). Several factors contribute to the prevalence of metabolic comorbidities in psychiatric disorders, including the psychopharmacological effects of medications and suboptimal lifestyle changes such as insufficient exercise, inadequate dietary patterns, substance abuse and elevated rates of smoking (Penninx & Lange, 2018). One of the most prevalent risk factors frequently addressed in research on metabolic syndrome is obesity. The onset of obesity and weight gain is also commonly observed in the course of psychiatric disorders (Chao et al., 2019). Furthermore, there is a notable prevalence of obesity among individuals with psychiatric disorders who develop metabolic syndromes during their lifespan making it crucial to investigate obesity within the context of psychiatric disorders.

A notable correlation is the association between psychiatric medications and weight gain, which often leads to obesity. Yet, it remains unclear whether the increased incidence of metabolic syndrome observed in psychiatric patients is primarily due to poor lifestyle choices, medication side-effects or the disease condition itself. Nevertheless, drug-naive individuals experiencing their first episode of SCZ have been shown to exhibit lower levels of fasting glucose tolerance and higher levels of plasma glucose, insulin, and cortisol compared to HC individuals, suggesting that the association between psychiatric disorders and obesity may be independent of medication effects (Ryan et al., 2003).

Neurobiological studies have indicated the existence of independent associations between psychiatric disorders and somatic illnesses, attributed to shared inflammatory pathways (Meyer et al., 2020; Najjar et al., 2013). Additionally, genetic studies have provided evidence of pleiotropy between somatic illness and psychotic disorders, suggesting a potential underlying mechanism

(Andreassen et al., 2023). Hence, there is a strong imperative to identify biological markers for stratifying patients with psychiatric disorders and to uncover the biological underpinnings of somatic comorbidity. Given the robust association between obesity and the development of metabolic syndromes, it is imperative for researchers to consider obesity as a trait to understand somatic comorbidities in psychiatric disorders. This is particularly crucial to address the high prevalence of metabolic syndromes and to implement effective mitigation strategies. Moreover, obesity, a central component of many somatic diseases, has been intricately linked to psychiatric disorders through clinical observations and shared biological mechanisms (Chao et al., 2019; Lopresti & Drummond, 2013; Weiss et al., 2020). Such endeavors will enhance the clinical delineation of psychotic conditions, enabling innovative intervention strategies aimed at mitigating such comorbidity risks, thereby reducing both mortality and morbidity rates.

Obesity

As per the WHO, obesity is a complex disease marked by an increase in body fat mass thereby causing health issues (Panuganti et al., 2024). Over the last decades, it has taken the form of a global pandemic and poses a major public health problem (Weiss et al., 2020). Moreover, it has been exacerbated by the COVID-19 pandemic, contributing to a substantial increase in mortality (Arulanandam et al., 2023; Steenblock et al., 2022). Based on the survey conducted by WHO in 2022, approximately one in every eight individuals suffers from obesity worldwide. Approximately 20% of the world's population are overweight, 11% are obese as well as 43% of adults above 18 years of age are overweight and 16% of adults are obese. Furthermore, 37 million children under 5 years worldwide are overweight (Phelps et al., 2024). The same survey showed that the prevalence of obesity has doubled in adults and, specifically in children and adolescents, obesity has become four-times in the past three decades (Phelps et al., 2024). The alarming rise of obesity worldwide is concerning, especially due to its associations with multiple noncommunicable diseases such as the diabetes, cardiovascular diseases, respiratory diseases, cancers as well as psychiatric disorders. In 2019, there were 5 million deaths among individuals affected by both overweight or obesity and noncommunicable diseases. Additionally, obesity can affect reproductive health, contributing to conditions like hyperthyroidism, polycystic ovary syndrome and disturbances in sleep patterns. Over the past decade, researchers have observed a greater incidence of obesity among individuals with psychiatric disorders compared to control groups. Moreover, obese individuals with psychiatric disorders tend to display higher treatment resistance than non-obese patients. However, interventions such as weight loss have shown promise in ameliorating the condition (Lopresti & Drummond, 2013).

Body mass index

In common practice, body mass index (BMI) is a widely accepted scale to measure and categorize the different levels of obesity. The BMI is computed by dividing weight measured in kilograms (kg) by square of height measured in meters (m^2) (Wolin, 2009). The concept of using height and weight was first devised by Adolphe Quetelet between 1830 and 1850. While conducting studies

to understand human growth, Quetelet observed that during infancy and puberty, “the weight increases as the square of the height”, which was then termed as the Quetelet Index (Eknoyan, 2008). The modern-day term ‘body mass index’ was later coined by Ancel Keys in 1972 (Keys et al., 1972). In his 1972 article, Keys promoted the usage of BMI as a measure to study body fatness and stated that “"if not fully satisfactory, at least as good as any other relative weight index as an indicator of relative obesity" due to the simple calculation as compared to the other used measures (Keys et al., 1972).

Classification of obesity based on BMI scale

According to the guidelines provided by the WHO broadly an adult with a BMI of less than 18.5 is considered as underweight, which may indicate eating disorders, malnutrition or other health issues. Next, a BMI of 25 or more is classified as overweight and a BMI of 30 or more is recognized as obese (Organization, 2005). A basic categorization has been outlined in Table 1. However, these scales can vary for different countries.

Table 1. Basic categorization of the BMI scale.

Category	BMI (kg/m^2)
Underweight (Severe thinness)	< 16.0
Underweight (Moderate thinness)	16.0 – 16.9
Underweight (Mild thinness)	17.0 – 18.4
Normal range	18.5 – 24.9
Overweight	25.0 – 29.9
Obese (Class I)	30.0 – 34.9
Obese (Class II)	35.0 – 39.9
Obese (Class III)	≥ 40.0

Note. BMI = Body mass index

Causes of obesity

The accumulation of fat leading to obesity stems from a physiological imbalance in energy, characterized by higher calorie intake and lower calorie expenditure. Excess energy is stored in the fat cells, a common characteristic of obesity pathology. Various factors contribute to the pathology of developing obesity such as the quality of food, genetic, epigenetic and environmental factors (X. Lin & Li, 2021).

Food intake

The primary cause of fueling the sudden increase in global obesity is due to the widespread availability of energy-dense food and a sedentary lifestyle, resulting in surplus energy accumulation as compared to expenditure, leading to fat accumulation (Yoo, 2018). Furthermore, the significant rise in fast-food culture, which promotes the consumption of sugary and fatty foods that are often irresistible in taste, stimulates the brain's reward region. Brain's reward region is also stimulated by intake of addictive substances such as heroin and cocaine. Put simply, foods which are high in sugar and are fat-rich are tailored to impact our brains much like drugs, thus, making them addictive (Sadeghirad et al., 2016). Individuals with obesity show higher levels of glucose, triglycerides, cholesterol and low-density lipoprotein levels and lower levels of high-density lipoprotein which are primary risk factors of somatic diseases such as cardiovascular disease. Most fast-foods are rich in cholesterol, trans-fat, and sugar, which can potentially contribute to obesity (Stadler & Marsche, 2020).

Genetic and epigenetic factors

Moreover, both genetic and epigenetic factors play vital roles in causing obesity. Some individuals show higher genetic susceptibility toward fat accumulation, attributed to problematic interactions between the homeostatic and reward circuits resulting in higher caloric intake. Increasing studies are showing that family history, lifestyle and psychological impact the likelihood of becoming obese due to fat accumulation or poor exercise habits. A cross-sectional study revealed that a child whose both the parents are obese has is ten times more susceptible to develop obesity as an adult, while a child with only one parent as obese is three times more susceptible to develop obesity as compared to a child whose parents are not obese (Corica et al., 2018). Furthermore, twin studies have revealed that over 40-70% of differences in obesity results from genetic factors. GWAS studies have identified 74 key genes for obesity. These genes are extensively interconnected and enriched in various biological processes associated with energy expenditure and homeostasis (Ang et al., 2023). Primarily, genetic mutations in the genes associated with obesity may lead to disruption of the homeostatic pathway causing more hunger, increased caloric intake, reduced control leading to overeating, causing fat accumulation and increased fat storage causing obesity (Koochakpour et al., 2019). Interestingly, epigenetic changes during early postnatal development may implicate the risk of obesity for a child, potentially leading to transgenerational transmission of this risk (Herrera et al., 2011).

Gut microbiota

Recent evidence has implicated the role of having healthy gut microbiome as a key to staying healthy without developing obesity. The gut microenvironment in obese individuals have been shown to support a more diverse range of viral species compared to leaner hosts. This environment is prone to generating pathogenic variants causing severe disease. Moreover, mouse studies have shown that germ-free mice with normal microbiota and normal total body fat gained body fat after cecal colonization with gut microbes, suggesting a role in metabolic rates and adipose tissue deposition (Bäckhed et al., 2004).

Although the exact causing mechanisms of obesity remains elusive, recent findings have suggested discrepancies in the hypothalamic–pituitary–adrenal axis (HPA) axis leads to the energy-homeostasis-imbalance. The imbalance affects brain regions such as the reward system, which are also implicated in many psychiatric disorders, making it necessary to address obesity within the context of psychiatric disorders.

Obesity in psychiatric disorders

Both overweight and obese individuals have a consistently higher risk of developing psychiatric disorders (Blasco et al., 2020). Conversely, patients suffering from psychiatric disorders are at risk of being overweight or obese (Mangurian et al., 2016). Patients with psychiatric disorders who exhibit higher risk factors for somatic diseases, including physical inactivity, poor diet and obesity have an elevated mortality risk of ~10 years earlier compared to the general population, primarily attributed to coexisting medical comorbidities (Schneider-Thoma et al., 2019). Clinical studies consistently showed an association of higher BMI with mental disorders such as SCZ, depression, bipolar, personality and anxiety disorders (Afzal et al., 2021). Furthermore, the prevalence of obesity and diabetes is also 2 to 3 times higher in individuals with psychiatric disorders than in the general population (Bellass et al., 2021).

1.2.2 Common neurobiological pathway between obesity and psychiatric disorders

Several reports have shown that both obesity and psychiatric disorders share multiple biological pathways, such as the neuroinflammatory pathway, hypothalamic–pituitary–adrenal (HPA) axis and the gut–brain axis (Martins et al., 2019).

Neuroinflammatory pathway

In obesity, an increase in adipocyte levels triggers the recruitment of immune cells, which in turn stimulates the production of inflammatory mediators (Gregor & Hotamisligil, 2011). Subsequently, adipocytes release cytokines that can reach the central nervous system, leading to neuroinflammation, particularly affecting regions like the hypothalamus and hippocampus (Castanon et al., 2015). Consumption of a high-fat diet, particularly one rich in saturated fats, has

been linked to inflammation in the hypothalamus, resulting in apoptosis of anorexigenic neurons within the arcuate nucleus. These neurons are vital for regulating satiety, and their reduced activity contributes to gain in weight (Velloso, 2009). Furthermore, peripheral cytokines can influence various processes within the central nervous system, including neurotransmitter metabolism and neuroendocrine activities, potentially leading to mood changes and behaviors commonly associated with depression (Dantzer et al., 2008).

HPA axis

Neuroendocrine changes are often reported in obesity, specifically concerning the HPA axis and with a particular involvement of the stress hormone, cortisol. This is noteworthy because activation of the stress system is commonly viewed as a perpetuating factor for mood episodes, worsening of psychosis and decline in cognitive functioning (Martins et al., 2019).

Gut microbiota

Emerging evidence indicate that the gut microbiota influences both brain function and obesity through its regulation of inflammatory responses and the HPA axis. It is possible that the development of obesity and psychiatric disorders stems from changes in the composition of gut microbiota, influenced by factors such as diet, medications, concurrent illnesses and genetic predispositions (Baothman et al., 2016). Changes in the gut environment may trigger immune cell activity in the intestinal lining, potentially affecting the communication between the gut-brain axis. This intricate relationship involves interactions between the gut, the brain and components such as the vagus nerve and enteric system. Notably, alterations in gut microbiota have been linked to increased permeability of the gut to large molecules, potentially leading to the translocation of gut bacteria. This phenomenon is commonly observed in individuals with obesity and those experiencing depression.

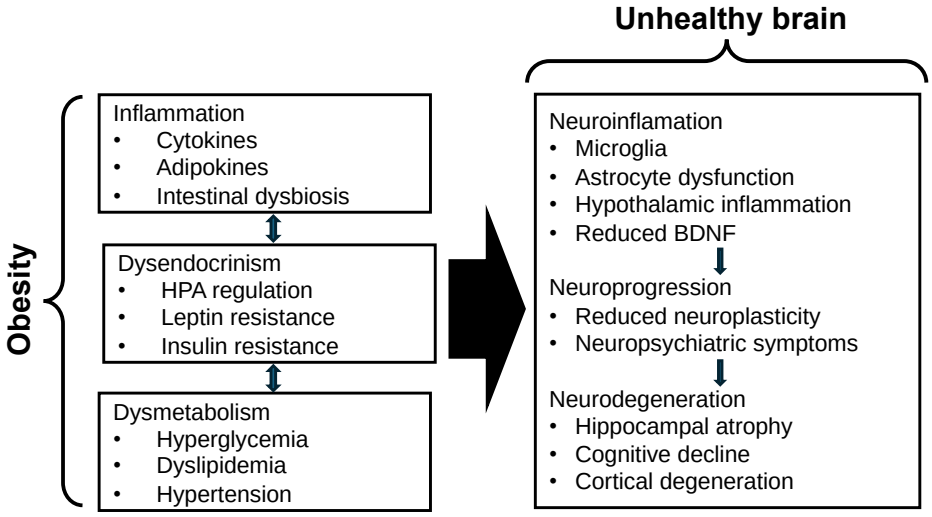

Figure 1. Obesity and neurobiological underpinnings (adapted from (Baothman et al., 2016))

1.3 Brain-based ageing in psychiatric disorders

1.3.1 Biological aspects of ageing

The process of ageing is described as a gradual decline in function over time that is marked by the progressive deterioration of physiological integrity which diminishes an individual's overall functionality and increases susceptibility to mortality (López-Otín et al., 2013). In simple terms as we age, we undergo changes in our body with respect to cells, tissues and our organs. The biological aspect of ageing is a highly complex process, which is yet to be fully unveiled. Multiple factors and biological processes are involved in the ageing process. Of which López-Otín et al. (2013) narrowed down the nine hallmarks of ageing (López-Otín et al., 2013). Epigenetic alterations, genomic instability, loss of proteostasis, telomere attrition contribute to cellular damage which is commonly observed in ageing. In response to this damage, nutrient sensing becomes dysregulated, stem cell exhaustion, mitochondria dysfunction, altered intercellular communication and cellular senescence often occur ultimately contributing to the observed process of ageing (López-Otín et al., 2013; Moskalev et al., 2013). Interestingly, humans do not undergo biological ageing uniformly, as observable differences in different ageing markers such as hair loss, skin wrinkles, and presbyopia, are apparent (Cole et al., 2019a).

Age-related deterioration serves as the primary risk factor for multiple health ailments such as diabetes, cardiovascular disorders, psychiatric conditions, and neurodegenerative diseases. Interestingly, these ailments have varying degrees of age of disease onsets. Consequently, biogerontological researchers are focusing on assessing the biological facets of ageing, with the goal of identifying age-related biomarkers that offer superior predictive capabilities for disease risks compared to chronological age alone (Cole et al., 2019a).

Biological age

The concept of biological age, distinctive from chronological age, first emerged from epigenetics research (Jackson et al., 2003; Oswald, 2000). Initially, biological age was loosely defined as the gap between a person's perceived life expectancy and the average life expectancy of a population cohort (Oswald, 2000). However, recent advancements have yielded a more nuanced comprehension of biological age. It is now evaluated by examining the interaction of multiple variables such as genetic factors, environmental factors influencing the epigenetics, lifestyle choices, overall health status, and lifetime experiences. This evaluation aims to pinpoint particular health characteristics and risk profiles associated to age-related conditions (Bocklandt et al., 2011).

1.3.2 Brain changes during ageing

The pioneering work by Pfefferbaum et al. (1994) established a milestone where they provided first evidence of brain changes with age. By using simple segmentation methods on MRI brain

scans, their study quantified brain morphometric changes in the brain from infancy to late adulthood (Pfefferbaum et al., 1994). They observed that GMV increases steadily until the age of four, after which it gradually decreases until around 70 years of age. In contrast, white matter volume exhibits a different trajectory. White matter volume continues to increase until the age of twenty, at which point it reaches a plateau. Subsequently, cerebral spinal fluid remains relatively stable until an individual reaches their twenties, after which it steadily increases. This seminal study laid the foundation for understanding the dynamic changes in brain morphometry across different stages of life, providing relevant perspectives into the process of ageing and the development of the human brain (Pfefferbaum et al., 1994). However, the underlying mechanisms linking brain morphology, function and causative factors remain to be fully elucidated.

Cognitive decline with ageing

The initial observation regarding the nexus between ageing and brain-functioning began to manifest nearly a century ago, particularly in the 1930s, when scholars initially observed decrement in cognitive functioning with progressing age (Miles, 1933). By 1976, Horn and Donaldson's work indicated that changes in cognitive functioning associated with ageing are domain-specific. Their work also proposed that certain facets of intelligence improve over adulthood, or at least resist decline in specific intelligence domains (Horn & Donaldson, 1976). Later, Salthouse et al. associated advancing age with a decline in the speed of processing information leading to impairments in cognitive functioning (Salthouse, 1996). By the 2000s it was established that chronological ageing leads to less efficiency in our mental processes and that the deficits in memory, attention and cognitive control are the core aspects of cognitive ageing (Hasher & Zacks, 1988). Furthermore, the concept of cerebral ageing emerged with evidence indicating that with an increase in age, the brain volume decreases, particularly in the frontal cortex. Moreover, older adults recruit additional brain regions while performing cognitive tasks which depend on frontal function when compared to young individuals (Park et al., 2001). Later, gradual advancements in neuroimaging techniques yielded key insights, such as the association between prefrontal volume loss and decreased memory and executive performance (Hedden & Gabrieli, 2004).

Brain atrophy

As mentioned before, significant changes occur in the structure and function in the brain of individuals, leading to cognitive decline and an elevated susceptibility to neurodegenerative conditions including dementia. Advancements in MRI, specifically VBM, a neuro-imaging technique used for quantifying volumetric variations in brain areas by using sMRI images, have enhanced our insights on typical and atypical neurodevelopment with respect to ageing. Specifically, the brain undergoes localized and non-linear patterns of highly synchronized phenomenon during its structural development and ageing processes. Brain changes can be progressive due to processes such as cell growth and myelination but can also be regressive due to processes such synaptic pruning processes during brain development (Spear, 2013).

Additionally, brain changes can lead to widespread atrophy during ageing (Franke et al., 2020; Franke & Gaser, 2019). In this context, atrophy refers to a decrease in the size or volume of specific brain tissue, a condition often associated with neurological conditions or ageing. Region-specific atrophy indicates consistent patterns of structural brain alterations in the throughout development and ageing, with certain regions of brain exhibiting more pronounced changes than other regions (Franke et al., 2020). Importantly, there may exist discrepancies between one HC individual's brain alterations as compared to the average brain alterations of a population with respect to GMV, white matter volume and cortical thickness. Such patterns of deviations from typical healthy brain-ageing profiles could imply potential underlying risk of developing cognitive ageing or age-associated brain diseases, prompting further investigation to study these brain changes.

1.3.3 Brain age gap estimation (BrainAGE) framework

A growing body of research has successfully established the framework for estimating individualized brain-based age by using different modalities of high-dimensional neuroimaging data such as structural and functional images (Franke et al., 2010, p. 200; Franke & Gaser, 2019; Koutsouleris et al., 2014). This method usually includes multiple parameters for each individual's brain images. Subsequently, by employing pattern recognition techniques, it is feasible to quantify the structural development and ageing of the brain across various stages of life. Unlike univariate methods, multivariate methods, as discussed later in section *1.4 Machine learning as a tool to capture comorbid patterns*, can identify and quantify both subtle and extensive deviations in the region-specific or voxel-wise brain structure throughout the brain, tailored to the individual's age (Franke & Gaser, 2019).

The overarching goal of a brain-age framework is to accurately estimate an individual's brain-based age, which serves as a biological indicator and has captured the specific structural brain patterns associated with age. To achieve this, the brain age model is developed using voxelized MRI scans from a large sample of cognitively HC individuals and identify the brain-ageing signatures. Subsequently, the age predictor is employed on new individuals to estimate individualized brain ages based on their MRI scans. Finally, the difference between individual's estimated brain age and chronological age reveals the brain age gap estimation (BrainAGE) score (Franke & Gaser, 2019). A positive BrainAGE score indicates advanced structural brain-ageing or accelerated ageing, while a negative BrainAGE score indicates delayed structural brain-ageing or decelerated ageing. For example, if an individual who is chronologically 55-year-old, scores BrainAGE of +5 years, it indicates that the structural brain properties of the given individual's brain resemble to the structural brain properties of a 60-year-old reference person. This finding may indicate accelerated ageing in the individual. Conversely, if a 55-year-old individual scores BrainAGE of -5 years, the person's brain properties resemble to a person who is chronologically 50-year-old.

BrainAGE and its association with general health factors

Several neuroimaging studies have examined aspects of brain-ageing with respect to general health factors. Conventionally, a lower BrainAGE score is considered as a healthy indicator during adolescence while at later stage (adulthood and later), a lower BrainAGE score is considered as healthy. Based on this, several studies have focused to examine and link BrainAGE with general health factors. During early developmental stages or adolescence, higher BrainAGE has been linked to better cognitive functioning, whereas a lower BrainAGE has been associated with heart defects and premature birth (Everwijn et al., 2019). During adulthood, various stress-inducing and lifestyle factors have been associated with brain-ageing alterations. Specifically, greater BrainAGE scores has been associated to factors such as early life stress inducers, high alcohol intake, smoking, and health issues like cardiometabolic risks and physical disorders (Angebrandt et al., 2022; Beck et al., 2022; Treur, 2022). Conversely, engaging in meditation, physical exercises and engaging in music have been linked to lower BrainAGE in adults (Adluru et al., 2020; Bittner et al., 2021; Luders et al., 2016; Rogenmoser et al., 2018). Additionally, particularly within the female population, physiological occurrences such as the monthly cycle and pregnancies have been linked to alterations in BrainAGE (de Lange et al., 2020).

1.3.4 Application of BrainAGE framework to psychiatric disorders

After the initial successful implementation of the BrainAGE framework to study the brain atrophy in patients with neurodegenerative disorders such as Alzheimer's Disease and furthermore to predict the individuals transitioning from mild cognitive impairments to Alzheimer's disease, many studies have used the BrainAGE framework to study brain atrophy in other neurodegenerative conditions such as dementia as well as in psychiatric disorders such as depression, SCZ, bipolar disorder (Franke et al., 2010; Gaser et al., 2013; Koutsouleris et al., 2014). The surge in interest in brain-age research has been driven by compelling evidence revealing biological connections between psychiatric disorders and premature ageing (Pearson et al., 2022).

The utilization of the brain age prediction model in individuals diagnosed with psychiatric disorders such as SCZ, CHR, and depression consistently reveals positive BrainAGE scores, indicative of accelerated brain-ageing. Neuroimaging studies consistently report elevated BrainAGE scores in SCZ patients compared to HC individuals, with scores ranging between +2.6 and +7.8 years across various studies (Constantinides et al., 2023). However, findings regarding depression are inconsistent, with BrainAGE scores varying between +4.0 years to showing no significant differences relative to HC individuals (L. K. M. Han et al., 2021). Furthermore, longitudinal data analysis unveils a progressive increase in BrainAGE scores during the initial years following the onset of illness. This temporal trajectory underscores the dynamic nature of brain-ageing in psychiatric disorders and emphasizes the importance of early intervention and monitoring (Schnack et al., 2016). Structural brain variations in common psychiatric disorders have been elaborately discussed in *Chapter 3*

Neurobiology of ageing

The most accepted theory for observing accelerated brain-ageing trajectories in such patients is due to earlier loss of GMV with the onset of psychosis or depression. Immunological findings have revealed that elevated proinflammatory cytokines, arising due to genetic predisposition or as response to environmental determinants, may cause dysfunctioning astrocytes and microglia activation, causing dendritic pruning and synaptic changes. Immune dysfunction plays a critical role in the development of psychiatric disorders such as both SCZ and depression, where heightened levels of cytokines such as interleukin 6 and C-reactive protein have been found. The heightened levels of cytokines are often associated with the loss of GMV, a phenomenon commonly observed during the process of ageing as well (Michaud et al., 2013)..

1.3.5 Need to address BrainAGE in psychiatric disorders

BrainAGE analysis can provide insights into structural brain alterations that occur early in the course of psychiatric disorders, potentially enabling early detection and diagnosis. Identifying these changes at an early stage may facilitate timely intervention treatment initiation, which is crucial for improving patient outcomes. The ageing process significantly impacts the brain, and individuals with chronic psychiatric or neurological disorders inevitably experience its effects over the course of their illness. Assessing the biological-age of the brain in individuals with psychiatric disorders holds promise for enhancing our understanding of disease susceptibility and resilience. This framework allows us to assess how the different psychiatric conditions influence the brain-ageing processes and further refine outcome predictions by capturing individual variations between ageing and specific disease condition (Cole et al., 2019a). This approach has the potential to offer valuable insights into disease progression, inform personalized treatment strategies and ultimately improve patient care and outcomes (Cole et al., 2019b).

1.4 Machine learning as tool to capture the comorbid patterns

1.4.1 History of machine learning

ML can be defined as a computational strategy enabling computer systems/algorithms/statistical models to automatically learn from data patterns with the hope of making meaningful and optimal decisions. The idea of artificial intelligence and machine learning was introduced during the 1950s and 1960s once electronic computers became prevalent and facilitated the creation of statistical models and the analysis of extensive datasets. From the beginning, the development of ML branched into three major categories such as the classical work in symbolic learning, as well as neural networks (Kononenko, 2001). The past two decades saw a vast methodological advancement of these ML branches (Kononenko, 2001). The use of statistical methods to identify patterns, including techniques such as Bayesian classifiers, k-nearest neighbors, discriminant analysis has shown promise. Additionally, the inductive learning methods such as the decision

trees has been noteworthy such as the chabox ELIZA regarded as the “computer therapist” (Weizenbaum, 1966). The past one decade has seen noteworthy advancements in artificial neural networks, such as the multilayered feedforward neural network which have been developed and applied across diverse fields. Interestingly, the idea of ML was based on a model of cell-cell interaction in the brain, which was created in 1949 by Donald Hebb as described in the book “The Organization of Behavior” where Heb’s perceptions on inter neuron communications has been described (Hebb, 1949).

Advancements of ML in health care sector

The application of ML methods in the field of medical sciences and health sector commenced shortly after the foundational concepts of ML were established. The focus in the field of artificial intelligence during the 1950s and 1970s was to develop ML algorithms to make inferences on specific tasks which were previously exclusive to human decision-making abilities. By the 1960s, ELIZA, a natural language processing algorithm, was developed. ELIZA used pattern matching techniques to mimic human conversation (Weizenbaum, 1966). After a slow phase in artificial intelligence development in medicine for three decades, often termed as “artificial intelligence winter”, the past two decades artificial intelligence and specifically ML witnessed seminal development in multiple sectors of health care. Accessibility of patient records to natural language processing algorithms allowed these tools to identify patient-specific information and facilitate precision medicine responses. By 2017, Bakkar et al identified RNA-binding proteins which were altered in amyotrophic lateral sclerosis, by the help of the supercomputer, Watson (Kaul et al., 2020). The ML have performed comparable or, at times, superior to clinicians, specifically in pattern recognition tasks, including the detection of skin cancer, lung cancer and eye disease (Kaul et al., 2020). Furthermore, companies have also already included ML algorithms in their ultrasound devices facilitating robust detection of breast cancer (e.g., Samsung, RS80A) (Cazacu et al., 2019). Importantly, the past decade witnessed widespread application of ML methods for detection of psychiatric disorders.

1.4.2 Use of machine learning in psychiatry

Etiologically, psychiatric disorders are heterogenous showing comorbid symptoms as compared to other neurological disorders making their diagnosis a challenging task. ML algorithms are beneficial in solving this challenge due to their robustness in detecting specific patterns. Diagnostic models assist clinicians in identifying the disease more accurately, and prognostic models are useful to predict the development course of the disease. The combined integration of ML and other branches, specifically neuroimaging in the past decade unlocked the potential of recognizing disorder-specific patterns, which otherwise may go unnoticed by clinicians. The efficacy ML methods in psychiatry have greatly influenced research towards the fields of early recognition, a subfield of psychiatry emphasizing on early diagnosis as well as in the emerging field of precision psychiatry, a branch in mental health care aiming to provide individualized

diagnosis, treatment, and prevention strategies by accounting multiple factors such as genetics, neuroimaging data as well as environmental factors. Furthermore, as discussed earlier, one of the key factors contributing to high mortality rate among patients with psychiatric disorders is the co-occurrences of other conditions such as obesity, cardiovascular risk factors, Type II diabetes as well as neurodegenerative disorders such as dementia (Arulanandam et al., 2023). Especially, given the challenge of disentangling the cause-effect relationship, particularly when it is unclear which conditions/symptoms are the cause and which are the effect, a task greatly improved after the emergence of ML. More advanced ML methods have facilitated in combining the disease-specific information from different data domains such as neuroimaging, genetics, clinical data or even social media records to provide a more refined and robust diagnosis (Franke & Gaser, 2019; Koutsouleris et al., 2014, 2021; Phelps et al., 2024). Another major challenge is the identification of biological factors in CHR individuals or those in the prodromal phase where an individual is susceptible to transitioning into psychotic disorder. ML has proved helpful as it can learn these specific patterns and identify the subgroups who show more disease vulnerability and similar pattern to those individuals who have already transitioned, thus facilitating early diagnosis and implementation of preventive methods. ML models can also cluster individuals exhibiting similar patterns, such as brain patterns, thereby assisting clinicians in making decisions based on the similarity in the profiles of these clustered individuals for further prognosis and treatment planning. Furthermore, ML has served as a favorable tool for comprehending differences at individual levels (e.g. in clinical sample), while simultaneously mapping these differences in relation to HC sample (Rutherford et al., 2022). The framework has been widely beneficial in brain-age and other predictive research queries, particularly in cases where it is necessary to compare the deviations of a clinical sample with respect to a reference group. Taken together, the power of ML has been useful to identify biomarkers specific to each condition and facilitate early recognition, prevention and personalized treatment strategies.

Classification analysis

In psychiatry, classification analysis refers to the utilization of models to categorize or predict individuals into distinct diagnostic groups using diverse features like neuroimaging data, genetic markers or clinical symptoms. Typically, the objective is to construct models capable of effectively discriminating between various psychiatric disorders or distinguishing individuals with psychiatric conditions from those without. Using GMV data, ML algorithms can classify subjects as SCZ patients or HC individuals, based on features extracted from the brain imaging data. A more advanced application involves distinguishing individuals who are in the process of transitioning to psychosis from those in high-risk states, determining whether an individual will convert to psychosis or not (Dwyer et al., 2018; Koutsouleris et al., 2018, 2021; Loch et al., 2023).

Regression analysis

A regression model is a type of ML model designed to predict a numerical, continuous output, such as a rating. Linear or polynomial regression models are common examples, which create a

line or curve to best fit the data in a dataset. Regression problems can also be transformed into classification problems by setting thresholds to categorize the continuous output variables into discrete categories. An example of regression-based problems is predicting brain age (Chekroud et al., 2021; Franke et al., 2010; Koutsouleris et al., 2014).

Common machine learning methods used in psychiatry

ML has been applied in various areas improving interventions, showing promising predictive diagnosis accuracies and prognosis of mental health disorders and comorbid conditions. Generally, these algorithms rely on large datasets to robustly learn the discriminative patterns to perform classification and predictive tasks. Supervised machine learning methods such as Support Vector Machine (SVM) is one of the most prevalent methods applied prediction of appropriate labels for a given data such as neuroimaging, genetics data.

Supervised learning

Supervised learning entails acquiring an understanding of the connection between a group of input variables and an outcome variable, which is then employed to anticipate the results of unseen data points (Iyortsuun et al., 2023). SVM are versatile tools used for both classification and regression tasks. In classification, SVM determines the optimal decision boundary, called the hyperplane, to effectively segregate data points into different classes in n-dimensional space. It then assigns new data points to the appropriate categories based on this learned boundary. SVM offers several advantages, including its capability to handle both semi-structured and structured data and its tendency to avoid overfitting. However, when dealing with large datasets, SVM's learning time may increase, which can impact its effectiveness. Consequently, when applying supervised methods to high-dimensional datasets such as neuroimaging data, it's common to include a feature selection step to derive low-dimensional representations. Despite its limitations with noisy datasets, SVMs have gained widespread acceptance in fields like psychiatry due to their reliable performance, user-friendly nature, and quicker computational times compared to alternatives like neural networks. In dissertations, SVMs are frequently utilized, with detailed explanations provided in subsequent sections. Another prominent supervised learning method is decision trees, which segment data into constant approximations and construct models based on basic decision rules derived from data attributes. Logistic regression, on the other hand, is often used for forecasting categorical outcomes. The Least Absolute Shrinkage and Selection Operator (LASSO) algorithm efficiently learns feature patterns while predicting specific disorders or clinical outcomes by simultaneously selecting relevant features. Likewise, the Relevance Vector Machine (RVM) uses a probabilistic framework, by employing automatic relevance determination to obtain sparse solutions while penalizing unnecessary model complexities. The effectiveness of RVM has been successfully demonstrated in quantifying neuroimaging biomarkers for PTSD and predicting treatment outcomes in depression. Additionally, RVM was incorporated into the inaugural BrainAGE framework as the prediction algorithm (Franke et al., 2010). Additionally, multi-task learning approaches are gaining traction for jointly leveraging complementary features

from various perspectives of neuroimaging data. Recent advancements utilized ML frameworks for more challenging tasks. The challenging task characterizes specific signatures of comorbid disease patterns among psychiatric disorders, dimensional approaches have been utilized to capture the complex linear relationship between high-dimensional datasets.

Multivariate methods such as canonical correlation analysis and partial least squares methods have been useful tools to capture associations across different data modalities (Mihalik et al., 2022). For example, canonical correlation analysis has been employed with resting-state fMRI (rs-fMRI) connectivity data. This approach successfully identified two low-dimensional components, each representing distinct disease dimensions, such as an anhedonia-related component and an anxiety-related component. These methods have successfully captured the associative components across specific brain regions associated with the respective clinical dimensions, thereby opening avenues to study the neural correlates of specific disease symptoms. Specifically, the method of using sparse partial least squares (SPLS) has been introduced explicitly later.

ML accuracy to detect psychiatric disorders

Initially, the application of ML in psychiatry was primarily centered around disease diagnosis. While ML has proven to be a powerful tool extensively used for classification and regression tasks, particularly in distinguishing patients with psychiatric disorders from HC individuals, the performance of these models exhibits significant variability. Each study utilizes diverse datasets, data domains, data processing pipelines, ML algorithms, model parameters, and validation approaches, which can potentially account for the observed differences in classification accuracies. A review article summarizing the findings of classification analyses conducted to differentiate SCZ patients from HC individuals using various supervised ML methods applied to different brain features revealed that model performances generally ranged between 55% and 70%. The highest classification accuracy of 73.5% was achieved using cortical thickness data and an SVM classifier (Cortes-Briones et al., 2022). Similarly, literature findings on classification accuracies for distinguishing patients with MDD from HC controls have also demonstrated varying results, ranging from 53% to 91% (Belov et al., 2024; Gao et al., 2018; Kambeitz et al., 2017). Furthermore, there are varying observed in regression methods when conducting predictive analyses. For instance, the mean absolute error (MAE), a common measure used to assess predictiveness in brain-ageing models, has been shown to vary between 2 and 10 years for both HC and patient samples. Additionally, ML research has demonstrated relatively lower accuracy in identifying comorbid conditions, highlighting the need for further attention and improvement in this area.

1.5 Aims of this study

As discussed earlier, addressing the somatic comorbidities of psychiatric disorders poses a significant challenge. Among the somatic diseases, metabolic comorbidities contribute

significantly to the high mortality and morbidity associated with psychiatric disorders such as SCZ and depression while their exact reasons remain poorly understood. Since obesity is a prominent risk factor for various metabolic diseases, it is crucial to explore the shared characteristics between obesity and psychiatric disorders. Furthermore, longitudinal studies have highlighted the high prevalence of obesity during the course of psychiatric diseases and particularly during relapses. Given that obesity and psychiatric disorders, both psychotic and affective, share common neurobiological pathways leading to similar brain alterations, understanding the underlying causes is of paramount importance.

Furthermore, aberrant brain-ageing processing is common occurrences in multiple psychiatric disorders and specifically more pronounced in psychotic disorders. Moreover, the process of brain-ageing can significantly impact the trajectory of psychiatric disorders, especially in the presence of metabolic risk factors, highlighting the importance of distinguishing between the individual processes. Additionally, it is crucial to establish associations between the clinical dimensions within each of the conditions. The aim of this dissertation is to overcome these limitations by leveraging ML methods.

The study's main aim is to understand the link between obesity, ageing, the associated brain alterations, clinically relevant variables and psychiatric disorders. Since BMI serves as a widely accepted and used tool for assessing obesity, we developed a multivariate BMI-predictor based on whole-brain GMV of HC individuals without psychiatric diagnoses. We propose an individualized brain-based BMI gap score (BMIgap) calculated as the difference between brain-estimated and observed BMI. Furthermore, we applied the BMI-predictive model to clinical populations comprising individuals suffering from SCZ and ROD as well as individuals at CHR states for psychosis. Moreover, we explored shared brain regions between obesity and SCZ and investigated the phenotypic associations between obesity, SCZ, and clinically relevant variables using SPLS.

2. Quantification of obesity related brain changes by using ML as a tool

The content of this chapter has been submitted as: Adyasha Khuntia, David Popovic, Elif Sarisik, Madalina O. Buciuman, Mads L. Pedersen, et al. **BMIgap: a new tool to quantify transdiagnostic brain signatures of current and future weight**, which is currently under review at Nature Mental Health. The content of this chapter has been paraphrased, and the tables and figures presented herein have been adapted from the aforementioned paper.

2.1 Association between psychiatric disorders and obesity

2.1.1 Why address obesity as a comorbidity in psychiatric disorders?

As introduced in Chapter 1, clinical studies have consistently revealed a higher prevalence of obesity among individuals with psychiatric disorders, including SCZ, MDD, bipolar disorder, personality disorders as well as anxiety disorders. Notably, these patients exhibit a two-to-three-fold higher incidence of obesity and metabolic syndromes compared to the general population (Bellass et al. 2019). However, the bidirectional relationship between obesity and psychiatric disorders remains poorly understood, including whether they share overlapping or distinct neurobiological pathways (Blasco et al., 2020; Luppino et al., 2010; Mangurian et al., 2016). Moreover, commonly prescribed anti-psychotics and anti-depressant medications are known to impact body fatness. Furthermore, there is an ongoing debate regarding the causes of weight changes, that is, whether medications implicate the neurobiological pathways leading to weight change or whether the onset of weight change is attributed to the progression of the psychiatric disease state. Given that obesity is a common feature of somatic diseases and strong association between somatic diseases and psychiatric disorders, it is paramount to address the complex and bidirectional relationship between obesity and psychiatric disorders, as it may have adverse prognostic implications. This underscores the importance of developing personalized tools bcapable of capturing the comorbid interactions associated with both obesity and psychiatric disorders.

In this chapter, our primary focus is to disentangle the intricate commonalities between obesity and psychotic disorders such as SCZ and CHR and affective disorders including ROD by using BMI to measure obesity. Consistent with the previous definitions, individuals with a BMI exceeding 30 units are considered obese. A higher BMI indicates a higher degree of obesity in a person.

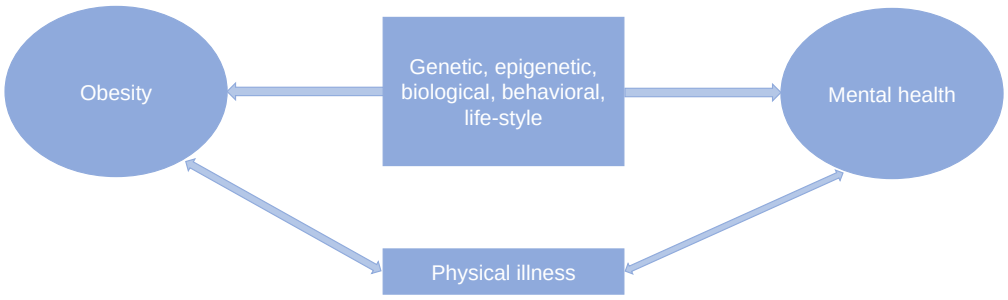

Figure 2. Interface between obesity and mental health

2.1.2 Obesity and SCZ

An estimated 40-60% of individuals suffering from psychotic disorders including SCZ, schizoaffective, brief psychotic, delusional disorders are overweight or obese, which is significantly higher than the general population. Individuals with such conditions have 2.5 times higher risk of early mortality as well as their life expectancy is ten to thirty years lower than the general population (DE HERT et al., 2009). One of the major causes of early mortality is cardiovascular disease, arising from higher rates of metabolic risk indicators such as hyperglycaemia, dyslipidaemia, obesity and hypertension (Mitchell, 2013). Specifically, patients with SCZ have a three-times higher likelihood of developing obesity (Annamalai et al., 2017; Vancampfort et al., 2015). Multiple factors, such as genetics, pathophysiology, lifestyle choices and medications significantly contribute towards prevalence of obesity in psychiatric patients Since obesity is the common cause of multiple metabolic syndromes, its impact extends to physical health, thereby contributing to elevated mortality rates (Figure 2). Moreover, obesity also affects mental health and brain structure notably. Evidence suggests that obesity may worsen the symptoms of SCZ by disrupting the white matter integrity and reducing connectivity between brain networks. Nevertheless, being underweight also poses health risks, and a low BMI can indicate self-neglect or physical fragileness.

Bidirectional Relationship between SCZ and obesity

Increasing studies have shown evidence that there is a bidirectional relationship between etiology of obesity and psychiatric disorders manifested through the comorbidity of obesity or metabolic syndromes with psychiatric disorders as well as the occurrence of psychotic and depressive symptoms in overweight or obese individuals. However, it remains elusive whether the pathology follows a "disorder-to-obesity" or "obesity-to-disorder" direction, or if the pathology is intertwined.

Multiple factors are contributing towards obesity including disruption of shared neurobiological pathways. The causes for obesity are elaborated in section *1.2 Somatic comorbidities associated with psychiatric disorders,* including sustained inflammation, disruption of endocrine system and

metabolic dyshomeostasis resulting in excess of energy accumulated in the fat cells. In fact, neuroinflammation has garnered special interest in this field characterized by a disparity between astrocytes and microglial cells where the microglial cells assume roles in multiple processes including the production of growth factors as well as metabolism of neurotransmitters. As time progresses, mechanisms of plasticity including synaptic production, remodeling, and neurogenesis gradually become impaired, especially in critical areas such as the PFC, hippocampus and hypothalamus. Ultimately, neurodegenerative processes may occur, characterized by permanent lesions such as gliotic scars and notably, a significant loss of neural cells in cortical regions. Such alterations of the brain-structure may partly contribute to the disruptions in cognitive, control and executive as well as reward activities in obese individuals and further development of psychiatric disorders development (Weiss et al., 2020). The manifestation of GMV loss in psychotic disorders, particularly in frontal-temporal regions and areas associated with reward and control, may inhibit the control for eating, leading to overconsumption of high-calorie food that provide a sense of reward, ultimately resulting in weight gain and obesity, a phenomenon also observed in patients with eating disorders. Conversely, the onset of negative psychotic symptoms or depressive symptoms may reduce appetite, resulting in weight loss, a common occurrence in psychiatric disorders including depression and anorexia nervosa. The hypothesis of overlapping symptoms across different subtypes of psychiatric disorders and the possibility of identifying and distinguishing brain-specific markers for these subtypes pose significant challenges. However, if achieved, it could have important therapeutic implications by facilitating, for example, the understanding of the cause-effect relationship between obesity and medication initiation, thereby enabling early interventions to prevent metabolic syndromes.

Obesity and SCZ

Obesity has a marked impact on brain structure and related psychiatric outcomes (Afzal et al., 2021; Bora et al., 2017; Luppino et al., 2010; Martins et al., 2019). Infact, neuroimaging findings have revealed that brain alterations occurring due to obesity shows similar alterations as observed in patients with SCZ such as a total GMV reduction. Infact, the widespread use of BMI as the obesity-variable has facilitated the neuroimaging research groups to use BMI to examine the brain changes in relation to both obesity and SCZ. For example, a study examining the relationship between BMI in patients with SCZ revealed that higher BMI is associated with lower total GMV, indicating a negative correlation between obesity and GMV. Specifically, this correlation was observed in brain regions such as the bilateral OFC and PFC, as well as the right hippocampal and frontal cortices. Another study compared the comorbidity of metabolic syndrome in patients with SCZ. Those individuals with metabolic syndrome showed smaller total brain volume and GMV, as well as smaller volumes of the OFC and insula, and larger ventricles, compared to those without metabolic syndrome. Also, the reward regions of the brain were reduced in the patient group with metabolic syndrome. Furthermore, individuals with metabolic syndrome exhibited reduced sizes in OFC and insula cortical surface areas relative to the patients without any metabolic syndrome (de Nijs et al., 2018). Although GMV loss and cortical thinning is a common

finding in both SCZ and obesity research, the cortical changes progress gradually with time for patients with SCZ. GMV reductions are also commonly attributed with the ageing process. Yet, it remains unclear whether such volumetric reductions are primarily associated with obesity, ageing or an interplay of both factors (S. R. McWhinney et al., 2022).

Obesity in high-risk individuals

Although not many studies investigated brain changes in high-risk individuals introspecting BMI changes, one study showed that such individuals showed low levels of physical activity while no significant BMI differences were observed compared to controls (Carney et al., 2016). Patients undergoing through first psychotic episode have shown high hyperglycemia, dyslipidemia and gain in weight during the initial weeks following the commencement of antipsychotic medications (Correll et al., 2014, De Hert et al., 2006, Foley and Morley, 2011). Such metabolic syndromes increase proportionally with illness-duration (De Hert et al., 2006, De Hert et al., 2011b). Individuals experiencing episodes of psychosis who have not previously been treated with antipsychotic medication have demonstrated abnormal glucose tolerance (Fernandez-Egea et al., 2009). Furthermore, among the individuals experiencing first episode of psychosis, BMI was associated with lower GMV in the left cerebellum (Kolenic et al., 2018).

Obesity and psychotic symptoms

Individuals showing negative symptoms such as emotional response deficits are more prone to being overweight and to developing metabolic syndrome. Less healthy lifestyle habits such having a more sedentary lifestyle is a common occurrence in such individuals, which might increase the risk factors for cardiovascular diseases (Arango et al., 2011). Furthermore, study showed that patients with SCZ patients showing metabolic syndrome as comorbidity exhibited poor cognitive functioning than those patients who did not exhibit any metabolic syndrome (Saxena et al., 2023). Furthermore, the HDL showed high positive correlation with BMI and the severity of psychiatric symptoms (Sahpolat et al., 2021). Another study, observed that both overweight and obese patients with SCZ with higher appreciation for body image specifically body functionality as assessed showed fewer positive psychotic symptoms (Mahfoud et al., 2023). The heightened intensity of residual symptoms, as indicated by elevated PANSS scores, was found to be associated with reduced volumes of the frontal lobe, PFC, insula, hippocampus, left hemisphere amygdala, and total white matter (Tsai et al., 2020). Furthermore, the negative psychotic symptoms were have been negatively associated with higher BMI in severe patients with SCZ which are primarily attributable to reduced levels of anhedonia and levels of asociality (Mezquida et al., 2018). Furthermore, longitudinal studies have indicated that around six years into the follow-up period, the increase in BMI is specifically associated with positive symptoms rather than negative symptoms, particularly notable before the commencement of antipsychotic treatment in antipsychotic-naïve patients diagnosed with SCZ. This suggests that the theory linking weight gain to antipsychotic initiation lacks substantial support (S.-H. Lin et al., 2021).

2.1.3 Obesity and depression

While the co-occurrence of obesity and depression had been frequently observed, until the beginning of the millennium, this association was predominantly perceived as coincidence (Stunkard et al., 2003). The meta-analytic review conducted by de Wit et al. identified a significant association between depression and obesity, reporting an 18% increased risk of obesity among individuals with depression. Additionally, studies focusing on adolescents revealed that MDD during adolescence predicted higher BMI in adulthood compared to individuals without a history of depression. Further analyses investigated potential mediating variables and identified factors such as sex, socioeconomic status and childhood experiences as contributors to the development of both depression and obesity. Additionally, it was suggested that genetic susceptibility to both depression and obesity may be influenced by environmental factors (Stunkard et al., 2003). Later, common molecular mechanisms linking obesity and depression became apparent, indicating the pivotal role of the HPA axis in both conditions. Cytokines such as IL-6, IL-18 and TNF-α, neuropeptides such as melanocortin, NPY, orexin and neurotransmitters including epinephrine, serotonin were identified as key players in both depression and obesity, while interacting within the HPA axis. Additionally, other factors such as persistent stress and variations in gene-expression are contributing factors towards the emergence of either condition or comorbid manifestations of both depression and obesity (Bornstein et al., 2006).

Neuroimaging studies using VBM examined the relationship between BMI and depression, specifically MDD and illness-duration. Higher BMI was associated with lower GMV, particularly in regions such as the thalamus, medial PFC, OFC and caudate nucleus. Moreover, within the patients diagnosed with MDD, patients showing higher BMI have shown severe disease chronicity. Additionally, both BMI and disease chronicity exhibited correlations with morphometric irregularities in the medial prefrontal regions. Moreover, these neurostructural alterations between the disease severity and obesity overlapped specifically in prefrontal areas engaged in impulse control and regulation of emotions (Opel et al., 2015). These findings imply that obesity maybe directly associated with higher disease chronicity.

Moreover, adult individuals with MDD exhibited thinner GMV in cortical regions as compared to HC individuals in several brain regions, including the brain regions of temporal lobe, OFC, insula, anterior and posterior cingulate. These structural brain changes were particularly pronounced in patients with early disease onset, appx before the age of twenty-one. The adolescents with MDD did not exhibit disparities in cortical thickness when compared to their HC counterparts. However, these patients displayed a decrease in overall surface area as well as exhibited localized reductions in regions specific to frontal areas, notably in the medial OFC, superior frontal gyrus, as well as brain regions associated with motor, somatosensory, primary and visual functioning. The most pronounced effects have been observed in recurrent adolescent patients. These findings indicate that MDD may exert a dynamic influence on brain structure, resulting in diverse patterns of alterations observed across different life stages (Luppino et al., 2010; Schmaal et al., 2017).

Obesity and depressive symptoms

Some studies including the work by ENIGMA working group did not establish significant associations between the brain derivatives and the depressive symptom scales (HDRS-17) (Schmaal et al., 2017). Community based studies have indicated that elderly individuals who are obese, regardless of gender, are less inclined to experience depressive symptoms than their counterparts with normal weight. The results offer support for the "jolly fat" hypothesis, initially proposed within Chinese traditional culture, indicating that favorable perceptions of obesity might act as a safeguard against depressive symptoms (Mulugeta et al., 2018).

2.1.4 Common neurobiological pathways

The neurobiological pathways common to both obesity and psychiatric disorders have been detailed in *1.2 Common neurobiological pathway between obesity and psychiatric disorders.* Briefly, among the biological pathways linking obesity to psychiatric disorders, increased neuroinflammation stemming from cytokine production in adipocytes is a well-established phenomenon. Additionally, high-sugar or LDL cholesterol-rich diets are known to elevate inflammation rates, impacting neurotrophic factors and the gut microbiome, which is a common observation in both obesity and psychiatric disorders (Marx et al., 2021). Psychosocial connections between physical and mental health are also significant, as psychiatric conditions can impede one's ability to derive enjoyment and pursue personal interests, thereby fundamentally affecting daily functioning and quality of life (Connell et al., 2014). Compromises to a healthy lifestyle habit, often resulting in decreased physical exercise, can contribute to gain in weight and subsequent obesity (McElroy, 2009). Furthermore, the common biological factors such as inflammation may mediate the progression from obesity to psychiatric disorders, alongside the disease burden of chronic metabolic syndromes.

ML to predict obesity

Given the recurrent challenges to disentangles the intertwined conditions of both obesity and different psychiatric disorders, whether ML can be a helpful tool, is yet to be fully understood. Until the time of study, not many studies had implemented the ML methods to reliably dissociate the brain signatures specifically occurring in obesity. To our knowledge Opel et. al (2017) had conducted the first study to associate BMI and neuroanatomical brain features (Opel et al., 2017). They found that higher BMI was significantly associated with medial prefrontal GMV decrease. The study, although promising did not assess the associations on psychiatric groups. The study, while promising, did not evaluate the associations within psychiatric groups, which forms an important basis of this study.

2.1.5 Influence of medication

Antipsychotics

The use of antipsychotic medication has emerged as an iatrogenic factor contributing to obesity in psychiatric disorders (Leutner et al., 2023). Numerous studies conducted within community settings have underscored the connection between medication usage and weight gain. For instance, research involving 5,756 individuals diagnosed with SCZ in France revealed a higher prevalence of obesity among patients consuming antipsychotic drugs such as clozapine, olanzapine, risperidone, or amisulpride compared to those not receiving any antipsychotic treatment (Limosin et al., 2008). Similarly, investigations within the Chinese community suggested that atypical antipsychotics might contribute to increased abdominal obesity (Kucukgoncu et al., 2019). Conversely, clinical observations among medication-naïve individuals at CHR and patients with affective disorders have indicated disturbances in glucose metabolism even before the occurrence of their initial psychotic episode (Kucukgoncu et al., 2019). Additionally, a recent study found that rapid weight gain associated with antipsychotic use is linked to diminished impulse control and alterations in brain regions implicated in impulsivity. Notably, this phenomenon varies across psychiatric populations and is strongly linked to chronic neuroinflammation (Grosu et al., 2024).

Antidepressants

Antidepressants such as paroxetine, amitriptyline and mirtazapine have been associated with a higher risk to weight-gain while some antidepressants, such as bupropion and fluoxetine, have been associated with weight-loss, including in already obese individuals. Notably, the combination of bupropion and naltrexone has shown to induce more significant weight loss compared to either drug alone (Ranjbar et al., 2013). The association between depression and obesity may involve dysregulation of the stress system, specifically the HPA axis, inflammation, oxidative stress and endocrine dysfunction, highlighting potential neurobiological mechanisms underlying both conditions (Bornstein et al., 2006). These findings underscore the complex interplay between medication usage, metabolic changes and neurobiological pathways in psychiatric populations.

2.1.6 Aims of the study

The study's main aim is to understand the association between obesity, the associated brain alterations clinically relevant variables and psychiatric disorders. Since BMI serves as a widely accepted and used tool for assessing obesity, we developed a multivariate BMI-predictor based on whole-brain GMV of HC individuals without psychiatric diagnoses. We propose an individualized brain-based BMI gap score (BMIgap) calculated as the difference between brain-estimated and observed BMI. Furthermore, we applied the BMI-predictive model to clinical populations comprising individuals suffering from SCZ and ROD as well as individuals at CHR states for psychosis. Furthermore, we examined the overlapping brain regions between both SCZ and obesity and investigated the phenotypic associations between obesity, SCZ as well as the clinically relevant variables using SPLS.

2.2 Methods

2.2.1 Sample characteristics

Neuroimaging datasets

The participants included in the current study are T1-weighted sMRI scans from four independent datasets including IXI dataset (https://brain-development.org/ixi-dataset/), Personalized Prognostic Tools for Early Psychosis Management (PRONIA; www.pronia.eu) study, Norwegian Centre for Mental Disorders Research (NORMENT) dataset (Wolfers et al., 2018) and the Munich Brain Imaging Database (MUC) (Koutsouleris et al., 2015).

PRONIA study

PRONIA is a multisite study where participants were recruited across nine sites in Finland, Germany, Italy, Switzerland, and the United Kingdom in accordance with the study's standardized recruitment protocol. The observational part of the protocol included follow-up examinations at three months interval further implemented by the nine PRONIA sites. The participants were pseudonymized twice after recruitment which was done locally at each site and centrally within the PRONIA-portal. This portal has a multi-user data-repository which hosting the defaced MRIs as well as information about each clinical and neurocognitive items of the participants. The organization of these database was first converted into digital questionnaires categorized as visits and cases. The portal also offered users a web interface to control the entry and upload of various acquired data into the corresponding questionnaires. Moreover, an implemented PRONIA@home mobile device interface allowed study participants to securely log in to the portal and complete the self-rating questionnaires for a given visit. The data underwent an automated process including quality control after completion of data-entry across all questionnaires for a given visit. This procedure involves executing approximately 1600 data integrity and dependency rules. These rules encompass various checks, including basic assessments of missing data and data ranges, evaluations of dependencies within individual questionnaires, and examinations of dependencies between two questionnaires within a single visit. Additionally, the procedure includes assessments of dependencies between two consecutive visits, ensuring uniformity, including checking the dates. The errors found are reported back to the defined user, thus facilitating for a manual correction of the encountered errors. This process is repeated until the quality of clinical questionnaires for the given visit is deemed sufficient, at which point the visit is locked (for details refer to Supplementary Methods, Koutsouleris et al., 2018)).

IXI dataset

The IXI dataset, comprising MRI images from healthy individuals, includes data collected at three hospitals in London: Guy’s Hospital, Hammersmith Hospital and the Institute of Psychiatry (https://brain-development.org/ixi-dataset/).

MUC dataset

The MUC database encompasses a diverse cohort, including both HC individuals and patients diagnosed with SCZ. Participants were recruited from the Department of Psychiatry and Psychotherapy at Ludwig-Maximilian University, Munich. Diagnostic assessments for patients were carried out using the Structured Clinical Interview for Diagnostic and Statistical Manual of Mental Disorders, Fourth Edition, Axis I Disorders. Symptom severity was evaluated utilizing the Positive and Negative Symptom Scale total score (PANSS). Age of onset for SCZ was retrospectively determined through semi-standardized interviews, providing insight into the temporal trajectory of the disorder. Additionally, illness duration, standing for the time interval between MRI acquisition and age of onset, was meticulously recorded. Hospitalization history, a critical aspect of disease progression, was quantified by tallying the number of in-patient or day-clinic admissions preceding MRI scans. Ethical considerations were paramount, with the study receiving approval from the local ethics committee and meticulously adhering to ethical guidelines outlined in the Declaration of Helsinki. Antipsychotic medication dosages administered at the time of MRI were converted to chlorpromazine equivalents for standardized assessment and analysis (Koutsouleris et al., 2015).

NORMENT dataset

Participants were recruited between October 27, 2004, and October 17, 2012, as part of the Thematically Organized Psychosis study, with subsequent reanalysis of data conducted in 2017 and 2018. The recruitment process targeted patients accessing inpatient and outpatient clinics within the Oslo region of Norway. Eligible patients who aged between 18 and 65 years, were required to be proficient in a Scandinavian language, possess an IQ above 70, and have no history of severe head trauma. Clinical assessments were conducted by trained physicians or clinical psychologists, employing the Structured Clinical Interview for DSM-IV Axis I Disorders to establish psychiatric diagnoses. HC individuals were randomly selected from national registries, provided neither they nor their relatives had a history of psychiatric disorders, alcohol or substance use disorders or cannabis usage within the preceding 3 months. Participating individuals underwent a comprehensive neuropsychological assessment encompassing domains such as processing speed, verbal learning and memory, executive functioning and working memory. Prior to participation, written informed consent was collected from all participating individuals. The study protocol, inclusive of magnetic resonance imaging procedures and cognitive and clinical data collection, adhered to strict deidentification protocols. Ethical approval was secured from the Regional Committee for Medical Research Ethics and the Norwegian Data Inspectorate (Wolfers et al., 2018).

Participant inclusion

Within the scope of the current investigation, the criteria for participant inclusion included a number of essential features. To begin with, the general inclusion/exclusion for the PRONIA participants are indicated in Table of Koutsouleris et al. (2018). Secondly, subjects from the IXI,

PRONIA, NORMENT, and MUC datasets were included in the study if they had been subjected to structural MRI scans and their processing through the VBM8 pipeline had been completed successfully. Furthermore, individuals were considered if they provided information on their sex, age, weight and height as well as if their BMI fell between the range of 18.5 (classified as underweight) to 35 kg/m^2 (classified as obesity class II and III) and their age spanned the range of 15 to 75 years. Finally, patients diagnosed with SCZ belonging to MUC database were considered for inclusion if they contained at least seventy percent of the clinical items as well as satisfied the criteria presented above.

The selection of HC participants adhered to specific additional criteria, ensuring the exclusion of individuals with existing or prior psychological illnesses. Our study comprised a total of 1504 HC subjects, categorized into two distinct groups: the discovery sample and the replication sample. The discovery sample encompassed 770 individuals, while the replication sample comprised the remaining 734 HC participants. Within the discovery sample, participants were meticulously chosen to represent a uniformly distributed spectrum of BMI. This involved dividing the entire HC sample into 33 BMI bins, each spanning a 0.5 increment, and sampling an equal number of subjects from each bin to approximate a uniform distribution. Additionally, ages of subjects within each BMI bin were carefully matched to minimize the potential influence of age on BMI, thereby mitigating any confounding age effects (Figure 3). The replication sample, comprising of the remaining 734 participants, was subsequently utilized for model validation purposes (Figure 4). The schematic representation of the workflow has been demonstrated in Figure 5.

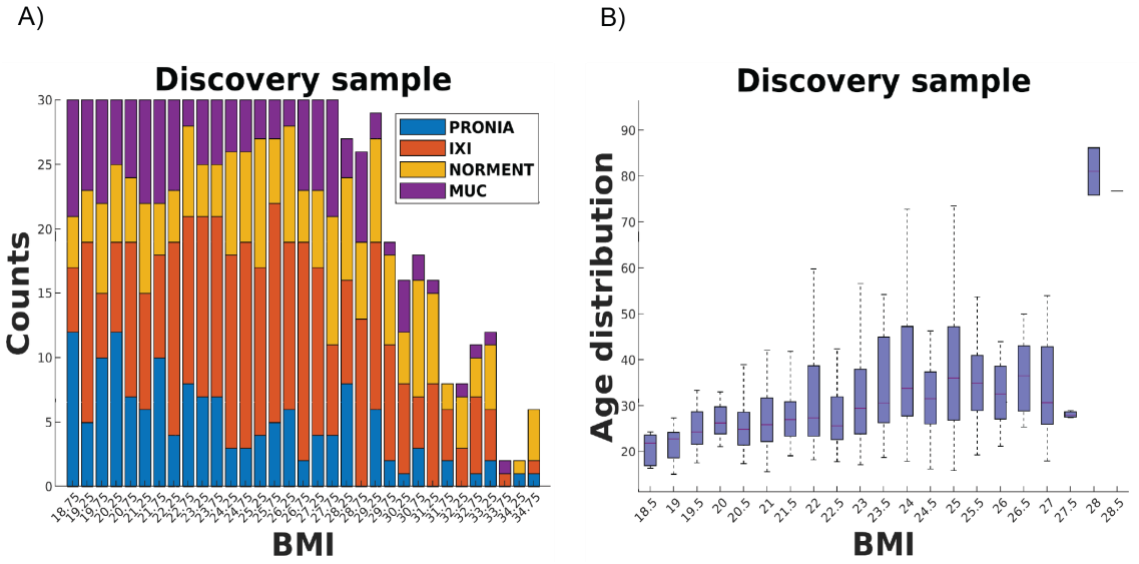

Figure 3. Sample for discovery data. Histogram for the BMI distribution for discovery sample showing the uniform-like BMI distribution with the different colors representing the four cohorts. Age distribution per BMI bin of 0.5 BMI units.

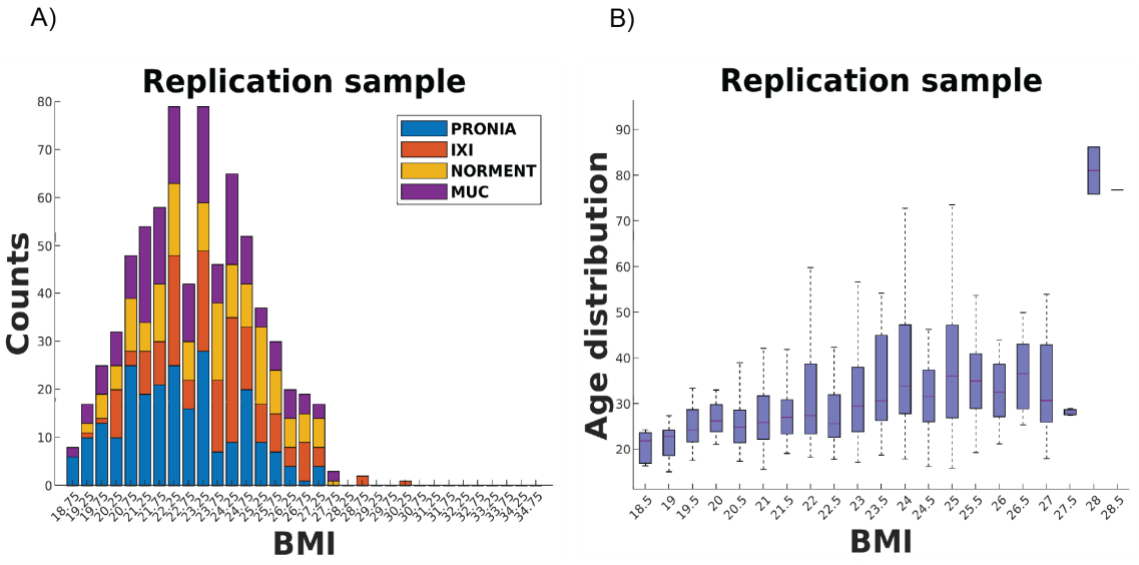

Figure 4. Sample for replication data. Histogram for the BMI distribution for replication sample showing the uniform-like BMI distribution with the different colors representing the four cohorts. Age distribution per BMI bin of 0.5 BMI units.

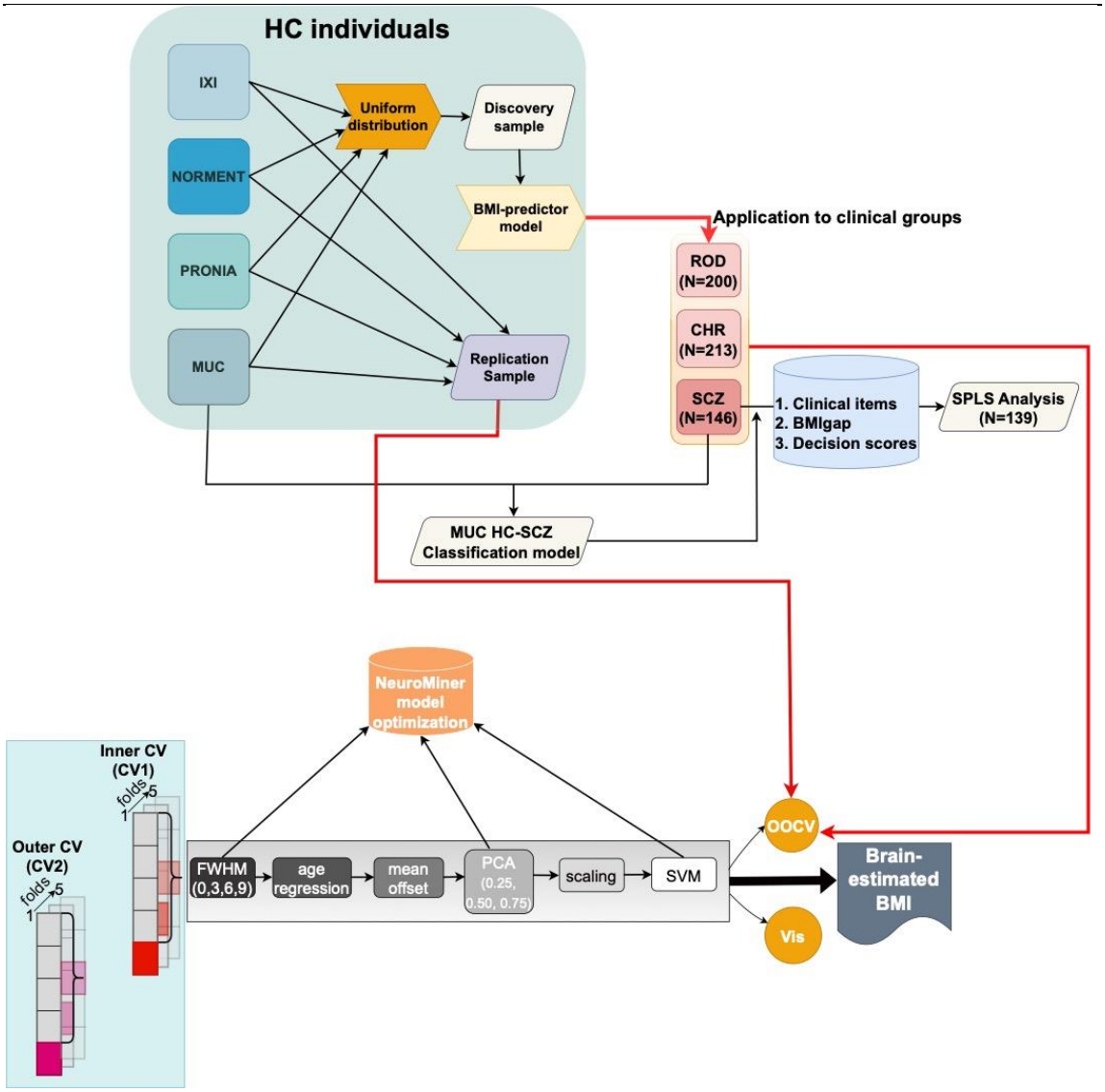

Figure 5. Schematic representation of analysis flow conducted in the study. Abbreviations: HC= healthy controls, MUC= Munich database, BMI= Body mass index, ROD= Recent onset depression, CHR= Clinical high-risk, SCZ= Schizophrenia, SPLS= Sparse partial least squares, CV= Cross validation, PCA= Principal component analysis, SVM= Support vector machine, Vis= Model visualization, OOCV= Out-of-sample cross-validation

MRI data acquisition and pre-processing

The specific MRI parameters for each dataset are provided in Table 2. The structural images underwent several preprocessing procedures using the VBM8 toolbox available at http://dbm.neuro.uni-jena.de/vbm . Firstly, we performed bias correction, tissue classification, and normalization to MNI space. This normalization technique employed a combination of linear transformation using 12 affine parameter and non-linear transformations within a unified model, which included high-dimensional DARTEL normalization. Subsequently, the gray matter segments were modulated solely by the non-linear components to preserve local gray matter values. Additionally, absolute threshold masking with a threshold value of 0.1 was applied. To enhance calculation speed and minimize noise, the GMV images were resampled to a uniform voxel resolution of 3x3x3 mm^3.

Table 2. MRI scanner systems and structural MRI sequence parameters used in BMIgap analysis

(table adapted from Koutsouleris et al. (2018)

Site	Model	Field Strength	Coil Channels	Flip Angle	TR (ms)	TE (ms)	Voxel Size (mm)	FOV	Slice Number
IXI database									
Hammersmith Hospital	Philips Intera	3.0T	-	8	9.6	4.6	-	208 x 208	-
Institute of Psychiatry	Philips Gyroscan Intera	1.5T	-	-	-	-	-	-	-
Guy's Hospital	General Electric	1.5T	-	8	9.8	4.6	-	208 x 208	-
NORMENT									
Oslo	SIEMENS Magnetom	3T	32	7	2730	3.93	1.33 × 0.94 × 1.0	240 x 240	160
Munich database									
LMU Hospital	SIEMENS Magnetom	1.5T	8	12	11.6	4.9	0.45 x 0.45 x 1.5	230 x 230	126
PRONIA									
Munich	Philips Ingenia	3T	32	8	9.5	5.5	0.97 x 0.97 x 1.0	250 x 250	190
Milan Niguarda	Philips Achieva Intera	1.5T	8	12	Shortest (8.1)	Shortest (3.7)	0.93 x 0.93 x 1.0	240 x 240	170
Basel	SIEMENS Verio	3T	12	8	2000	3.4	1.0 x 1.0 x 1.0	256 x 256	176
Cologne	Philips Achieva	3T	8	8	9.5	5.5	0.97 x 0.97 x 1.0	250 x 250	190
Birmingham	Philips Achieva	3T	32	8	8.4	3.8	1.0 x 1.0 x 1.0	288 x 288	175
Turku	Philips Ingenuity	3T	32	7	8.1	3.7	1.0 x 1.0 x 1.0	256 x 256	176
Udine	Philips Achieva	3T	8	12	Shortest (8.1)	Shortest (3.7)	0.93 x 0.93 x 1.0	240 x 240	170
Muenster	Siemens Magnetom PRISMA-FIT	3T	20	8	2130	2,28	1x1x1	256	192
Duesseldorf	Siemens Prisma	3T	32	8	2000	3.37	1.0x1.0x1.0	256x256	176
Bari	Philips Ingenia	3T	32	8	8.1	3.7	1.0 x 1.0 x 1.0	256 x 256	180

Note. TR = repetition time, TE = echo time, FOV = field of view.

2.2.2 ML analysis

BMI-prediction model

We have included the whole brain GMV maps as features to train the BMI-prediction model. All the ML analysis have been conducted using the MATLAB-based open-source ML toolbox NeuroMiner (v1.1; https://github.com/neurominer-git/NeuroMiner_1.1).

Nested cross-validation

In the model, we implemented a repeated nested cross validation (CV) set-up which is a robust method for model generalization and prevention of information leakage while mitigating overfitting of model. In the CV structure, the outer CV cycle is designated as CV2 and the inner CV cycle is designated as CV1. Models are trained in the CV1 cycle and to select the best tuning parameters. The best-performing models are applied to the data in the CV2 cycle and evaluate the model performance. The CV settings included five folds and five permutations at the inner and outer CV cycles each, producing 625 CV1 training and test partitions. Model overfitting was prevented by restricting the hyperparameter optimization to the inner folds only while guaranteeing the selection of optimized model. Moreover, in NeuroMiner, models were retrained on the CV1 training and test data using the optimal hyperparameter combination before being applied to the CV2 validation data. To ensure robustness, the final prediction for a given individual in CV2 is computed by averaging the predictions of multiple models. These models are trained on different subsets of the data, excluding the individual in question from both the training and hyperparameter optimization stages. By averaging the predictions of these models, we obtain a more stable and reliable estimate of the individual's BMI.

Pre-processing

The pre-processing of the data involved several pre-processing steps. Firstly, the model optimized the Gaussian smoothing between 0, 3, 6 or 9 mm full-width-at-half maximum (FWHM) kernel widths. Second, the age effects using partial correlation analysis as a regression method. Third global-mean offset correction was employed to remove site-specific effects, as explained below. Next, principal component analysis (PCA) was used to reduce the feature dimensions where the model optimized the PCA levels between 0.25, 0.50 and 0.75.

Subsequently, a linear kernel type nu-support vector machine regression algorithm was employed for modeling, with a regularization parameter set to 1. This algorithm was chosen based on its suitability for regression tasks and its ability to handle nonlinear relationships between predictors and the target variable.

Model performance was evaluated using several metrics which we calculated on both the CV1 test and CV2 validation datasets. These metrics included the MAE, Pearson's correlation coefficient (r), and the coefficient of determination (R^2)). The MAE was specifically chosen as the optimization criterion, aiming to minimize the average absolute difference between observed and

predicted BMI values. Optimization of the model involved finding the combination of hyperparameters that yielded the lowest MAE across different iterations of the cross-validation process. This optimization was conducted by exploring various combinations of hyperparameters, including smoothing, PCA and nu, resulting in a total of 12 combinations. Additionally, the statistical significance of the BMI prediction model was assessed using permutation testing. This involved randomly permuting the BMI labels 1000 times and recalculating the model's performance metrics. The significance level was established at $\alpha=0.05$, providing a rigorous evaluation of the model's effectiveness.

Site-correction

Previous research has indicated that sMRI data may be influenced by site or scanner variations. To address this concern, we utilized data from four cohorts, two of which were multi-site studies. To mitigate the potential impact of site-effects, we implemented a global mean correction procedure within the nested cross-validation framework. This correction procedure involves several steps. Initially, it involves calculating the mean feature-score of each site. Subsequently, the overall mean across all sites is determined. Next, the mean difference between each site's mean and the overall mean is computed. Ultimately, this mean difference is subtracted from every feature of the respective sites. Through the application of this correction, our objective is to standardize the data and mitigate the impact of site-specific variations, thereby augmenting the robustness and generalizability of our analyses.

Post-hoc BMIgap correction for true BMI

To mitigate the influence of BMI on BMIgap in the discovery, replication, and clinical groups, we utilized a stepwise calibration method that makes use of k-fold cross-validation. At first, we partitioned the discovery sample into five smaller subsets. During each iteration of the process, one subset was designated as a hold-out set, which functioned as the test set. The remaining samples, equivalent to the training group, were used to calculate the beta values using partial correlation. Afterwards, the beta coefficient that was generated was used on the hold-out subgroup of the discovery sample, as well as on the complete replication sample and the clinical groups, in order to obtain the corrected BMIgap values. This iterative approach proceeded until all subsets had been used as the hold-out test set once. Ultimately, we calculated the average BMIgap for all subsets in order to provide a revised BMIgap score for each person. By employing this iterative calibration technique, our objective was to minimize the influence of BMI on BMIgap in various groups, thereby ensuring more precise and dependable evaluations.

Classification model for MUC HC/SCZ

Within NeuroMiner, we created a classification model using sMRI data to differentiate persons with SCZ from HC individuals. Our objective was to identify brain patterns that are unique to individuals with SCZ. To guarantee consistency across models and concentrate exclusively on disparities between BMI-predictive and HC-SCZ separating brain voxels, we developed the

classification models by employing the same pre-processing procedures as those utilized in the BMI prediction model. The steps involved in the analysis were as follows: applying Gaussian smoothing with kernel widths of 0, 3, 6, and 9 mm FWHM, removing age effects through partial correlation analysis, conducting PCA with different energy levels including 0.25, 0.50, 0.75 to reduce the dimensionality of the image space, and scaling each voxel value from 0 to 1, in line with the parameters used in the BMI prediction model. The method was carried out using a repeating nested CV cycle consisting of 5 folds for both the inner and outer cycles. Each cycle had 5 permutations, also, with the same setting as used for the BMI regression model. In addition, a brain mask specifically targeting the GMV to preserve just the voxels that are relevant to GMV regions was used. The classification algorithm used was a linear class-weighted SVM, with model-optimization performed for the regularization parameter C_{SVM} over the range of $2^{[-4\ to\ +4]}$, resulting in 11 parameters. In order to evaluate the performance, we employed sensitivity, specificity, accuracy, and balanced accuracy (BAC) measures on the CV1 test and CV2 validation datasets. The optimization criterion was based on the BAC metric. The optimization process consisted of selecting the combination of hyperparameters among 4 (smoothing), 3 (PCA), and 11 (C_{SVM}) that resulted in the highest BAC value across the CV1 test data partition. This entailed a total of 132 possible combinations. Ultimately, we generated visual representations of the predictive voxels of the diagnostic separability by employing the sign-based consistency metric as detailed below.

Model visualization

We evaluated the statistical significance of classification/regression model performances by comparing the observed respective optimization criterion BAC/r with an empirical null-distribution of the respective out-of-training BAC/r obtained by permuting the group labels 1000 times and retraining the models within the cross-validation scheme. Afterwards, we computed the probability of the observed BAC/r as the number of cases in which the permuted BAC/r was equal or higher than the observed BAC/r divided by 1000 and evaluated statistical significance at α=0.05, using FDR correction to control for multiple comparisons. For the visualization of the predictive features, we primarily employed a measure of feature stability termed grand mean cross-validation ratio (CVR) (described in detail in Koutsouleris et al., 2021 and adapted from Krishnan et al., 2011) (Koutsouleris et al., 2018; Krishnan et al., 2011). This is calculated by summing up the selected CV1 median weights across all the CV2 folds and dividing them by the standard error of the selected CV1 weights for each feature, similar to the bootstrap ratio (BSR) approach in partial least squares studies (8,9). The BSRs show how reliably each source is contributing to the observed pattern. Similar to BSR, CVR thresholded at ±2 is considered as stable. Additionally, we computed a metric of feature importance called sign-based consistency, which evaluates feature relevance by counting the instances where a particular feature maintains the same sign (positive or negative) throughout the ensemble, conceptually adapted from the method of Gómez-Verdejo et al., 2019 and detailed in Koutsouleris et al., 2021 (Gómez-Verdejo et al., 2019; Koutsouleris et al., 2021). To create a more intuitive visualization of the predictive brain voxels in

the BMI-predicting model, we initially binarized the sign-based consistency maps to preserve the significant voxels thresholded at α=0.05. Subsequently, we multiplied the CVR with the binarized sign-based consistency maps. The resulting map showed the significant stable CVR with the warm and cool colored regions differentiating regions with positive and negative correlation of GMV and estimated BMI, respectively. The open-source 3-dimensional rendering software MRIcroGL (McCausland Center for Brain Imaging, University of South Carolina; https://www.nitrc.org /projects/mricrogl/) was used to overlay the thresholded map on the MNI template to produce 3-dimensional renderings and axial mosaic slices. Additionally, the automated anatomical labelling (AAL3) atlas was overlaid to visualize predictive ROIs in a spider-plot. Then, we applied the discovery model to the independent validation sample to assess the model's generalizability. Further, the discovery model was applied to the SCZ, ROD and CHR individuals to obtain brain-based BMI predictions. The HC individuals' and patients' BMIgap was calculated by subtracting the original from the predicted BMI scores.

Overlapping brain regions

For identifying brain regions associated with both obesity and SCZ, we initially binarized the FDR-corrected sign-based consistency maps. This was done by retaining the significant voxels ($P<0.05$) from the visualization of the regression and classification models only. Next, we overlapped the two binarized maps to produce a brain mask consisting of the overlapping regions shared between SCZ and obesity. The associations between GMV, BMIgap, SCZ-expression score, and clinical variables including age of disease onset, PANSS total score, number of hospitalizations and illness duration were examined by using this specific mask as a neuroanatomical search-space.

SPLS analysis

SPLS has been used to investigate the relationships between obesity, SCZ, and clinically significant variables including age of disease onset, PANSS total score, number of hospitalizations and illness duration. SPLS is a statistical method frequently used in multivariate analysis, particularly in situations where there are numerous predictor variables relative to the number of observations. SPLS was introduced as an improvement over the partial least squares method to address its difficulty in interpreting models with high-dimensional datasets (Lê Cao et al., 2008). It tackles this challenge by initially selecting a subset of relevant features to be included in the model, enhancing interpretability. SPLS is especially beneficial when dealing with high-dimensional data, such as whole brain data, as it automatically identifies the most relevant voxels for the model (Monteiro et al., 2016). This analysis used the SPLS Toolbox developed by Popovic et al. 2020 conceptualized on the SPLS framework by Monteiro et al., 2016 (Monteiro et al., 2016; Popovic et al., 2020). The analysis included only the SCZ participants who had less than 30% missing data in clinical variables, resulting in a sample size of 139. The primary objective was to identify correlations between the neuroimaging and clinical data domains for the SCZ participants. The neuroimaging data matrix, consisting of overlapping GMV regions identified from significant

voxels generated by the BMI prediction and classification models and a feature matrix that includes clinical dimensions such as BMI gap values, SCZ expression score, and clinical items such as PANSS total score, age of disease onset, illness duration, and number of hospitalizations.

SPLS method

The SPLS algorithm utilizes singular value decomposition to produce latent variables (LV) that represent unique multivariate associative effects between the two data matrices. Each LV consists of a pair of weight vectors, with u representing the brain pattern and v representing the clinical-dimension pattern of the LV. The feature weights range from -1 to 1, reflecting both the direction and magnitude of the covariance between the corresponding features. A consistent signum between two feature weights (u, v) implies positive covariation, while an opposing signum suggests negative covariation. A zero weighting indicates that the feature does not make a meaningful contribution to the respective covariance signature.

In addition, the two weight vectors combine to form a new hidden space, where individuals are represented by their latent scores. These scores are computed by combining the customized clinical and brain data with the corresponding clinical and brain vectors of the LV. The scores produce two numerical values that indicate the participants' individual loadings on the weight vectors. The correlation between latent scores for all individuals indicates the degree to which the weight vector pair is successful in maximizing covariance.

The significance of associative effects from the SPLS analysis was assessed by performing 5000 random permutations of the brain-clinical design matrix. This was followed by bootstrap resampling to uncover stable brain-clinical features in the important LVs. The significant patterns were subsequently assigned to the 17-network parcellation solution of the Yeo-Buckner atlas in order to visualize them. The BSRs were graphed individually for clinical and brain-based observations.

2.3 Results

2.3.1 Sociodemographic and clinical group-level comparisons

The statistical analysis comparing demographic variables revealed notable group-level distinctions among the discovery, replication, and patient populations, particularly concerning age, sex and BMI. Specifically, in the discovery cohort, the mean BMI was 25.10 (SD=4.03), whereas in the replication cohort, it was 23.03 (SD=2.07). A t-test examining BMI values demonstrated a significant disparity ($t = 12.49$, $P < 0.001$). Additionally, a one-way ANOVA conducted on the BMI values of HC individuals across the discovery sample, as well as SCZ, CHR, and ROD individuals, revealed significant differences ($F=12.43$, $P < 0.001$). For detailed demographic comparisons, please refer to Table 3 and Table 4. Table 5 shows sample characteristics of clinical items for patients with SCZ.

Table 3. Sociodemographic differences between discovery, replication individuals

	HC		t/χ^2
	Discovery	**Replication**	
Sample, number of participants (N)			
Total	770	734	
PRONIA	146	234	
IXI	308	172	$\chi^2_3 = 66.06$***
MUC	133	174	
NORMENT	183	154	
Age, Mean (SD)			
Total	41.26 (15.51)	32.24 (12.75)	$t_{1502} = 12.29$***
PRONIA	25.44 (6.70)	24.98 (5.55)	$t_{378} = 0.72$
IXI	52.02 (14.50)	41.50 (17.80)	$t_{478} = 7.01$***
MUC	37.76 (12.37)	31.66 (10.07)	$t_{305} = 4.76$***
NORMENT	38.31 (10.03)	33.56 (9.19)	$t_{335} = 4.50$***
Sex - Female, N (%)			
Total	435 (56.49)	373 (50.82)	
PRONIA	96 (65.75)	121 (51.71)	
IXI	170 (55.19)	92 (53.49)	$\chi^2_3 = 27.41$***
MUC	75 (56.39)	92 (52.87)	
NORMENT	94 (51.37)	68 (44.16)	
BMI, Mean (SD)			
Total	25.10 (4.03)	23.03 (2.07)	$t_{1502} = 12.49$***
PRONIA	23.81 (3.99)	22.40 (1.99)	$t_{378} = 4.59$***
IXI	25.42 (3.74)	23.62 (1.95)	$t_{478} = 5.90$***
MUC	24.18 (3.91)	22.89 (2.02)	$t_{305} = 3.74$***
NORMENT	26.27 (4.20)	23.48 (2.09)	$t_{335} = 7.50$***

Note. N= number of participants, SD= standard deviation, χ2= Chi-square test statistic, t= t-statistic, HC= healthy controls, BMI= Body mass index. Significant P values are stated as: *P≤0.05, **P≤0.01, ***P≤0.001

Table 4. Sociodemographic differences between discovery HC individuals and psychiatric groups

	HC	Patients			F
	Discovery	**SCZ**	**CHR**	**ROD**	
Sample, number of participants (N)					
Total	770				
PRONIA	146		213	200	
IXI	308				
MUC	133	146			
NORMENT	183				
Age, Mean (SD)					
Total	41.26 (15.51)				$F_{4,1567}$ = 164.42***
PRONIA	25.44 (6.70)		23.92 (5.24)	26.02 (6.37)	
IXI	52.02 (14.50)				
MUC	37.76 (12.37)	30.83 (9.97)			
NORMENT	38.31 (10.03)				
Sex - Female, N (%)					
Total	435 (56.49)				
PRONIA	96 (65.75)		103 (48.36)	96 (48.00)	
IXI	170 (55.19)				
MUC	75 (56.39)	34.00 (23.29)			
NORMENT	94 (51.37)				
BMI, Mean (SD)					
Total	25.10 (4.03)				$F_{4,1567}$ = 12.43***
PRONIA	23.81 (3.99)		23.46 (3.42)	24.01 (3.57)	
IXI	25.42 (3.74)				
MUC	24.18 (3.91)	24.02 (3.40)			
NORMENT	26.27 (4.20)				

Note. N= number of participants, SD= standard deviation, F= F-statistic, HC= healthy controls, SCZ= Schizophrenia, CHR= Clinical high-risk, ROD= Recent-onset depression, BMI= Body mass index. Significant P values are stated as: *P≤0.05, **P≤0.01, ***P≤0.001

Table 5. Clinical characteristics of the SCZ sample.

	SCZ
Number of participants (N)	139
Clinical Items, Mean (SD)	
PANSS total	51.45 (28.76)
Illness-duration	4.40 (6.70)
Age of onset	25.49 (7.92)
Number of hospitalizations	1.98 (2.12)
CPZ-equivalent dose (mg)	358.9 (382.4)

Note. MUC HC= Munich healthy control individuals belonging to discovery sample, SCZ= Schizophrenia, N= number of participants, SD= standard deviation, χ2= Chi-square test statistic, t= t-statistic, PANSS= Positive and Negative Syndrome Scale total score, CPZ= chlorpromazine. Significant P values are stated as: *P≤0.05, **P≤0.01, ***P≤0.001.

2.3.2 Individualized BMI prediction

The BMI-predictor predicted BMI in the discovery sample with an MAE of 2.75 kg/m^2. The R^2 between the true and predicted BMI was 0.28, P<0.001. This model application to the replication sample, generalized with a MAE of 2.29 and the R^2 between true and predicted BMI was 0.26, P<0.001. Figure 6A depicts the correlation between true and predicted BMI for the discovery and replication groups. The BMI-prediction model applied to the clinical groups predicted BMI with an MAE of 2.85, R^2 = 0.25 for the SCZ patients, 3.07, R^2 = 0.16 for CHR individuals and 2.73, R^2 = 0.10 in the ROD populations significantly (P<0.001). The Figure 6B depicts the correlation between true and predicted BMI scores in the psychiatric groups. Table 6 outlines the result of the regression analysis in details.

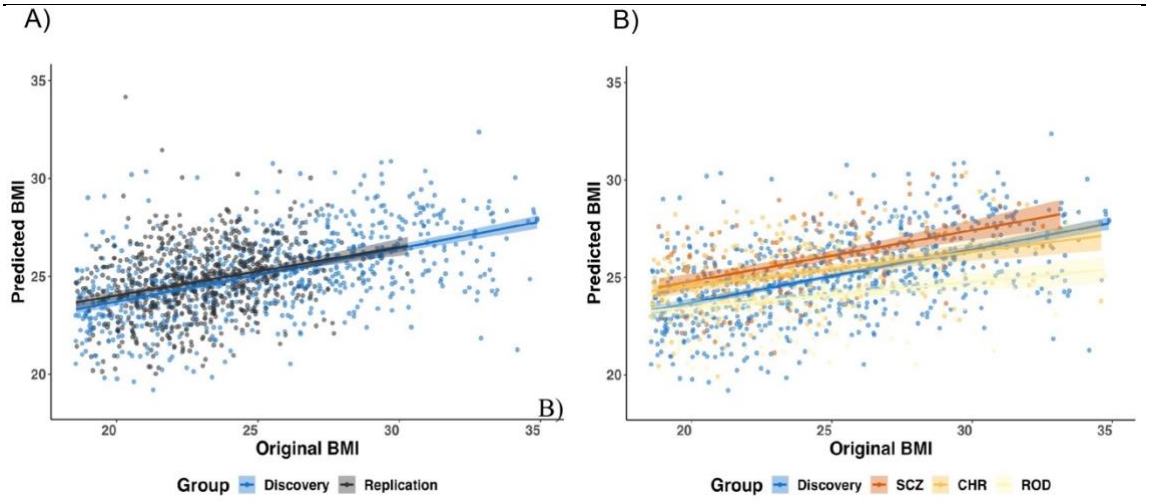

Figure 6. Regression model to estimate brain-based BMI. A) Original BMI score v/s predicted BMI score with a linear curve fit; the regression line with 95% confidence interval (CI) for the discovery group in blue and the replication group in black. B) Original BMI score v/s predicted BMI score with a linear curve fit; the regression line with 95% CI for the discovery group in blue, the SCZ patients in dark orange, CHR individuals in light orange and ROD individuals in yellow.

Table 6. Model performances of the regression analysis for the discovery model and its application to the replication and patient groups.

	N	BMIgap uncorrected	BMIgap	MAE	R^2	r
Discovery	770	-0.01 (3.4)	0 (1.78)	2.75	0.28	0.53***
Replication	734	1.73 (2.2)	0.23 (1.68)	2.29	0.26	0.51***
SCZ	146	1.83 (3.0)	1.05 (1.53)	2.85	0.25	0.50***
CHR	213	1.70 (3.26)	0.51 (1.68)	3.07	0.16	0.40***
ROD	200	-0.03 (3.48)	-0.82 (1.64)	2.73	0.1	0.32***

Note. The mean BMIgap has been reported with the standard deviation in brackets for the uncorrected BMIgap and the corrected BMIgap after regressing out the effects of body mass index. N= total number of participants, r= correlation coefficient measured by Pearson correlation, MAE= mean absolute error, R2= coefficient of determination, SCZ= Schizophrenia, CHR= Clinical high-risk, ROD= Recent-onset depression. Significant P values are stated as: *P≤0.05, **P≤0.01, ***P≤0.001

Model visualization

The BMI-predictive brain signatures showed negative GMV associations in the cerebellar, prefrontal, occipital, and insular cortices, the postcentral gyrus, hippocampus, and thalamus while, positive GMV associations were observed in the left hemisphere involving the cingulate, cerebellar, inferior occipital and temporal cortices, as well as in the right hemisphere covering parts of the precuneus, putamen and Rolandic operculum. The significant BMI-predictive regions are depicted in Figure 7.

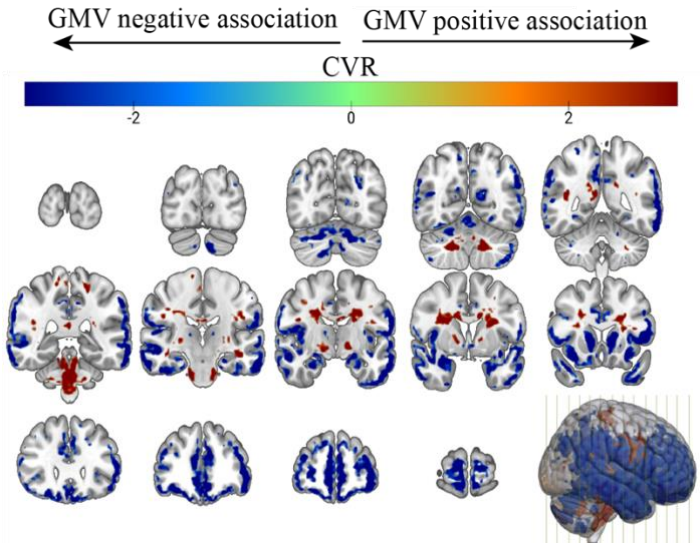

Figure 7. Visualization of the brain voxels predictive of BMI. The reliability of the predictive voxels was assessed by visualizing a grand mean cross-validation ratio map, thresholded based on the FDR-corrected sign-based consistency map with α =0.05. Cool colors indicate voxels with a negative association of GMV and estimated BMI, whereas warm colors represent a positive correlation. Abbreviations: GMV= Gray matter volume, CVR= Cross validation ratio.

BMIgap estimation across clinical groups

The BMIgap exhibited variations between HC individuals in both the discovery and replication cohorts, as well as clinical groups. Statistical analysis revealed significant differences between HC individuals and patient groups in both the discovery (F [HC discovery vs. patient groups] = 33.90, P<0.001) and replication (F [HC replication vs. patient groups] = 32.36, P<0.001) cohorts, as depicted in Figure 8.

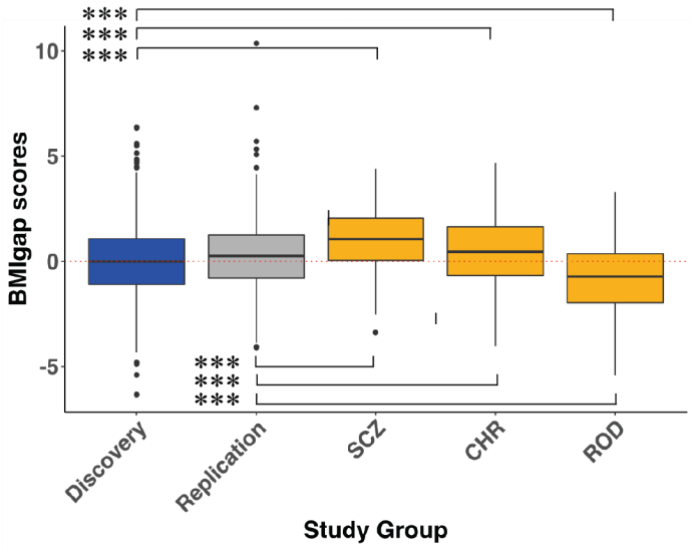

Figure 8. Group comparison between BMIgap scores. Boxplots for BMIgap for different discovery, replication, and patient groups. Abbreviations: BMI= body mass index, SCZ= Schizophrenia, CHR= clinical high-risk, ROD= recent-onset depression. **P≤0.001.

Further analysis through post-hoc pairwise comparisons unveiled that individuals in the SCZ group demonstrated the highest BMIgap scores (mean (SD) = 1.05 (1.53); t = 8.24, P<0.001; Cohen's d = 0.82), followed by individuals in the risk of developing psychosis (ROD) group (mean (SD) = -0.82 (1.64); t = -7.03, P<0.001; d = -0.82) and individuals in the CHR group (mean (SD) = 0.51 (1.68); t = 4.41, P<0.001; d = 0.51). Post-hoc comparisons were conducted to assess the mean BMIgap values in the replication group, revealing significant differences in comparison to all patient groups. Specifically, the SCZ group exhibited a t-value of 6.41 (P<0.001) with d = 0.82, the CHR group displayed a t-value of 2.37 (P=0.019) with d = 0.27 and the ROD group showed a t-value of -9.05 (P<0.001) with d = -1.05.

Notably, a significant difference in BMIgap was observed between HC individuals from the discovery and replication cohorts (t=3.75, P<0.001, d=0.23). These discrepancies may be attributed to marked variations in BMI distributions between the two samples (Figure 3A, C), evidenced by a significant difference in the variances of the BMI distributions (F= 3.8018, P< 0.001). This suggests differences in sample characteristics rather than limitations in model generalizability.

Moreover, effect sizes in the replication group were comparatively smaller than those observed in the patient groups. Additionally, the overlapping regression lines (Figure 6A) underscored the generalizability of the BMIgap model across different cohorts.

We did not find significant differences were observed in the BMIgap values among fully naïve (N=80, 37.56%), antipsychotics-naïve (N=153, 71.83%), antidepressant-naïve (N=108, 50.70%), and concurrently antidepressant-antipsychotics-treated (N=133, 62.44%) individuals classified as CHR (F=0.6, P=0.6244). Similarly, there were no statistically significant differences in the BMIgap values among fully naïve (N=59, 29.50%), antipsychotics-naïve (N=173, 86.50%), antidepressant-naïve (N=63, 31.50%), and concurrently antidepressant-antipsychotics-treated (N=141, 70.50%) individuals classified as at ROD (F=0.002, P=0.9964). Additionally, we did not observe significant correlation was between BMIgap and chlorpromazine equivalents (*r*=-0.01; P=0.86) for patients diagnosed with SCZ.

2.3.3 HC-SCZ Classifier

In the MUC sample, the classification model achieved a balanced accuracy (BAC) of 72.4%, with a sensitivity of 72.2% and a specificity of 72.6%, demonstrating statistically significant performance (P<0.001) in distinguishing individuals with SCZ from HC individuals (Figure 8A). This classification model was specifically designed to identify brain regions uniquely associated with SCZ. Notably, significantly predictive voxels were localized in various brain regions, including the inferior, middle, and superior frontal gyrus, hippocampal, thalamic, insular, Rolandic operculum, postcentral, cerebellar, and basal ganglia structures (P<0.05). Moreover, on the right hemisphere, the lingual, fusiform gyrus, and mid-temporal lobe were also identified as significantly predictive of the diagnostic pattern (P<0.05), as illustrated in Figure 8B.

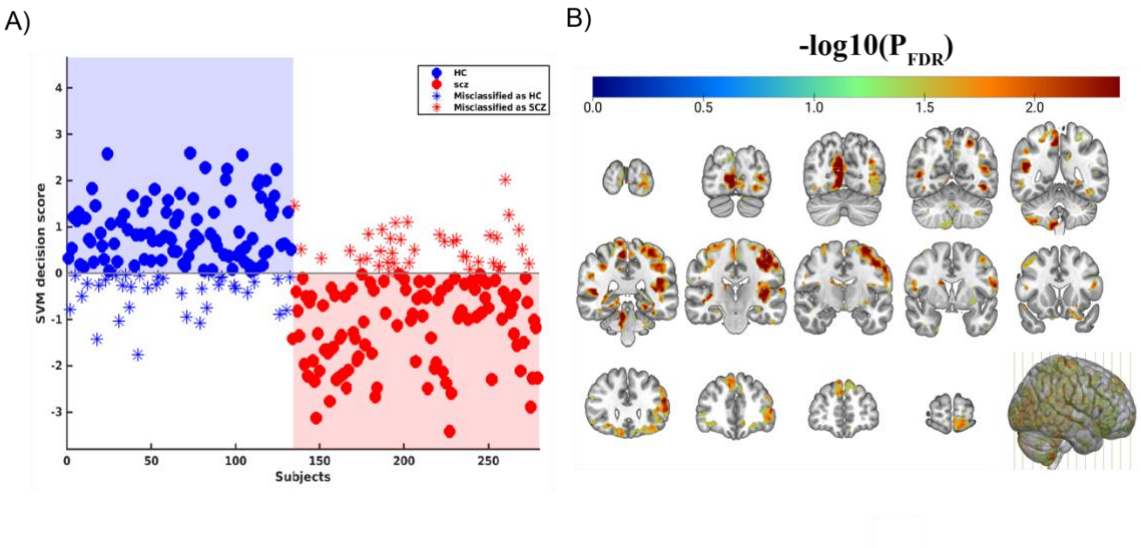

Figure 9. Model performance and visualization of classification model to classify patients with SCZ from HC individuals. A) Classification performance. B) The reliability of the predictive voxels visualized using FDR-corrected sign-based consistency map thresholded at α=0.05. Abbreviations: FDR= False discovery rate, HC= Healthy controls, SCZ= Schizophrenia

2.3.4 BMIgap, SCZ-expression and clinical dimension

The neuroanatomical features corresponding to both BMI-predictor and SCZ-classifier exhibited overlapping patterns in various brain areas, such as the inferior, middle, and superior frontal gyrus, caudate, putamen, Rolandic operculum, right precuneus, and middle temporal lobe regions as depicted in Figure 10.

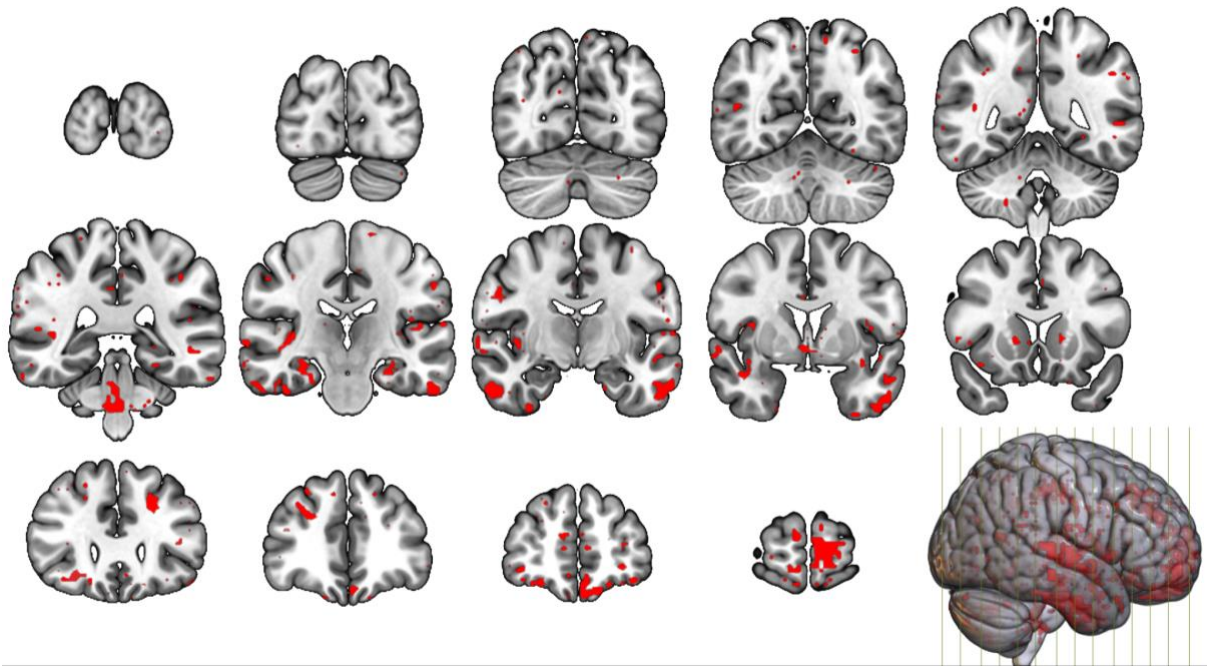

Figure 10. Overlapping brain regions between BMI-predictivity and SCZ-likelihood. Overlapping regions across schizophrenia and obesity obtained by binarizing and multiplying the sign-based consistency maps from the regression and classification models (α=0.05).

Within this defined neuroanatomical search space, SPLS analysis revealed five significant LVs, each representing distinct levels of association with clinical features of the disease, as illustrated in Figure 11 and Figure 12. Our analysis was primarily focused on investigating the correlations between clinical dimensions, BMIgap, and psychiatric disease expression within the SCZ-group. Given that the SCZ-group exhibited notably higher BMIgap values compared to other clinical groups, we considered it a reliable basis for our study.

In LV1 (r=0.87, P<0.001), lower BMIgap scores and higher SCZ expression-scores were related to decreased GMV in the ventral attention network and increased GMV in the default mode network (DMN) (auditory), somatomotor B, control (C and B), and central visual networks (Figure 12A).

In LV2 (r=0.84, P<0.001), higher BMIgap, SCZ expression-scores, age of onset, number of hospitalization and illness duration were related to decreased GMV more pronounced in the DMN specifically in the A, B and C subcomponents, visual, somatomotor A, attention, salience, limbic, and control networks and increased GMV in DMN (auditory) and somatomotor B networks, as illustrated in Figure 11A.

In LV3 (r=0.85, P<0.001), higher BMIgap and higher SCZ expression-scores were related to decreased GMV in the DMN B and increased GMV in the DMN D (auditory) (Figure 11B).

In LV4 (r=0.44, P=0.025), higher SCZ expression-scores, illness duration, age of onset, and number of hospitalizations and lower BMIgap and PANSS total scores were related to decreased

GMV in the limbic as well as control A and B , DMN A and B, somatomotor A and B, salience, dorsal and ventral attention, and peripheral visual networks and increased GMV in non-overlapping subcomponents DMN C and control C networks (Figure 12B).

In LV5 (r=0.58, P<0.001), we observed a signature independent of BMIgap. Lower PANSS total score, illness duration, and age of onset and higher SCZ expression-score were related to decreased GMV in DMN (C) and control (C) networks, and increased GMV in the DMN (A, B), somatomotor (B), dorsal attention (B), and salience networks (Figure 11C).

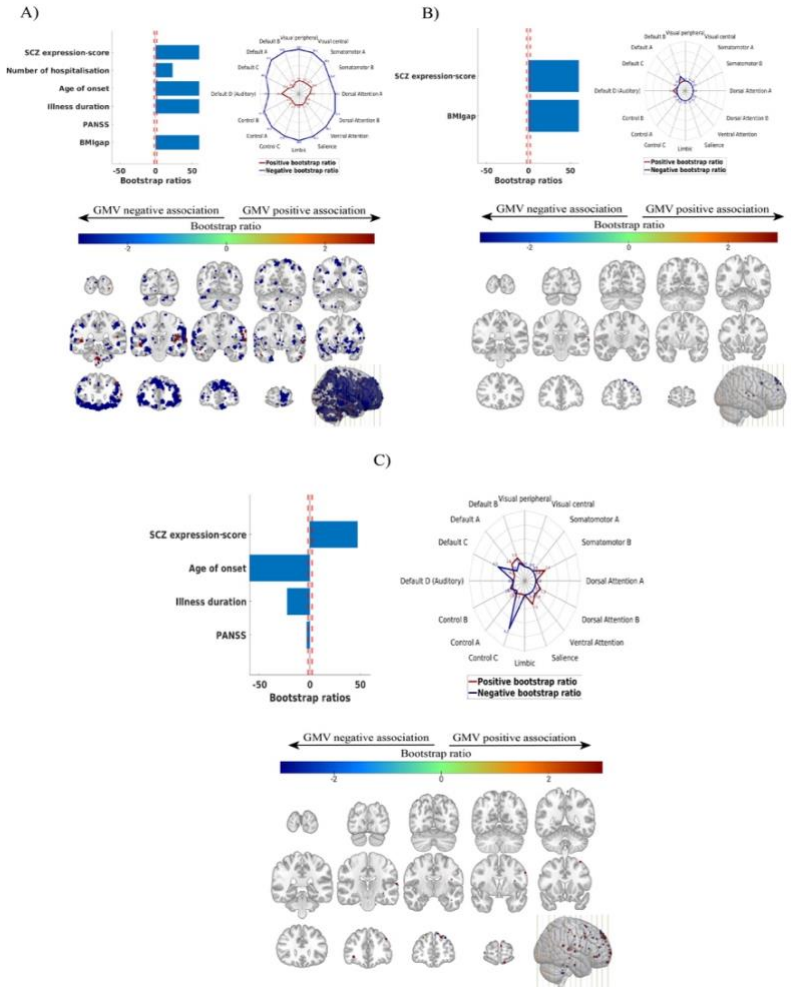

Figure 11. Signatures exhibiting a positive association between SCZ-expression score and BMIgap effects. A) LV2 and B) LV3 represent signatures showing positive association between SCZ-expression score and BMIgap. C) LV5 represents a BMIgap-independent signature of LV5. Bar plots visualize the correlation of each variable with the LV, blue identifies variables significantly contributing to the LV. The x-axis denotes BSR in the x-axis (interpretable as z-scores) and the y-axis denotes BMIgap, SCZ expression score and other clinical items. The red dotted line in the graph represents a BSR of 1.96 (equivalent to a 95% confidence interval). The contribution of individual voxels is shown using BSR in MNI space. Cool colors indicate voxels with a negative correlation of GMV and clinical items, whereas warm colors represent a positive correlation. The spider-plot illustrates the voxel contribution within the 17-network parcellation solution extracted using the Yeo-Buckner atlas (Thomas Yeo et al., 2011). The network names and the cerebral cortical regions that compose the 17 networks are from the supplementary video in Baker et al. (2014) (Baker et al., 2014). Abbreviations: BSR= bootstrap ratios, LV= Latent variable, SCZ= Schizophrenia, BMIgap= body mass index gap score, PANSS= Positive and Negative Symptom Scale total score

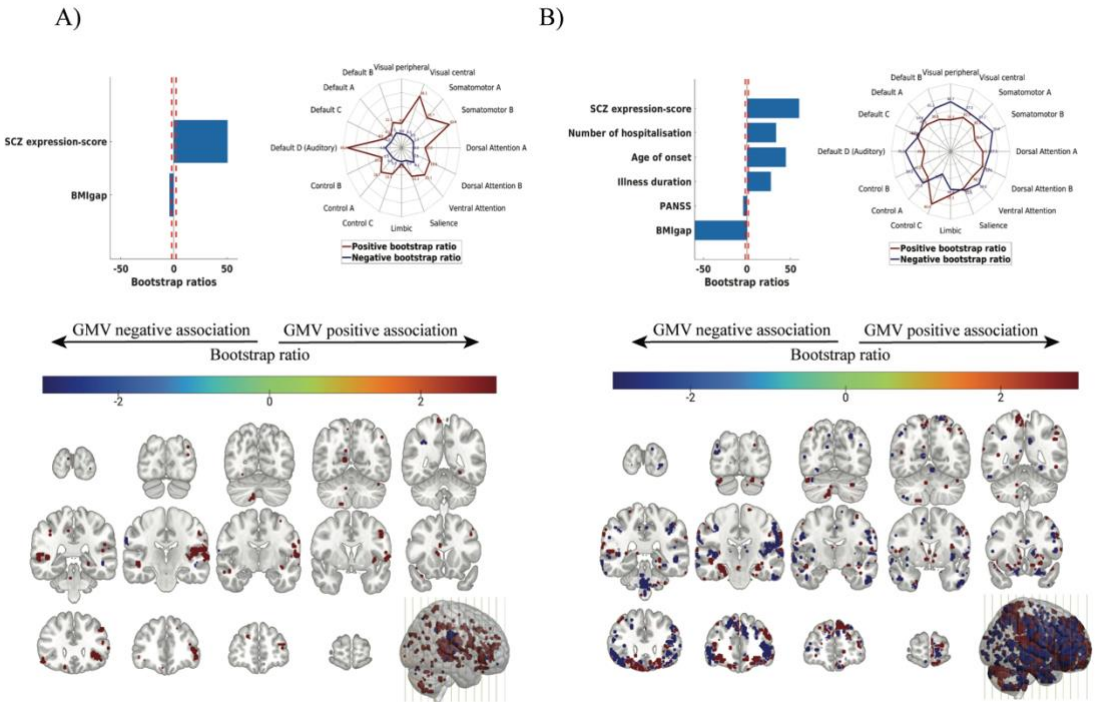

Figure 12. Signature exhibiting negative association between SCZ-expression score and BMIgap effects. SPLS analysis results for A) LV1 and B) LV4. Bar plots visualize the correlation of each variable with the LV, blue identifies variables significantly contributing to the LV. The x-axis denotes bootstrap ratios (BSR) (interpretable as z-scores) and the y-axis denotes BMIgap, SCZ expression-score and other clinical items. The red dotted line in the graph represents a BSR of 1.96 (equivalent to a 95% confidence interval). The contribution of individual voxels is shown using BSR in MNI space. Cool colors indicate voxels with a negative correlation of GMV and clinical items, whereas warm colors represent a positive correlation. The spider-plot illustrates the voxel contribution within the 17-network parcellation solu-tion extracted using the Yeo-Buckner atlas (Thomas Yeo et al., 2011). The network names and the cerebral cortical regions that compose the 17 networks are from the supplementary video in Baker et al. (2014) (Baker et al., 2014). Abbreviations: LV= Latent variable, SCZ= Schizophrenia, BMIgap= body mass index gap score, PANSS= Positive and Negative Symptom Scale total score

2.4 Discussion

In this study, we introduce 'BMIgap' as an innovative tool for assessing obesity-related brain changes in both psychiatric and non-psychiatric populations. We identified patterns of BMI-associated brain alterations and brain changes observed in psychiatric disorders. We observed an association between lower GMV in frontal and temporal regions and higher BMI, explaining a significant portion of BMI variation in individuals without psychiatric disorders. Next, individuals with SCZ and those at CHR exhibited positive BMIgap scores, whereas individuals with ROD demonstrated negative BMIgap scores compared to those without psychiatric disorders. Furthermore, we identified overlaps between the separability of SCZ individuals from HC individuals and structural brain variations associated with BMI, particularly in regions implicated in inhibitory control and reward processing. BMIgap scores accounted for 6.25% of the variance in SCZ expression scores. SPLS analysis revealed that the predominant patterns linking brain-based SCZ diagnostic separability and BMI predictiveness were associated with longer illness duration, later disease onset and a higher number of hospitalizations.

2.4.1 BMI predictive brain regions

Our findings provide further evidence supporting previous research findings showing associations between structural variations in the brain and obesity (S. R. McWhinney et al., 2022; Opel et al., 2017). The negative relationship observed between BMI and GMV within the reward and salience systems suggests a potential role in regulating eating behavior (Li et al., 2022). This negative association underscores the possibility that alterations in these brain regions may influence the way individuals respond to food cues and rewards, potentially contributing to overeating and weight gain. In our study, we noted reductions in GMV associated with BMI predictive regions of the brain implicated in taste perception, reward processing and inhibitory control among individuals without psychiatric disorders (HC individuals). These changes may contribute to the development of maladaptive eating patterns, thereby fostering obesity. Specifically, reductions in GMV in prefrontal regions have been associated with diminished inhibitory control, which might increase vulnerability towards consuming excessive calories. Additionally, our findings revealed negative associations between GMV and BMI in the occipital gyrus, a brain region crucial for processing visual and gustatory information related to food, consistent with previous investigations into obesity (Herrmann et al., 2019). These observed alterations in brain structure may arise from the physiological effects of obesity on the central nervous system thereby establishing a feedback loop between impaired cognitive control and obesity-related changes in the brain.

2.4.2 Obesity and SCZ

Our findings revealed notable reductions in prefrontal volume among individuals diagnosed with SCZ compared to HC individuals. This aligns with the previous findings that impaired inhibitory

control constitutes a fundamental aspect of SCZ. This impairment is evident in the challenges individuals face in suppressing automatic or dominant reactions to stimuli, as well as in deficits in cognitive control (Ursu et al., 2011; Yan et al., 2022). Furthermore, our analysis unveiled that significant brain patterns distinguishing SCZ mapped onto regions of the brain predictive of BMI such as areas associated with inhibitory control, reward processing and cognitive regulation (Tsai et al., 2020). This observation suggests potential interconnected pathways between obesity and SCZ, consistent with prior research. Prefrontal deficits, characterized by reduced cognitive drive and impaired inhibitory control, may exacerbate the susceptibility of individuals with SCZ to engage in addictive behaviors. This heightened risk could manifest in overeating behaviors, thereby contributing to elevated BMI levels within this population.

2.4.3 Conceptualizing BMIgap

The concept of BMIgap offers a means to quantify structural brain variations that are predictive of obesity. A positive BMIgap observed in patients with SCZ and those at CHR state suggests that their brain-estimated BMI exceeds their actual BMI, implying brain alterations akin to those typically associated with higher BMI levels. This intriguing finding hints the possibility that underlying pathophysiological mechanisms in psychiatric disorders may influence brain structure in a manner resembling the alterations observed in obese individuals. Furthermore, these interaction effects seem to be more pronounced in patients with SCZ as compared to those in CHR individuals, likely due to the more advanced disease stage in the former group, leading to a higher observed BMIgap. These results suggest that the co-occurrence of obesity and SCZ may lead to more substantial brain changes compared to individuals with only one of these conditions. Notably and conversely, ROD individuals exhibited a negative BMIgap score. This suggests that their brain alterations align more closely with those typically seen in individuals with lower BMI levels. This observation is supported by previous research demonstrating overlapping brain patterns between depressed individuals and those who are underweight, as well as elevated depression scores in patients with anorexia nervosa (Bohon & Welch, 2021). Future application of the BMI prediction model to patients with MDD and bipolar disorder holds promise for shedding further light on the potential pathophysiological processes underpinning BMI-related brain phenotypes.

2.4.4 Association between medications and BMIgap

Antipsychotics and antidepressants have been associated with the promotion of obesity, as documented in previous studies (Fava, 2000; Gill et al., 2020; Panariello et al., 2011). The mesolimbic dopaminergic system and the ventromedial nucleus play pivotal roles in modulating behavioral responses to environmental stimuli and regulating both intake of food and the body-weight homeostasis. These mechanisms contribute to weight-gain following the administration of antipsychotic medications (Panariello et al., 2011). While most antidepressants are known to induce weight gain, certain agents, such as fluoxetine and bupropion, may lead to weight loss as

well (Gill et al., 2020). Interestingly, our study did not uncover a correlation between BMIgap and antipsychotic dosage in patients with SCZ, as measured by chlorpromazine equivalents. It's worth noting that the chlorpromazine equivalency method offers only a rough estimate and does not capture the individual patient's pharmacodynamic and pharmacokinetic profiles across different antipsychotic compounds. Despite this, our analysis did not reveal significant differences when comparing BMIgap scores among fully naive, partly naive, and concurrently treated individuals with both antidepressants and antipsychotics, within the CHR and ROD samples implicating that medication effects may not fully account for the variability in BMIgap. Moving forward, it is imperative for future research to meticulously investigate the distinct, neurotransmitter-specific effects of antidepressants and antipsychotics on BMIgap, employing longitudinal study designs. This approach will allow for a deeper understanding of how these medications influence brain structure alterations related to obesity over time. Such insights could inform more tailored treatment strategies and interventions for individuals with psychiatric disorders, with a focus on mitigating the risk of obesity-related complications.

2.4.5 Association between BMIgap, SCZ expression-score and clinical variables

Our analysis identified four out of the five significant LVs that govern structural brain variations associated with both control and reward systems. These variations were found to be associated with the SCZ-expression score, BMIgap and clinical parameters in distinct ways: LV2 and LV3 exhibited positive associations between SCZ expression-scores and BMIgap, while LV1 and LV4 displayed only negative associations. Moreover, the positive clinical loadings were observed exclusively in LV2 and LV4, indicating specific connections between BMIgap, SCZ, and clinical features. The observed patterns characterized by high BMIgap-SCZ expression scores were associated with a decrease in GMV within networks such as the limbic network, coupled with increased GMV within networks like the DMN (specifically, the auditory network). These networks are known for their involvement in reward circuit, food motivation, executive and affective control, as evidenced by research on obesity (Avery et al., 2017; Dugré et al., 2019). Additionally, these networks have been implicated in SCZ research, particularly in impaired processing of negative emotions and have shown heightened network-specific functioning in these individuals (Jamea et al., 2021; Tamminga et al., 1992). Furthermore, positive loadings in clinical variables, indicating late disease onset, high hospitalization frequency and longer illness duration, were associated with both high BMIgap and SCZ-expression scores. This suggests a potential association between the severity of SCZ and the presence of obesity-related traits. Overall, these findings underscore a complex interplay between common neurobiological pathways and environmental factors contributing to both SCZ and obesity.

However, the two LVs exhibiting negative associations between BMIgap and SCZ expression scores may suggest the presence of distinct neurobiological pathways underlying SCZ and obesity. This divergence could arise from the considerable neurobiological heterogeneity often

observed in SCZ (Luckhoff et al., 2022). Certain subgroups, possibly characterized by depressive symptoms, might reduce the appetite, leading to lower BMI and diminished obesity-related brain changes, while still maintaining high diagnostic separability (Bohon & Welch, 2021). Furthermore, positive loadings in three out of four clinical variables may reflect a pronounced effect of SCZ on disease severity. Conversely the negative loadings in both BMIgap and PANSS total score may arise from specific symptom profiles strongly associated with higher BMI or metabolic dysregulation (S.-H. Lin et al., 2021). Lastly, we observed a pattern primarily reflecting the impact of SCZ on brain systems, which appeared distinct from BMI-related macroscopic brain variation. However, counterintuitively, this pattern exhibited negative loadings for clinical items associated with high SCZ diagnostic separability. This finding could suggest a divergent clinical course, where individuals with an earlier onset, shorter duration of illness, and milder symptoms may be less prone to showing elevated SCZ diagnostic scores. This nuanced correlation highlights the intricate nature of SCZ subtypes and indicates possible variations in how the disorder manifests and progresses. In summary, these findings indicate the presence of both common and differing pathways contributing to the shared alterations in brain structure related to both SCZ and BMI. This opens up opportunities for investigating the characterization of potential psychiatric subtypes and uncovering the precise neurobiological pathways underlying each condition.

2.4.6 Limitations

The study has many limitations that warrant consideration. First, our study lacked adequate representation of individuals with extreme BMI values (BMI >35 or <18.5) due to sample size limitations. This gap in representation highlights the need for future research utilizing our BMIgap model to investigate neural mechanisms in both underweight and highly obese individuals. However, conducting such research may be challenging, particularly in the case of underweight individuals, given the increasing prevalence of conditions like anorexia nervosa. Secondly, our study lacked data on essential metabolic markers such as lipid profile, fasting glucose levels, and HOMA-IR (Homeostatic Model Assessment of Insulin Resistance). These markers are crucial for understanding potential shared pathophysiological mechanisms that influence both brain structure and clinical correlations between obesity and psychiatric disorders. Despite this limitation, the use of BMI, a widely employed metric in similar studies, allowed us to make initial and direct comparisons with previous research findings. In essence, while our study provides valuable insights, there are areas for improvement and further exploration (Herrmann et al., 2019; S. R. McWhinney et al., 2022). Future research endeavors should aim to address these limitations by including a more diverse range of BMI values by incorporating additional metabolic markers to deepen our understanding of the complex interplay between obesity and psychiatric disorders at both neurobiological and clinical levels.

2.4.7 Conclusion

This study provides further evidence supporting the widespread associations between BMI and GMV. Consistent with previous research, we identified overlapping brain regions that are predictive of both BMI and SCZ, suggesting that individuals affected by both obesity and SCZ may exhibit more pronounced brain alterations compared to those with either condition alone. Our BMIgap model emerges as a promising tool for disentangling the personalized risk of neurostructural changes associated with obesity and psychiatric disorders. Moreover, it is imperative for future investigations to explore whether these observed brain alterations serve as modifiable risk factors in psychiatric disorders and whether the obesitogenic effects of antipsychotic medications contribute to their associations with alterations in brain structure. Longitudinal neuroimaging studies, incorporating datasets with metabolic markers and spanning from at-risk to relapsing disease stages, are essential. Such studies will enable us to evaluate the prognostic and monitoring potential of BMIgap for obesity-related comorbidities in mental disorders. This holistic approach will offer valuable insights into the complex interplay between obesity, psychiatric disorders and brain structure, ultimately informing more effective interventions and treatments for individuals with these conditions.

3. Brain-age estimation in multisite studies

Parts of the content of this chapter has been published as: Adyasha Khuntia, Madalina-Octavia Buciuman, John Fanning, et al. **Towards collaborative data science in mental health research: The ECNP NeuroImaging Network Accessible Data Repository. Neuroscience Applied, 2025, 4, 105407; https://doi.org/10.1016/j.nsa.2024.105407.** The content of this chapter has been paraphrased, and the tables and figures presented herein have been adapted from the aforementioned paper.

3.1 Brain-ageing in common psychiatric disorders

Psychotic and affective disorders commonly exhibit clinical and brain changes that correlate with age (Ballester et al., 2022). As patients with SCZ age, they typically experience improvements in positive functioning but may also encounter a decline in cognitive functionality (Folsom et al., 2006). Additionally, the frequency of depressive episodes tends to rise significantly, increasing by 90% after the onset of the third episode as these patients age (Burcusa & Iacono, 2007). These observations have motivated the scholars of this millennium to focus on brain-ageing research targeting disease-specific brain signatures and their underlying biological processes. It has been fourteen years since Franke et al. (2010) first conceptualized BrainAGE as a metric to capture ageing associated brain deviations at individual level (Franke et al., 2010). The BrainAGE concept, also known by alternative terms such as brain age score (Beheshti et al., 2018), brain-predicted age difference (brainPAD) (Cole & Franke, 2017) or brain age delta (Smith et al., 2019), has been extensively researched and utilized in the field of psychiatry. The initial framework outlined by Franke et al. (2010) included measuring the brain-based age estimates, by first building a feature matrix constituting of brain derived measures of psychiatrically healthy individuals. The brain derived features are given as input to a multivariate ML algorithm such as a regression to predict chronological age for each individual. The difference between the predicted age by the ML model and the chronological age is then calculated. This model is further applied to different psychiatric groups to estimate the respective brain-age and assess their deviation from the norm. Over the years, this framework, although still efficient and widely used, has also evolved by incorporating different methodological strategies such as neuronal networks (Hahn et al., 2022) by using the brain-derived features to build a deep-learning model that predicting the chronological age. Although VBM8 extracted whole brain GMV images were initially used as input features, the concept has been extended to use other brain measures derived from other imaging modalities such as the diffusion-weighted magnetic resonance imaging, rs-fMRI data, as well as inclusion of data-fusion methods to combine different modalities. Moreover, it is no longer limited to assess only the GMV alterations rather other brain derivatives such as WMV, cortical thickness has also been studies extensively. Importantly, extension of the BrainAGE analysis to include longitudinal datasets as well, has been extensively done. Moreover, it is crucial to validate brain-age models to separate, unseen healthy sample. This step is essential for mitigating

generalizability bias. A systematic framework to derive BrainAGE is depicted in Figure 13. Regardless of the specific methodology used, BrainAGE has been widely applied to assess age-related abnormalities across psychiatric disorders.

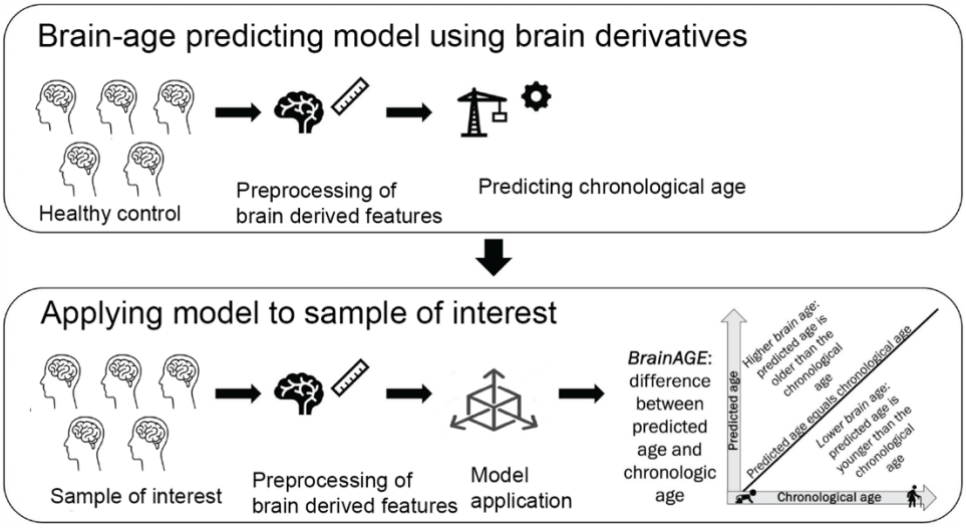

Figure 13. Schematic depiction of a standard framework to estimate BrainAGE (adapted from (Seitz-Holland et al., 2024))

3.1.1 BrainAGE in SCZ

A prevailing hypothesis posits SCZ as a syndrome of accelerated ageing (Kirkpatrick et al., 2008). If substantiated, accelerated and potentially pathological brain atrophy should be identifiable early, preceding the onset of clinical symptoms. In this context, comparing brain atrophy to that of normal brains becomes pertinent, with the straightforward and efficient approach being the application of a BrainAGE model trained on HC individuals to estimate deviations in these patient groups. BrainAGE analysis has emerged as a valuable tool for investigating structural brain alterations in SCZ. Studies employing BrainAGE in SCZ have unveiled accelerated brain-ageing trajectories in affected individuals, characterized by significant deviations from expected brain-ageing patterns. These deviations often present as widespread reductions in GMV and alterations in white matter integrity, indicating a complex interplay between disease pathology and age-related changes in brain structure.

Patients having psychotic disorders have repeatedly displayed a significantly higher BrainAGE score as compared to HC individuals. The first ever study to apply the brain age prediction method to estimate BrainAGE scores in patients with SCZ was conducted by Koutsouleris et al. (2014) by using SCZ participants ranging between 18 and 60 years and they showed that patients displayed a positive BrainAGE score with respect to HC individuals (Koutsouleris et al., 2014). More recent application of this concept to patients belonging to SCZ spectrum such as schizophreniform, schizoaffective or psychotic disorder have shown that BrainAGE can reach

upto 7.8 years (Shahab et al., 2019) (Shahab et al. (2019)). Kaufmann et al. (2019) conducted a comprehensive investigation on brain-ageing in patients with SCZ (Kaufmann et al., 2019). They trained an XGBoost model by using brain thickness, area, and volume features derived from structural MRI data as input features from a training cohort of 35,474 individuals, while building separate models trained for each gender. This analysis revealed a significant BrainAGE with a Cohen's d effect size of 0.51. Additionally, age prediction models trained using features from specific brain regions such as cerebellar or subcortical regions showed no increased in BrainAGE, but a substantial effect in the frontal lobe. These findings imply that neuroanatomical characteristics related to brain-ageing vary throughout the brain, suggesting that each region may have its own distinct ageing pattern and rate. BrainAGE discrepancies have also been observed in longitudinal studies. Schnack et al. (2016) conducted a longitudinal analysis with repeated measures, demonstrating a strong association between the onset of SCZ and the acceleration of brain-ageing (Schnack et al., 2016). The rate of brain-ageing reached its peak immediately following the onset of SCZ, after which the acceleration rate diminished, becoming non-significant after approximately five years and eventually normalizing to one year per year. More recent studies utilizing advanced machine-learning and deep-learning methods have also shown similar BrainAGE trends in SCZ group. Utilizing more advanced ML techniques such as transfer learning, Chen et al. (2020) illustrated that employing pre-trained models from diverse databases or data types alongside brain-age prediction models using diffusion MRI data revealed comparable differences in BrainAGE between patients with SCZ and HC individuals. Furthermore, analysis using structural covariance networks also demonstrated similar BrainAGE scores of +5.52 years for SCZ patients (Kuo et al., 2020). Lastly, by employing deep neural networks, Bashyam et al. (2020) build a deep brain network using MRI scans from 11,729 individuals yielding distinct BrainAGE differences between SCZ and HC, contingent upon the degree of model fit to the data (Bashyam et al., 2020). Although the deep learning models exhibited greater robustness with lower MAE, they also yielded lower BrainAGE scores (~3 years) for the SCZ group.

Only a limited studies have focused on exploring the phenomenon of accelerated brain-ageing in patients experiencing their first psychotic episode and CHR individuals. Notably, Hajek et al. (2019) conducted a study that demonstrated significant differences in BrainAGE between medication-naïve individuals with their first-episode schizophrenia-spectrum disorders and HC individuals (Hajek et al., 2019). The findings from this study revealed that the group experiencing their first psychotic episode displayed a BrainAGE deviation of 2.65 years compared to the HC group. Furthermore, studies have investigated the BrainAGE deviations for CHR individuals as well. The CHR individuals in the NAPLS 2 study, exhibited a higher BrainAGE score for the CHR group as compared to the HC individuals. However, this outcome was associated with the age of onset of psychosis. Although, the CHR individuals who developed psychosis between the age of 12 and 17 showed an overestimation of brain-age, the CHR individuals whose age of disease onset was between 18 and 21 did not show similar overestimation (Chung et al., 2018).

BrainAGE and clinical characteristics in SCZ

Recently studies have aimed to elucidate the relationship between brain age and psychopathology (Demro et al., 2022). Their findings indicated that advanced brain-ageing was associated with lowering of cognitive performance as well as reduced general functioning. Notably, the cognitive performance and schizotypal symptoms of the patient relatives correlated with BrainAGE, suggesting that advanced brain-ageing process may be associated with subtle manifestations related to psychosis (Demro et al., 2022). Interestingly, the large cohort ENIGMA study did not observe any statistically significant connections between BrainAGE and various clinical parameters such as age-of-onset, illness duration, severity of symptoms as measured by PANSS total and SAPS global scores, severity of negative symptoms as measured by SANS global score, antipsychotic medication usage as well as CPZ-equivalent dosage. Furthermore, they did not observe significant effects when comparing typical versus atypical medication groups, or when comparing both typical and atypical medication groups versus atypical medication groups alone, Kaufman et al. (2019) investigated the association between BrainAGE and various clinically relevant variables in patients with SCZ, revealing a link between higher BrainAGE and poorer functioning (Kaufmann et al., 2019). Specifically, elevated BrainAGE levels were correlated with lower levels of functioning, as indicated by a negative correlation between BrainAGE and Global assessment of functioning (GAF) symptom and function scores. Furthermore, BrainAGE demonstrated positive correlations with more severe negative symptoms of SCZ, as assessed by PANSS negative scores. Among the studies investigating brain-ageing in first-episode psychosis individuals, there is consistent evidence indicating that accelerated brain-ageing occurs very early in the illness-course. Furthermore, in CHR individuals, greater brain-age deviation has been associated to an increased risk of transitioning to psychosis and exhibiting a pattern of persistently poor functioning over time. However, this association seems to be particularly pronounced among younger CHR adolescents (Chung et al., 2018).

3.1.2 BrainAGE in depression

Research findings regarding brain-ageing in individuals with depression remain inconclusive. Some studies have identified a positive BrainAGE deviation score compared to HC individuals, albeit to a lesser extent than observed in individuals with SCZ (Christman et al., 2020; L. K. M. Han et al., 2021). Conversely, other studies report no significant differences between individuals with depression and HCs in terms of BrainAGE deviation (Bashyam et al., 2020; Kuo et al., 2020). One of the first studies showing accelerated brain-ageing in patients with MDD was by Koutsouleris et al. (2014) (Koutsouleris et al., 2014). The ENIGMA study comprising the largest sample size with 2675 participants to study BrainAGE showed significant BrainAGE differences between the MDD and the HC individuals and BrainAGE of 0.86 years (L. K. M. Han et al., 2021). Subsequently, another study by Besteher et al. (2019) reported no significant differences between the BrainAGE scores between the MDD and HC groups, yet the MDD group exhibited a BrainAGE of +0.41 years, albeit with a limited sample size (Besteher et al., 2019). Kaufman et al. (2019)

investigated the BrainAGE patterns in a larger sample size and showed no significant BrainAGE differences compared to the HC individual group, albeit exhibiting 0.86 years of BrainAGE for the patient group (Kaufmann et al., 2019). Similarly, other researchers have reported no significant differences as well (Bashyam et al., 2020; Christman et al., 2020). Structural covariance networks approach by incorporating the relationship among specific brain regions to predict brain age exhibited a considerable BrainAGE of +1.99 years between MDD and HC groups, although it did not reach statistical significance (Kuo et al., 2020). Similarly, Dunlop et al. (2021) utilized resting-state functional MRI data to predict brain-age. Despite reporting a high MAE in their final model, they observed a substantial BrainAGE standard deviation of 12.65 in the MDD group (Dunlop et al., 2021).

BrainAGE and clinical characteristics of depression

The range of negative events and consequences, including environmental adversities, early onset of depression during adolescence and impairment in functioning, have been associated to an increase in BrainAGE. Moreover, investigating the distinct impacts of each indicator, while considering the presence of others, requires examination in larger study populations. Deviation from chronological age may reflect general health status rather than being specific to any particular exposure or outcome (Drobinin et al., 2022).

In the extensive ENIGMA study, notable BrainAGE differences were observed between individuals with remitted depression, those currently experiencing depression, individuals using antidepressant medication during scanning, medication-free depressed patients, patients with late adult-onset depression, mid-adulthood onset depression, early-onset depression, first-episode depression, and recurrent depression compared to controls. However, there were no significant associations found between depression severity or current depressive symptoms, as measured by self-reported Beck depression inventory-II (BDI-II) or clinical-based Hamilton depression rating scale (HDRS-17) questionnaires, at the time of scanning within the MDD sample.

3.1.3 GMV association with age

Studies investigating age-related changes in the brain have revealed that GMV tends to increase during late childhood followed by a gradual decline (Franke & Gaser, 2019; Koutsouleris et al., 2014). Initial research by Good et al., 2001 indicated a global GMV atrophy which was directly correlated with increase in age (Good et al., 2001; Terribilli et al., 2011). Furthermore, they observed that the accelerated GMV loss was localized in regions such as the insula, central sulci, superior parietal gyri and cingulate sulci, while brain regions including the amygdala, hippocampi and entorhinal cortex did not show significant brain changes with ageing, indicating relative preservation (Good et al., 2001). Subsequent studies by other researchers further corroborated that age specific GMV loss primarily localized in brain areas such as frontal and parietal regions as compared to other regions such as temporal and occipital lobes (Resnick et al., 2003).

Moreover, longitudinal investigations provided valuable insights into the rate and distribution of age-related brain alterations. These studies have revealed that healthy individuals who remained free from pathological conditions and sustained both physical and cognitive well-being exhibited slower rates of brain atrophy compared to those with pathological conditions (Resnick et al., 2003). Furthermore, the findings of ageing-related reductions in frontal volume associated during adulthood may be implicated by late-stage brain maturation processes (Resnick et al., 2003). These alterations involve increase in synaptic pruning and myelination, both of which are associated with a noticeable decrease in GMV (Sowell et al., 2004). The divergent patterns of age- and region-specific gray matter alterations observed in non-elderly adults may be attributed to differential timing in the maturational processes of myelination and synaptic pruning within the brain (Terribilli et al., 2011). Furthermore, in Kaufman et al. (2019) BrainAGE analysis using large datasets with 35,474 individuals, a substantial effect was observed specifically in the frontal lobe. This indicates that the neuroanatomical changes associated with brain-ageing are not uniformly distributed throughout the brain (Kaufmann et al., 2019). Instead, it suggests that each brain region may exhibit its own unique pattern and rate of ageing.

3.1.4 BrainAGE in regions-of-interst (ROI) studies

Using voxelized whole brain images as feature inputs is a common practice in BrainAGE studies, often referred to as data-driven strategies. However, this approach has several drawbacks, particularly regarding its application in clinical settings. Firstly, the processing of MRI images is pipeline dependent which might take a lot of processing time and computational infrastructure. Secondly, the method of extracting a single predictive-value from the whole brain or total GMV images can be considered as black-box. Thirdly, there has been evidences that the brain-ageing process is restricted to specific regions of the brain and doesn't occur in the entire brain. These challenges motivated the researchers to develop methods to calculate individualized BrainAGE in a simpler, faster and computationally effective way while not losing any crucial neurobiological information. Measurement of the regional brain volume has been established and accepted specifically to understand cognitive functioning in brain. While the reduction in image-processing time may not be guaranteed with the implementation of ROI maps, there is a definitive decrease in the computational power and time while developing the models. Particularly, it has been demonstrated that newer ML and DL approaches necessitate extensive datasets and significant computational resources to construct models such as neural networks, resources that are often constrained to clinicians.

Previously, Baecker et al. (2021) conducted a comparative study to evaluate the predictive abilities of ML models utilizing region-based and VBM data (Baecker et al., 2021). They used brain data from 10,824 HC individuals from the UK Biobank and demonstrated that model performance was affected by the choice of data modality. They found that VBM data, coupled with dimensionality reduction methods, proved to be more robust compared to the low-dimensional ROI data, despite using the same model algorithm. The lowest MAE using ROI data

was 4.06 years (Baecker et al., 2021). Another previous study showed no differences in the MAE values while using different brain derivatives such as volume, cortical-thickness and ROI, rather the MAE improved after combining all the features improved the MAE value (Gutierrez Becker et al., 2018). Another study while utilizing cortical thickness measures only showed a MAE of 4.05 years (Aycheh et al., 2018).

Furthermore, the multi-site study consortium ENIGMA has successfully conducted BrainAGE analysis by using ROI data in various psychiatric groups. The findings revealed a significant elevation in BrainAGE by +3.55 years in SCZ patients compared to HC individuals after adjusting for age, age^2, sex and scanning site. Moreover, in separate study but using same image processing pipeline brain regions, the consortium found that MDD group exhibited a BrainAGE score +1.08 years higher than HC individuals after adjusted for age, age^2, sex and scanning site (Constantinides et al., 2023).

3.1.5 BrainAGE and obesity

There are consistent associations between BrainAGE and obesity, and overweight and obesity have been identified as risk factors for accelerated brain-ageing, as observed in neurodegenerative disorders (Xu et al., 2015). Studies have found that among psychiatrically healthy individuals, the obese individuals exhibit a higher BrainAGE as compared to individuals with normal weight (Ronan et al., 2016; Zeighami et al., 2022). Similar findings have been observed amongst psychiatric groups as well (S. McWhinney et al., 2021). Notably, Kolenic et al. (2018) showed that participants experiencing first-episode psychosis who are obese or overweight displayed the highest BrainAGE scores, while those individuals who had normal weight exhibited the comparatively lower BrainAGE scores (Kolenic et al., 2018). Furthermore, in the same study, they did not find association between BrainAGE and LDL, HDL or triglyceride levels as well as usage of psychotropic medication or other clinical items such as hypertension (Kolenic et al., 2018). Another longitudinal analysis assessing the brain changes with respect to both obesity and ageing in first-episode psychosis individuals revealed that although, first-episode psychosis individuals showed higher brain-ageing as compared to HC individuals, however the annual rate of brain-ageing was similar for both groups. In both cohorts, a higher baseline BMI was associated with accelerated brain-ageing. Specifically, for every additional BMI point, the brain-aged by an extra month per year (S. R. McWhinney et al., 2022). Moreover, it was revealed that individuals who underwent weight loss due to bariatric surgery experienced a reduction in age-related brain abnormalities measured by the BrainAGE score, amounting to approximately a 2.5 year decrease (Zeighami et al., 2022). This improvement in brain-age related changes was accompanied by widespread enhancements in cardiometabolic factors as well. This suggests that obesity plays a significant role to understand the relationship between brain-ageing in individuals having psychotic episodes. Moreover, it suggests a potential linkage between brain alterations associated with both ageing and obesity in psychiatric patients, highlighting the need for further exploration.

3.1.6 Normative modelling framework

Normative modeling is a relatively new approach emerged during the mid 2010s specifically aimed to capture individual level differences in a clinical population with respect to a reference population model derived from a larger population. In psychiatry the traditional categorizing individuals into the so called ‘healthy control’ and ‘clinical’ groups assumes no heterogeneity within these groups. The normative modelling framework addresses this inherent heterogeneity commonly occurring within these groups by focusing on individual variations rather than simple group comparisons, thus providing a more nuanced understanding of psychiatric conditions. Various statistical approaches have been suggested for normative modeling, such as regression, support vector machines, and Gaussian process modeling (Marquand et al., 2019).

We will use the framework to build the BrainAGE model using ROI data. We will utilize data from large cohort studies to understand the normative distribution within the healthy population. Next, we will generate probabilistic assessments regarding participants who deviate from this normative pattern in a separate HC group and patient population. Henceforth, we will statistically identify the brain regions associated with these deviations.

3.1.7 Aims of this study

The primary aim of this study is to understand brain-ageing as a comorbidity in HC individuals as well as in psychiatric cohorts. While brain-ageing has been extensively researched during the past decade and an accelerated brain-ageing has been a consistent finding specifically in SCZ patients, there still exists limitation relating to model replicability as well as less studies using ROI specifically in large cohort studies albeit the choice of using ROI maps being computationally more efficient as well as more realistic in clinical set-up. We assessed BrainAGE predictions in two analysis setups: 1) using GMV ROIs extracted from 1170 HC individuals within the recently established large and multi-site European College of Neuropsychopharmacology Neuroimaging Network Accessible Data Repository (ECNP-NNADR) consortium, 2) using the whole brain GMV voxels of the 770 HC individuals utilized in the discovery sample for constructing the BMI-predicting model. Subsequently, we plan to evaluate the predictive capabilities of the models using independent samples of HC individuals and various psychiatric groups, including SCZ, CHR, ROD and MDD. Our aim is to derive the utility of the BMIgap tool developed in the previous chapter to address the association between brain-age and obesity, as well as to understand the influence of obesity on brain-ageing, particularly in patients with SCZ. We intend to correlate individualized BrainAGE and BMIgap scores across both HC and clinical groups, as well as BrainAGE score and SCZ-expression scores. Finally, we aim to investigate the associations between BMIgap, BrainAGE scores, SCZ expression scores and various clinical variables using SPLS analysis, particularly for patients with SCZ.

Our first hypothesis is that the BrainAGE model developed using ROI data should perform better than the model using whole-brain voxelized data. Additionally, we expect that all patient groups

will show accelerated ageing effects. Furthermore, we hypothesize that the frontal regions associated with cognitive control will be commonly implicated in the contexts of obesity, brain-age and SCZ expression. Lastly, we anticipate obtaining differential brain-clinical signatures showing distinct levels of association, specifically showing patterns of comorbidity.

3.2 Methods

3.2.1 BrainAGE model using GMV-ROI data

Sample characteristics

To date, seven European sites representing six different countries participate in the ECNP-NNADR project: The Ludwig-Maximilian University Hospital in Munich, Bavaria, Germany; NORMENT Centre, Division of Mental Health and Addiction, Oslo University, Oslo, Norway; Bellvitge Biomedical Research Institute-IDIBELL, Universitat de Barcelona, Barcelona, Spain; University of Edinburgh, Edinburgh, Scotland; Università degli Studi di Milano, Milan, Italy; University of Turku, Turku, Finland; Università degli Studi di Verona, Verona, Italy. Across the participating sites, patients were included if they had complete demographic information including age, sex, diagnosis, and at least one complete score set in one of the clinical scales or MRI data. All included studies were approved by their respective local ethics committees. In total the repository consists of clinical and MRI data from 21 cohorts across the seven sites, resulting in a total sample size of 4,829 participants, including HC individuals and eleven distinct psychiatric conditions showcasing. Details about the MRI parameters for each site is detailed in Table 7.

Table 7. Magnetic resonance imagining acquisition parameters

Site	Subcohort	Scanner	Field strength	TR (ms)	TE (ms)	Flip angle	Voxel size (mm)	FOV	Slice num.
Munich	LMU Munich cohort	Siemens Magnetom	1.5T	11.6	4.9	NA	0.45 x 0.45 x 1.5	512 x 512	126
Barcelona	BARCENONA_PIE	Philips Ingenia	3T	10.46	4.79	8	0.75 x 0.75 x 0.75	320 x 320	233
Barcelona	BARCENONA_TEC	Philips Achieva	3T	8.2	3.7	8	0.94 x 0.94 x 1.0	256 x 256	160
Barcelona	BARCENONA_ANTICS	GE Signa Excite	1.5T	11.8	4.2	15	1.17 x 1.17 x 1.2	256 x 256	130
Barcelona	BARCENONA_PROV SIMPT	GE Signa Excite	1.5T	11.8	4.2	15	1.17 x 1.17 x 1.2	256 x 256	130
Barcelona	BARCENONA_FAM OCD	GE Signa Excite	1.5T	11.8	4.2	15	1.17 x 1.17 x 1.2	256 x 256	130
Barcelona	BARCENONA_HOARDING	GE Signa Excite	1.5T	11.8	4.2	15	1.17 x 1.17 x 1.2	256 x 256	130
Barcelona	BARCENONA_EXTPOR	Siemens Verio	3T	2100	2.67	9	1.0 x 1.0 x 1.0	256 x 256	176
Barcelona	BARCENONA_FISAX	Philips Ingenia	3T	10.68	4.96	8	0.75 x 0.75 x 0.75	320 x 320	220
Barcelona	BARCENONA_COMPULSE	Philips Ingenia	3T	10.68	4.96	8	0.75 x 0.75 x 0.75	320 x 320	220
Barcelona	BARCENONA_RESP_CBT	Philips Ingenia	3T	10.68	4.96	8	0.75 x 0.75 x 0.75	320 x 320	220
Edinburgh	GS-Imaging Aberdeen Subset	Philips Achieva	3T	1968	3.8	8	1.0 x 1.0 x 1.0	240 x 240	160
Edinburgh	GS-Imaging Dundee Subset	Siemens Prisma-FIT	3T	1740	2.62	8	1.0 x 1.0 x 1.0	256 x 256	208
Turku	TEPS1	Philips Ingenia	3T	8.1	3.7	7	1.0 x 1.0 x 1.0	256 x 256	176
Turku	TEPS2	Philips Ingenia	3T	8.1	3.7	7	1.0 x 1.0 x 1.0	256 x 256	176
Milan	15	Philips Achieva	1.5T	7.2	3.3	8	1.00 x 0.93 x 0.93	240 x 240	162
Milan	30_1	Philips Achieva	3T	9.8	4.6	8	1.00 x 0.94 x 0.94	NA	185
Milan	30_2	Philips Achieva	3T	7.06	3.4	8	1.09 x 1.04 x 1.04	NA	165
Milan	30_3	Philips Achieva	3T	NA	NA	8	1.0 x 1.0 x 1.0	NA	160
Verona	FIRST&PICOS	Siemens Allegra	1.5T	2060	3.93	15	0.46 x 0.46 x 1.25	NA	144
Verona	PREVENT & CARIVR &	Siemens Magnetom	3T	2300	3.93	12	1.0 x 1.0 x 1.0	NA	160
Oslo	top15	Siemens Magnetom	1.5T	2730	3.93	7	1.33 x 0.94 x 1.0	240 x 240	160

Note. TR – repetition time, TE – echo time, FOV – field of view.

MRI data processing

The MRI image processing was harmonized across sites, such that the T1-weighted structural images were processed using the morphometric analysis pipeline implemented in CAT12 (version 12.8, optimized for multi-site deployment; https://neuro-jena.github.io/enigma-cat12/). MATLAB-based scripts and instruction files were developed at LMU and were designed to cater to the needs of all participating sites, offering both standalone versions that do not require a MATLAB license or standard versions. By distributing these resources to all sites, we aimed to streamline and facilitate the harmonization process of MRI image processing, thereby contributing to the reliability and comparability of our neuroimaging analyses. The pipeline produced GMV and WMV measures for a set of ROIs parcellated according to the Schaefer-200 (GMV and WMV), AAL3 (GMV) and Hammers (GMV and WMV) atlases (Hammers et al., 2003; Rolls et al., 2020; Schaefer et al., 2018). ROIs were utilized instead of voxel-level data due to size constraints within the data sharing platform of ViPAR, which currently limits the entry of large matrices.

ROI based brain-age prediction model

For the BrainAGE analysis, we developed a multivariate age-predicting model, based on GMV ROIs extracted using three atlases from HC individuals. This age-prediction model was then applied separately to an independent HC sample and to patients with SCZ, and the study participants' BrainAGE scores were computed as the difference between the person's predicted age and observed chronological age.

Sample selection

In accordance with the normative framework, our initial aim was to select a large sample representative of all age ranges. We selected 1170 HC individuals from the total pool of 2357 HC individuals. This selection process involved dividing the total sample into 12 age bins and sampling individuals from each bin. By meticulously conducting this selection process, we aimed to ensure a balanced representation of individuals across various age groups. This approach facilitated the creation of a normative age model capable of capturing variability across different age ranges. As a result, we mitigated the risk of underrepresentation of age extremes, which could have otherwise skewed the normative sample. Figure 14 illustrates the age distributions of HC individuals both before and after the selection process for the normative sample. We will refer to this selected HC individuals as the 'HC normative' sample. The remaining 1161 HC individuals were retained as an independent dataset for model validation, which we refer to as the 'HC left-out' sample. The final HC normative model was then applied to both the HC left-out individuals 503 patients with SCZ and 591 patients with MDD to evaluate clinical effects on brain-ageing.

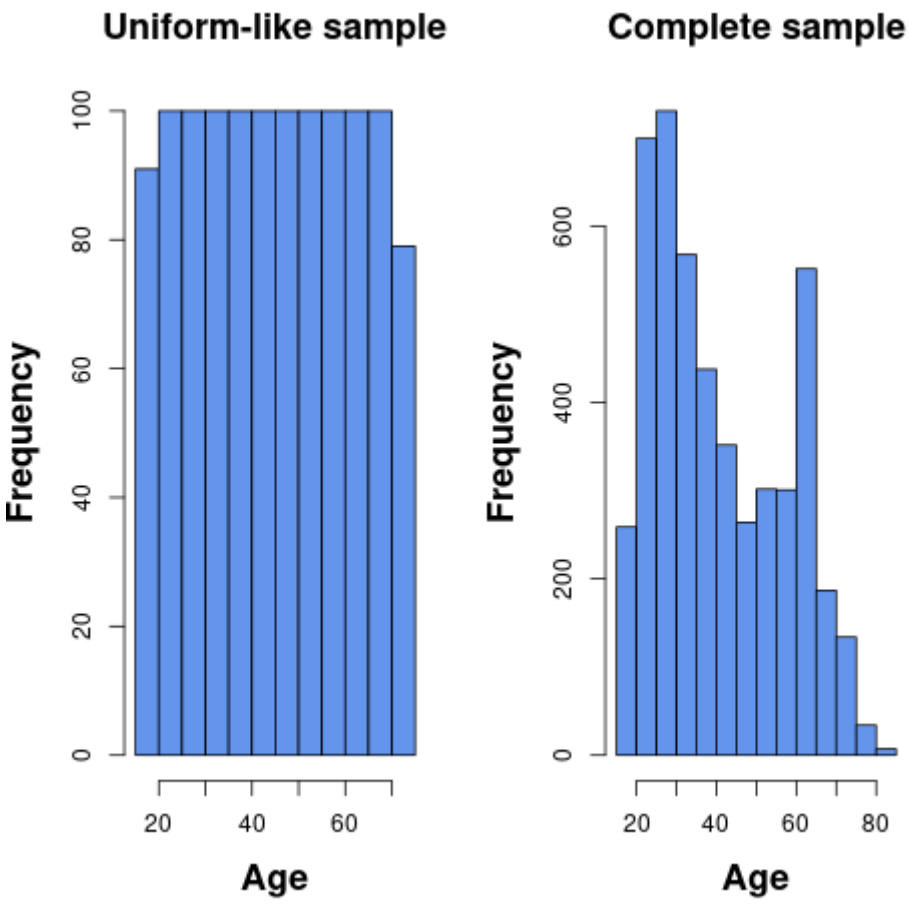

Figure 14. Sample of HC individuals included in the regression analysis. Histogram of the age distribution for the sample showing the full-range and uniform-like distribution of HC individuals.

ML analysis

At first, all GMV ROIs underwent an initial correction for total intracranial volume by dividing the value of each ROI by the total intracranial volume. The input features in the brain-age analysis were GMV ROI values from AAL3, Hammers, and Schaefer atlases. Additionally, each analysis was repeated with the data from individual atlases separately. All analyses were conducted using MATLAB (R2022a) and R software (v4.1) within the ViPAR environment. The classification and regression ML analyses were conducted using the open-source ML in R toolbox (mlr, v4.1) (15).

The R scripts used for all the proof-of-concept analyses are freely available in our GitHub repository (https://github.com/adyasha95/ECNP-NNADRrepo/).

ML pipeline

Following a methodology similar to previous ML analyses, all ML models were developed within a nested repeated CV framework. This framework consisted of 5 folds in both the inner CV1 and outer CV2 cycles, with 5 permutations applied to each cycle. In this approach, CV1 is employed

for hyperparameter tuning, where a set of hyperparameters is selected for each CV2 cycle. Subsequently, the model is trained on each outer training set using the optimal hyperparameters, and its effectiveness is assessed on the outer test sets. This comprehensive approach was adopted to prevent information leakage between train and test data and enhance the generalizability of the models (Parvandeh et al., 2020).

The data preprocessing included feature scaling between –1 and 1 and a global mean offset correction to mitigate site-effects present in the MRI ROI data (14). The site-correction method for global-mean offset correction follows the same conceptual framework as the method used in the BMIgap model. The code has been translated into R and integrated as a wrapper within the MLR package. Concretely, we used the HC individuals to estimate site-specific means, to avoid the removal of clinically relevant effects. Then, we computed differences between the site means and the overall mean for each feature and finally subtracted these mean differences from the entire data of each respective site (HC individuals and SCZ patients), in order to mean-center the data to the overall mean of the training data. All preprocessing steps were embedded within the nested cross-validation framework. A L2-Regularized L1-Loss Support Vector Regression algorithm (LiblineaRL2L1SVR) available in the mlr R package was used as the prediction algorithm. We evaluated the accuracy of the model's predictions using several metrics, including MAE, *r* and R^2, calculated between individual chronological age and predicted age. MAE was selected as the optimization criterion, consistent with previous regression analyses.

Post-hoc analysis

Initially, the predicted age values were corrected for their chronological age, addressing the overestimation at lower age ranges and underestimation at higher age ranges using linear regression analysis, as a common practice in BrainAGE research (Zhang et al., 2023). Similar to the approach used in the BMIgap model, beta-coefficients were computed through partial correlation analysis utilizing the HC normative sample. Subsequently, these coefficients were applied to the HC left-out and SCZ samples to derive corrected predicted-age values. Furthermore, the individualized BrainAGE scores were calculated by subtracting the chronological age from the corrected predicted age for both HC and SCZ individuals.

Post-hoc two-sample t-tests assessed group differences between the BrainAGE scores of HC normative and left-out individuals as well as normative HC and SCZ individuals at α=.05.

3.2.2 BrainAGE model using voxelized GMV data

To essentially show whether brain-obesity derivates and brain-ageing derivates are associated or not, we built a brain-age predictor by using similar model parameters as used in the BMIgap model as described in *Chapter 2: Quantification of obesity related brain changes by using ML as a tool* specifically elaborated in the section *2.2.2 ML analysis.* Furthermore, we used the same HC individuals as the discovery sample in the brain-age model as used in the BMIgap model for reliable comparison between BrainAGE and BMIgap scores.

ML analysis

Whole brain GMV maps belonging to the HC individuals in the discovery sample of the BMIgap model were used as features to predict brain-estimated age. To summarize the pre-processing procedure, Gaussian smoothing with kernel widths of 0, 3, 6 and 9 mm FWHM was initially applied. Following this, the removal of BMI effects was carried out using partial correlation analysis. The step ensured that prediction model is free from BMI effects. Next, global-mean offset correction was employed to remove site-specific effects. Subsequently, PCA was conducted to decrease the dimensionality of the image space at energy levels of 0.25, 0.50 and 0.75. Finally, voxel-wise scaling between 0 and 1 was implemented. Similar to the BMIgap-predictor, a used a linear kernel type nu-SVM regression algorithm was employed for modeling, with a regularization parameter set to 1. These pre-processing steps were executed using a repeating nested CV cycle with 5 folds for both inner and outer cycles with 5 permutations each. Additionally, a GMV specific brain mask was employed, ensuring that only relevant voxels within GMV regions were retained. Ultimately, we generated visual representations of the predictive voxels by employing the sign-based consistency metric.

Post-hoc analysis

The predicted age was adjusted to account for the common occurrence of both overestimation and underestimation of age at the extremes, a standard practice in BrainAGE studies, as implemented in the BMIgap model and BrainAGE model using GMV ROIs as described in *3.2.1 BrainAGE in the ECNP-NNADR sample*. The BrainAGE score for the discovery group was calculated by taking the difference between the predicted age from the chronological age. Next, the brain-age predictor was applied to the replication HC individuals, patients with SCZ and CHR individuals and their BrainAGE scores were calculated respectively. Group-level comparisons of the calculated BrainAGE scores between the discovery HC individuals and the patient groups were conducted using a two-sample *t*-test.

Correlation analysis

We conducted partial correlation analyses to investigate whether there was a correlation between the BrainAGE scores and the BMIgap scores of both the HC individuals and the clinical groups as well as correlation between BrainAGE scores and SCZ-expression scores.

Overlapping brain regions

We created a brain-mask to identify brain regions that are associated with ageing, obesity and SCZ-separability. For this purpose, following the previous approach, we initially binarized the FDR-corrected consistency maps based on sign from the brain-age predictor. This involved retaining only the statistically significant voxels ($P<0.05$) identified during the visualization of the brain-age prediction model. Subsequently, we overlapped this binarized map with the brain mask previously established to contain the overlapping predictive voxels from the BMIgap model and SCZ-classification models. This combined mask comprises the predictive voxels relevant to brain-

age, obesity, and SCZ diagnostic separability. The associations between GMV, BrainAGE, BMIgap, SCZ-expression score and clinical variables including age of disease onset, PANSS total score, number of hospitalizations and illness duration were examined by using this specific mask as a neuroanatomical search-space.

3.3 Results

3.3.1 BrainAGE model using GMV-ROI data

Below, we present the performance metrics for models utilizing GMV ROIs pooled across all atlases as features. Tables 8-11 provide detailed performances of models using GMV ROIs from individual atlases and when combined from all atlases.

The brain-age model predicted age with a MAE of 7.16 years (R^2 = 0.77, P<0.001) and a mean (SD) BrainAGE of ~0 (8.90) in the HC-normative group (Figure 15). Upon application of this model to the left-out HC individuals, the MAE was 6.97 years (R^2 = 0.74, P<0.001) with a negligible deviation in the BrainAGE [mean (SD) = 0.12(8.89)]. Subsequently, application of this model to patients diagnosed with SCZ yielded a MAE of 7.79 (R^2 = 0.79, P<0.001) and a BrainAGE score of 4.49 (8.90) and application to the MDD group produced the least MAE while using the data extracted using Hammers atlas with a MAE of 8.44 years (R^2 = 0.79, P<0.001) and a BrainAGE score of 1.26 years (10.43). Notably, we did not observe significant differences between the BrainAGE scores of normative and left-out HC samples [t(df) = -0.35(2329), P=0.73]. BrainAGE scores differed between HC and SCZ individuals, with the SCZ group exhibiting higher BrainAGE compared to HC normative (t(df) = -9.46(1671), P<0.001) and the left-out HC samples (t(df) = -9.19(1662), P<0.001). Furthermore, we observed varying results for the MDD group, with the BrainAGE score differing significantly between the HC-normative and MDD groups in the model using data extracted with Schaefer's atlas (t(df) = -2.66 (1759), P<0.01). Compared to the left-out HC sample, the MDD group exhibited significant BrainAGE differences for both Schaefer's (t(df) = -2.46 (1759), P=0.01) and Hammers' atlases (t(df) = -2.89 (1750), P<0.01). For detailed overview of the model performance based on individual atlas data, please refer to Table 8 and Figure 15. Additionally, for post-hoc comparisons between BrainAGE scores of HC normative, HC left-out and patient groups samples, please refer to Table 9-13.

Table 8. Model performances of the brain-age model using GMV ROIs in HC and SCZ samples.

	R^2	MAE	r	BrainAGE (mean ± SD)
HC normative				
All Atlases	0.77	7.16	0.88***	1.0907e-14 (8.90)
Schaefers	0.78	7.10	0.90***	6.6803e-15 (8.78)
AAL3	0.78	6.98	0.88***	6.0487e-15 (8.65)
Hammers	0.79	6.95	0.89***	7.6277e-15 (8.62)
HC left-out				
All Atlases	0.74	6.97	0.86***	0.12 (8.89)
Schaefers	0.74	7.02	0.86***	0.09 (8.81)
AAL3	0.78	6.35	0.89***	-0.11 (8.09)
Hammers	0.78	6.45	0.88***	-0.28 (8.27)
SCZ				
All Atlases	0.79	7.79	0.78***	4.49 (8.90)
Schaefers	0.62	8.10	0.79***	3.85 (9.13)
AAL3	0.67	7.10	0.82***	3.72 (8.39)
Hammers	0.64	7.85	0.80***	4.11 (9.05)
MDD				
All Atlases	0.55	10.11	0.74***	0.67 (12.54)
Schaefers	0.63	8.44	0.79***	1.26 (10.43)
AAL3	0.59	9.27	0.77***	0.87 (11.27)
Hammers	0.65	8.63	0.80***	1.05 (10.55)

Note. r = Correlation coefficient measured by Pearson correlation, MAE = Mean absolute Error, R^2 = Coefficient of determination, BrainAGE = Brain age estimation, SD = Standard deviation, HC = Healthy controls, SCZ = Schizophrenia, ***P≤0.001

Table 9. Post-hoc comparison of BrainAGE scores in HC individuals

	BrainAGE HC normative (mean, SD)	BrainAGE HC left-out (mean, SD)	T	P
All Atlases	1.0907e-14 (8.90)	0.12 (8.89)	-0.3512	0.73
Schaefers	6.6803e-15 (8.78)	0.09 (8.81)	-0.2472	0.80
AAL3	6.0487e-15 (8.65)	-0.11 (8.09)	0.32	0.75
Hammers	7.6277e-15 (8.62)	-0.28 (8.27)	0.79	0.43

Note. BrainAGE = Brain Age Estimation, SD = Standard deviation, HC = Healthy control, T = t-statistics assessed by two-sample *t*-test.

Table 10. Post-hoc comparison of brain-age deviation scores between HC-normative individuals and SCZ patients.

	BrainAGE HC normative (mean, SD)	BrainAGE SCZ (mean, SD)	T	P
All Atlases	1.0907e-14 (8.90)	4.49 (8.90)	-8.82	9.8890e-21
Schaefers	6.6803e-15 (8.78)	3.85 (9.13)	-8.12	8.8699e-16
AAL3	6.0487e-15 (8.65)	3.72 (8.39)	-8.14	7.4632e-16
Hammers	7.6277e-15 (8.62)	4.11 (9.05)	-8.82	2.9091e-18

Note. BrainAGE = Brain Age Estimation, SD = Standard Deviation, HC = Healthy Controls, SCZ = Schizophrenia patients, T = t-statistics assessed by two-sample *t*-test, P = P value.

Table 11. Post-hoc comparison of brain-age deviation scores between left-out HC individuals and patients with SCZ.

	BrainAGE HC left-out (mean, SD)	**BrainAGE SCZ (mean, SD)**	**T**	***P*-value**
All Atlases	0.12 (8.89)	4.49 (8.90)	-9.19	1.1310e-19
Schaefers	0.09 (8.81)	3.85 (9.13)	-7.90	5.0313e-15
AAL3	-0.11 (8.09)	3.72 (8.39)	-8.78	4.0264e-18
Hammers	-0.28 (8.27)	4.11 (9.05)	-9.66	1.6296e-21

Note. BrainAGE = Brain age estimation, SD = Standard deviation, HC = Healthy controls, SCZ = Schizophrenia, T = t-statistics assessed by two-sample *t*-test.

Table 12. Post-hoc comparison of brain-age deviation scores between HC normative individuals and patients with MDD.

	BrainAGE HC normative (mean, SD)	**BrainAGE MDD (mean, SD)**	**T**	***P*-value**
All Atlases	1.0907e-14 (8.90)	0.67 (12.54)	-1.29	0.20
Schaefers	6.6803e-15 (8.78)	1.26 (10.43)	-2.66	0.007
AAL3	6.0487e-15 (8.65)	0.87 (11.27)	-1.80	0.07
Hammers	7.6277e-15 (8.62)	1.05 (10.55)	-2.25	0.02

Note. BrainAGE = Brain age estimation, SD = Standard Deviation, HC = Healthy controls, MDD = Major depressive disorder, T = t-statistics assessed by two-sample *t*-test.

Table 13. Post-hoc comparison of brain-age deviation scores between left-out HC individuals and patients with MDD.

	BrainAGE HC left-out (mean, SD)	BrainAGE MDD (mean, SD)	T	*P*-value
All Atlases	0.12 (8.89)	0.67 (12.54)	-1.03	0.30
Schaefers	0.09 (8.81)	1.26 (10.43)	-2.46	0.01
AAL3	-0.11 (8.09)	0.87 (11.27)	-2.09	0.03
Hammers	-0.28 (8.27)	1.05 (10.55)	-2.89	0.0039

Note. BrainAGE = Brain age estimation, SD = Standard deviation, HC = Healthy controls, MDD = Major depressive disorder, T = t-statistics assessed by two-sample *t*-test.

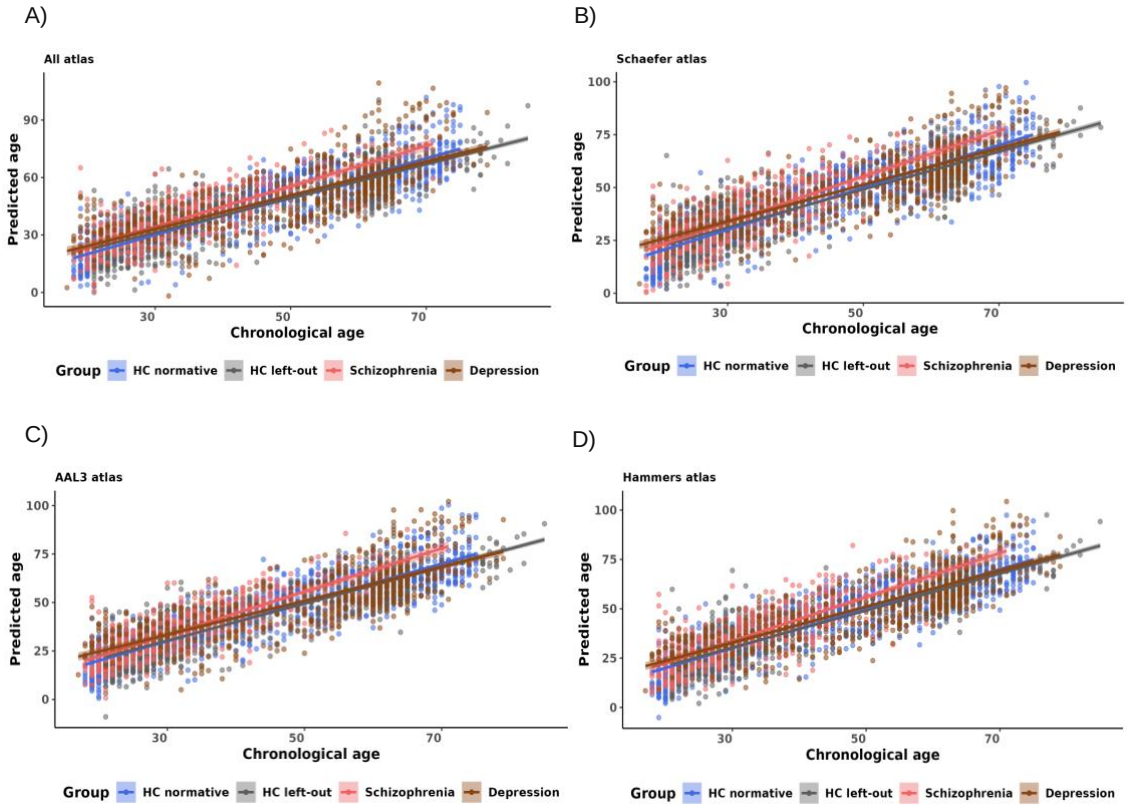

Figure 15. Results of the brain-age prediction model based on ROI GMV maps. Chronological age v/s predicted age with a linear curve fit; the regression line with 95% confidence interval for the HC individuals in blue and the SZ group in red for the model using GMV ROI values from A) all atlases pooled B) Schaefers, C) AAL3 and D) Hammers atlases.

3.3.2 BrainAGE model using voxelised GMV images

Brain-age predictions within BMIgap model datasets

The brain-age model using the discovery sample and similar model parameters as used for the BMIgap model predicted age with a MAE of 4.73 years and a mean (SD) BrainAGE of ~0 years in the discovery HC sample. The R^2 between the true and predicted age was 0.86, P<0.001. This model during application to the replication HC sample, generalized with a MAE of 4.79 years and the R^2 between true and predicted age was 0.82, P<0.001. Figure 16A depicts the correlation between true and predicted age for the discovery and replication groups. The brain-age prediction model applied to the clinical groups predicted BMI with an MAE of 9.67 years, R^2 = 0.80 for the SCZ patients, MAE of 4.67 and R^2 = 0.57 for CHR individuals and MAE of 4.01 years, R^2 = 0.57 in the ROD populations significantly (P<0.001). The Figure 16B depicts the correlation between true and predicted BMI scores in the psychiatric groups.

The mean BrainAGE scores for the HC replication group were 0.49 (6.05) years, showing no statistically significant difference from the BrainAGE score of the discovery group, indicating robust model generalizability. Moreover, the BrainAGE deviation for patients with SCZ was +9.49 (5.06) years, +1.31 (5.72) for CHR individuals and +0.27 (5.10) for ROD individuals. A significant difference in BrainAGE scores was observed between the SCZ group and the discovery HC sample (t = 2.80, P<0.01), as well as between the CHR group and the discovery HC sample (t = 2.80, P<0.01). However, there was no significant difference in BrainAGE between the discovery HC and ROD individuals. Further details of the brain-age analysis are presented in Table 12 and Table 13.

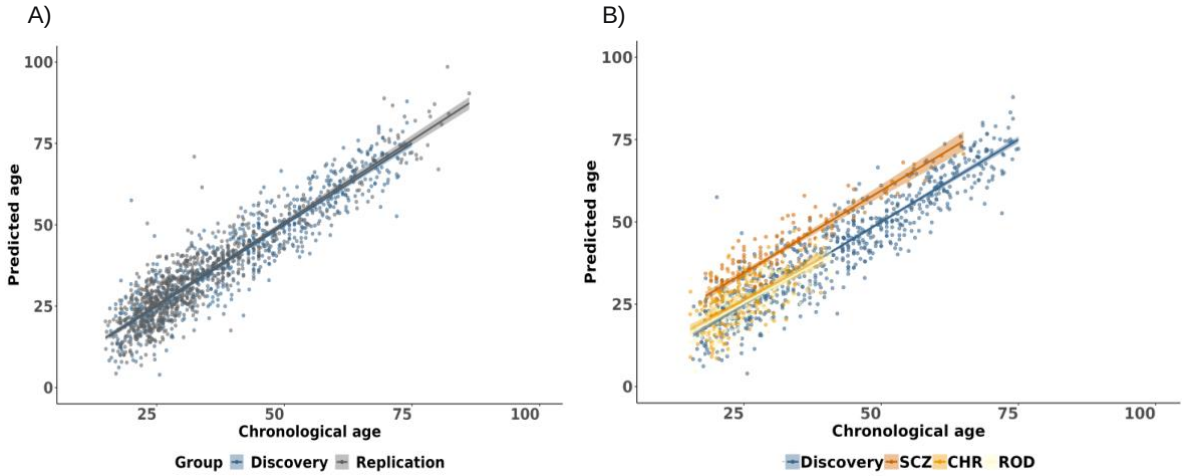

Figure 16. Regression model to estimate brain-based BMI. A) Chronological age v/s predicted age with a linear curve fit; the regression line with 95% confidence interval (CI) for the discovery group in blue and the replication group in black. B) Chronological age v/s predicted age with a linear curve fit; the regression line with 95% CI for the discovery group in blue, the SCZ patients in dark orange, CHR individuals in light orange and ROD individuals in yellow.

Table 14. Model performances of the brain-age model using whole brain images in HC and clinical samples.

	N	BrainAGE	MAE	R^2	*r*
PRONIA+IXI+ NORMENT+ MUC (discovery)	770	-2.9852e-15 (6.14)	4.73	0.86	0.93
PRONIA+IXI+ NORMENT+ MUC (replication)	734	0.49 (6.05)	4.79	0.82	0.91
SCZ	146	9.4984 (5.06)	9.6666	0.80	0.89***
CHR	213	1.31 (5.72)	4.67	0.57	0.64***
ROD	200	0.27 (5.10)	4.01	0.57	0.75***

Note. The mean BMIgap has been reported with the standard deviation in brackets for the uncorrected BMIgap and the corrected BMIgap after regressing out the effects of body mass index. N= total number of participants, r= correlation coefficient measured by Pearson correlation, MAE= mean absolute error, R^2= coefficient of determination, SCZ= Schizophrenia, CHR= Clinical high-risk, ROD= Recent-onset depression. Significant P values are stated as: *P≤0.05, **P≤0.01, ***P≤0.001

Table 15. Post-hoc comparison of brain-age deviation scores between replication HC individuals, clinical groups from discovery HC sample.

	N	BrainAGE	t-test
PRONIA+IXI+ NORMENT+ MUC (replication)	734	0.49 (6.05)	1.57
SCZ	146	9.4984 (5.06)	2.80 **
CHR	213	1.31 (5.72)	2.80**
ROD	200	0.27 (5.10)	0.58

Note. The mean BMIgap has been reported with the standard deviation in brackets for the uncorrected BMIgap and the corrected BMIgap after regressing out the effects of body mass index. N= total number of participants, *r*= correlation coefficient measured by Pearson correlation, MAE= mean absolute error, R^2= coefficient of determination, SCZ= Schizophrenia, CHR= Clinical high-risk, ROD= Recent-onset depression. Significant P values are stated as: *P≤0.05, **P≤0.01, ***P≤0.001

Model visualization of the most predictive brain-regions

The visualization of the most predictive voxels for brain-ageing revealed that the brain-voxels are significant (P<0.05) across the frontal, temporal and parietal regions specifically, in brain regions such as the caudate, right hemispheric mid frontal lobe, parahippocampal gyrus, inferior parietal lobe and medial temporal lobe. Additionally, significant voxels were identified in the left hemispheric cerebellum, inferior temporal lobe and superior parietal lobe. The visualization of the brain-age predictive voxels can be seen in Figure 16.

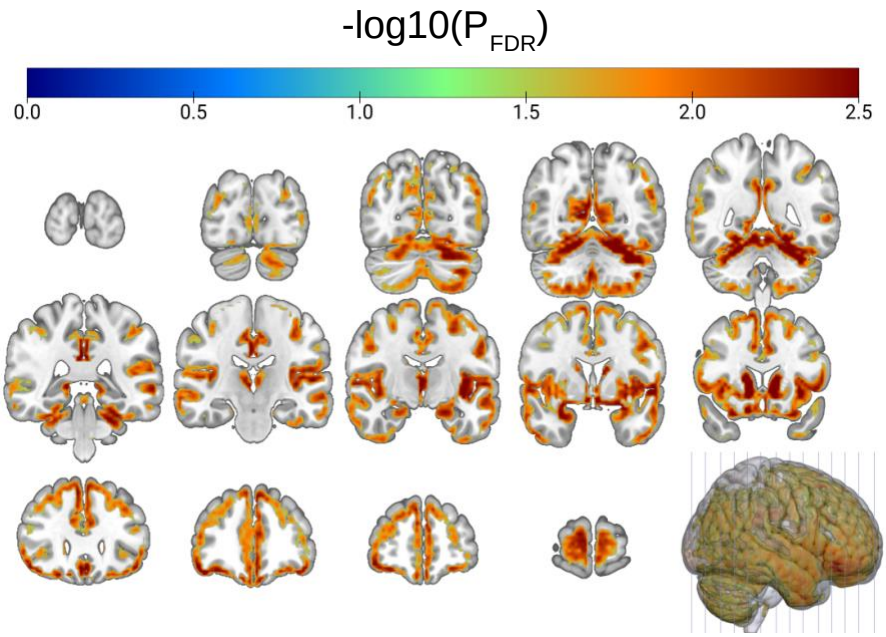

Figure 17. Brain-age predictive voxels. The reliability of the predictive voxels visualized using FDR-corrected sign-based consistency map thresholded at α=0.05. Abbreviations: FDR= False discovery rate

Correlation between BMIgap and BrainAGE scores

The correlation analysis revealed significant relationships between groups. In the discovery group, there was a moderate positive correlation (r = 0.29, P<0.001). The replication group showed a stronger positive correlation (r = 0.38, P<0.001). Moreover, within the clinical groups, the patients with SCZ showed the highest correlation was the highest (r = 0.49, P<0.001). The CHR individuals also demonstrated a high positive correlation (r = 0.48, P<0.001). Lastly, the ROD group exhibited a substantial positive correlation as well (r = 0.45, P<0.001). Moreover, the SCZ-expression correlated with r = 0.55, P<0.001 for the patients of MUC SCZ. Detail results of the correlation analysis has been outlined in Table 14. Furthermore, the correlation between the BrainAGE and BMIgap together for HC and patient group showed a (r = 0.39, P<0.001).

Furthermore, the visualization of the most predictive voxels overlapping across the brainage and BMI-predictor revealed significant regions (P<0.05) in multiple areas of the brain specifically in frontal and parietal brain regions such as the precentral gyri, cerebellum, parahippocampal gyri, left hemispheric hippocampus, anterior cingulate, right hemispheric temporal and inferior frontal gyri regions (Figure 18).

Table 16. Correlation between BMIgap and BrainAGE scores

	N	BMIgap	BrainAGE	*r*
PRONIA+IXI+ NORMENT+ MUC (discovery)	770	0 (1.78)	-2.9852e-15 (6.14)	0.29 ***
PRONIA+IXI+ NORMENT+ MUC (replication)	734	0.23 (1.68)	0.49 (6.05)	0.38***
SCZ	146	1.05 (1.53)	9.4984 (5.06)	0.49***
CHR	213	0.51 (1.68)	1.31 (5.72)	0.48***
ROD	200	-0.82 (1.64)	0.27 (5.10)	0.45***

Note. The mean BMIgap and BrainAGE have been reported with the standard deviation in brackets. N= total number of participants, *r*= correlation coefficient measured by Pearson correlation, R^2= coefficient of determination, SCZ= Schizophrenia, CHR= Clinical high-risk, ROD= Recent-onset depression. Significant P values are stated as: *P≤0.05, **P≤0.01, ***P≤0.001

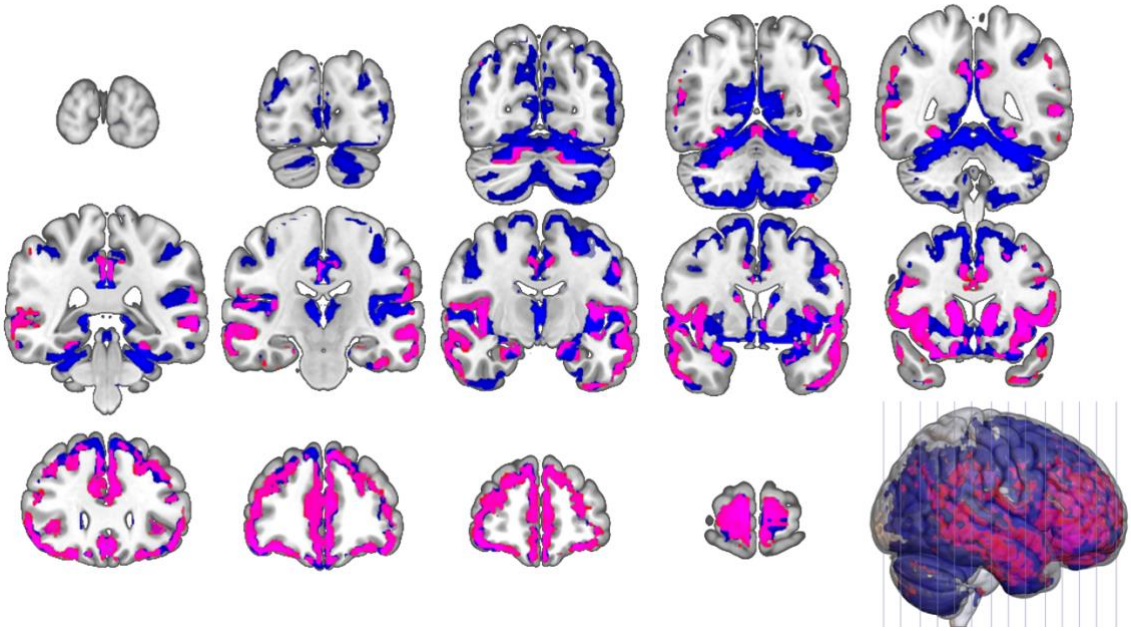

Figure 18. Overlapping brain regions between voxels predictive of brain-age and obesity are depicted in pink and non-overlapping voxels are in blue. Overlapping regions across **brain-age** and obesity obtained by binarizing and multiplying the sign-based consistency maps from the regression models (α=0.05).

Overlapping patterns between brain-age-predictor, BMI-predictor and SCZ-classifier

The visualization of the most predictive voxels for brain-ageing revealed significant regions (P<0.05) in multiple areas of the brain. Specifically, significant voxels were localized in the temporal regions, including the left hemispheric superior temporal lobe, middle temporal lobe and right hemispheric middle temporal lobe. In the frontal regions, significant voxels were found in the OFC, frontal superior medial region and left hemispheric medial OFC. Additionally, significant voxels were identified in the precentral region, cerebellum, and cingulum, specifically the left hemispheric posterior cingulum and right hemispheric anterior cingulum as well as other regions such as the Rolandic Operculum, parahippocampal regions, precuneus and left hemispheric inferior parietal lobe.

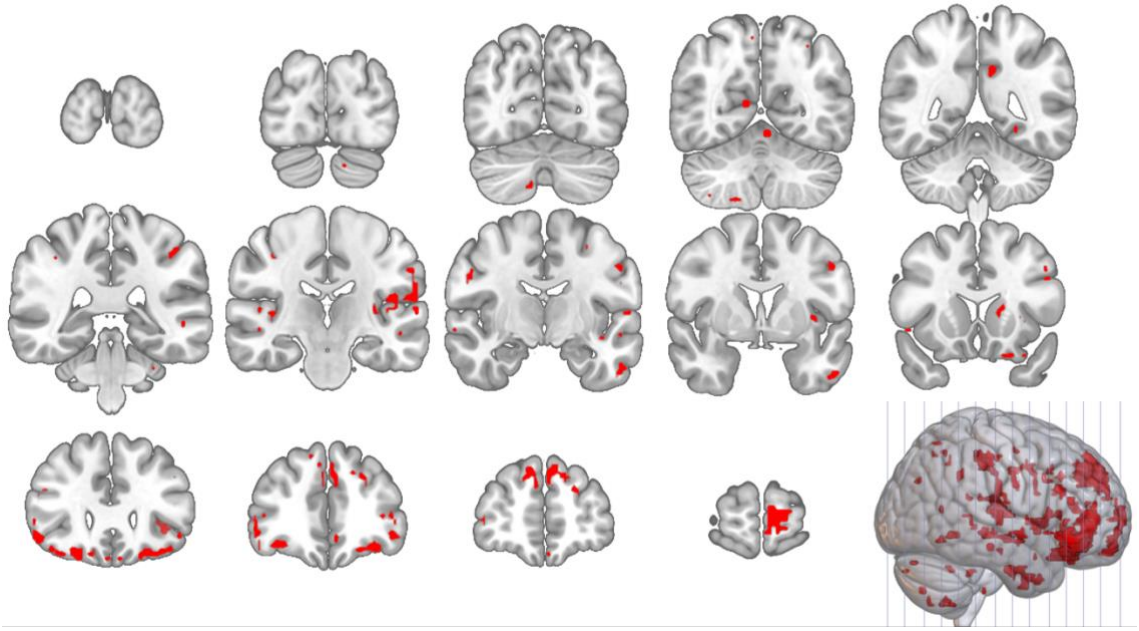

Figure 19. Overlapping brain regions between brain-age, obesity and SCZ-expression. Overlapping regions across schizophrenia**,** brain-age and obesity obtained by binarizing and multiplying the sign-based consistency maps from the regression and classification models (α=0.05).

3.3.3 Association between BrainAGE, BMIgap, SCZ-expression score and clinical variables

Within the defined neuroanatomical search space defined by the overlapping brain regions predictive of obesity, brain-ageing, SCZ expression and clinical variables, the findings from the SPLS analysis revealed five relevant LVs, showing distinct levels of association between the items, as illustrated in Figure 20-22.

Comorbid signature of brain-ageing and obesity: LV1 (r=0.88, P<0.001). Lower SCZ expression-score and higher BMIgap, BrainAGE and PANSS total scores and lower BMIgap scores were related to predominant decreased GMV particularly in the somatomotor, salience, DMN attention and control networks (Figure 20A).

SCZ defining signature: In LV2 (r=0.63, P<0.001), higher BrainAGE, SCZ expression-scores, age of onset, illness duration, PANSS total score and hospitalization frequency were related to decreased GMV predominantly in the control, salience, limbic and DMN networks as well as increased GMV prominently in visual, attention networks (Figure 21B).

Obesity-SCZ expression signature: LV4 (r=0.62, P=0.007). Higher SCZ expression-scores and BMIgap were related to predominant decreased of GMV in the control, DMN, limbic, salience networks and increased GMV in the visual, somatomotor and attention networks (Figure 23).

Comorbid signature of brain-ageing and obesity: LV3 (r=0.70, P<0.001): Higher SCZ expression-scores, BMIgap, BrainAGE, age of onset, number of hospitalization and lower PANSS total scores were related to decreased GMV in the DMN, limbic networks as well as increased GMV predominantly in regions such as visual and attention networks (Figure 20B).

SCZ defining signature: In LV5 (r=0.80, P<0.001), higher SCZ expression-score, BMIgap, number of hospitalizations, PANSS total score were and lower BrainAGE were related to decreased GMV localized across limbic, control, visual networks and increased GMV across DMN and salience networks (Figure 21B).

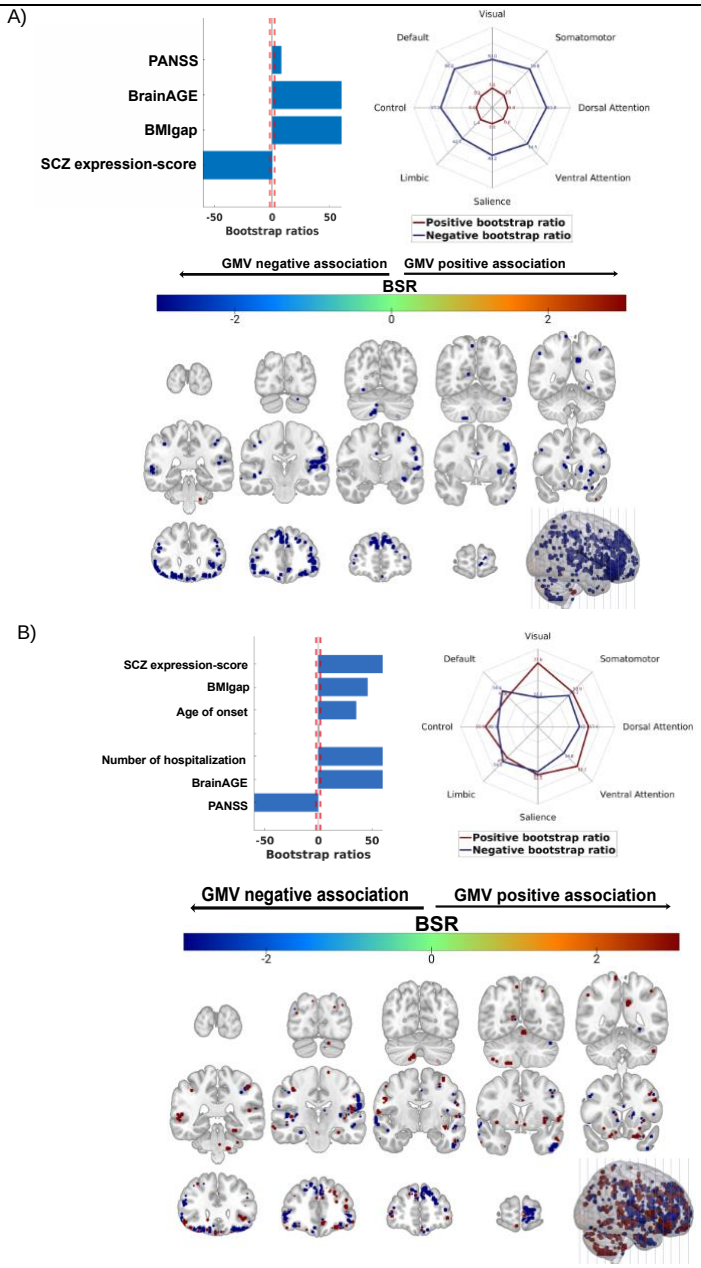

Figure 20. Comorbid signature of brain-ageing and obesity. SPLS analysis results for A) LV1 and B) LV3. Bar plots visualize the correlation of each variable with the LV, blue identifies variables significantly contributing to the LV. The x-axis denotes bootstrap ratios (BSR) (interpretable as z-scores) and the y-axis denotes BMIgap, SCZ expression-score and other clinical items. The red dotted line in the graph represents a BSR of 1.96 (equivalent to a 95% confidence interval). The contribution of individual voxels is shown using BSR in MNI space. Cool colors indicate voxels with a negative correlation of GMV and clinical items, whereas warm colors represent a positive correlation. The spider-plot illustrates the voxel contribution within the 7-network parcellation solution extracted using the Yeo-Buckner atlas (Thomas Yeo et al., 2011). The network names and the cerebral cortical regions that compose the 7 networks are from the supplementary video in Baker et al. (2014) (Baker et al., 2014). Abbreviations: LV= Latent variable, SCZ= Schizophrenia, BMIgap= body mass index gap score, BrainAGE = brain age gap estimation, PANSS= Positive and Negative Symptom Scale total score

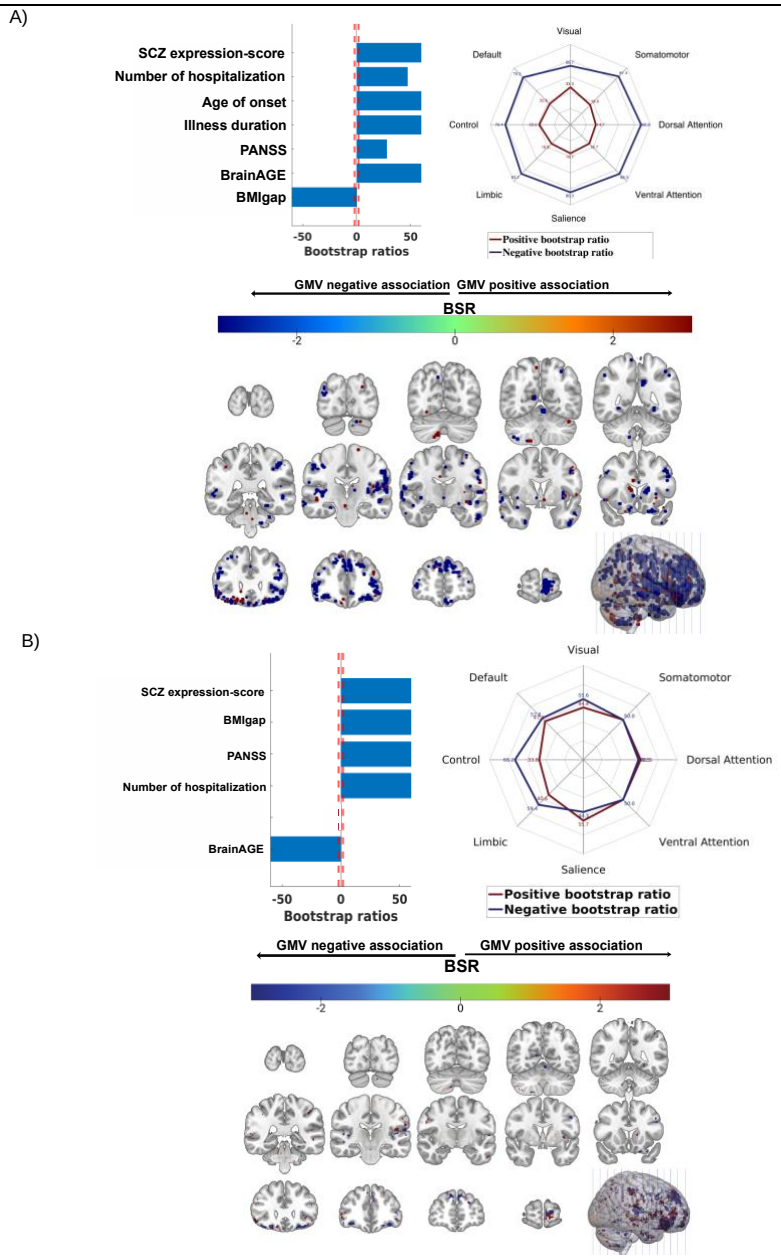

Figure 21. SCZ defining signature. SPLS analysis results for A) LV2 and B) LV5. Bar plots visualize the correlation of each variable with the LV, blue identifies variables significantly contributing to the LV. The x-axis denotes bootstrap ratios (BSR) (interpretable as z-scores) and the y-axis denotes BMIgap, SCZ expression-score and other clinical items. The red dotted line in the graph represents a BSR of 1.96 (equivalent to a 95% confidence interval). The contribution of individual voxels is shown using BSR in MNI space. Cool colors indicate voxels with a negative correlation of GMV and clinical items, whereas warm colors represent a positive correlation. The spider-plot illustrates the voxel contribution within the 7-network parcellation solution extracted using the Yeo-Buckner atlas (Thomas Yeo et al., 2011). The network names and the cerebral cortical regions that compose the 7 networks are from the supplementary video in Baker et al. (2014) (Baker et al., 2014). Abbreviations: LV= Latent variable, SCZ= Schizophrenia

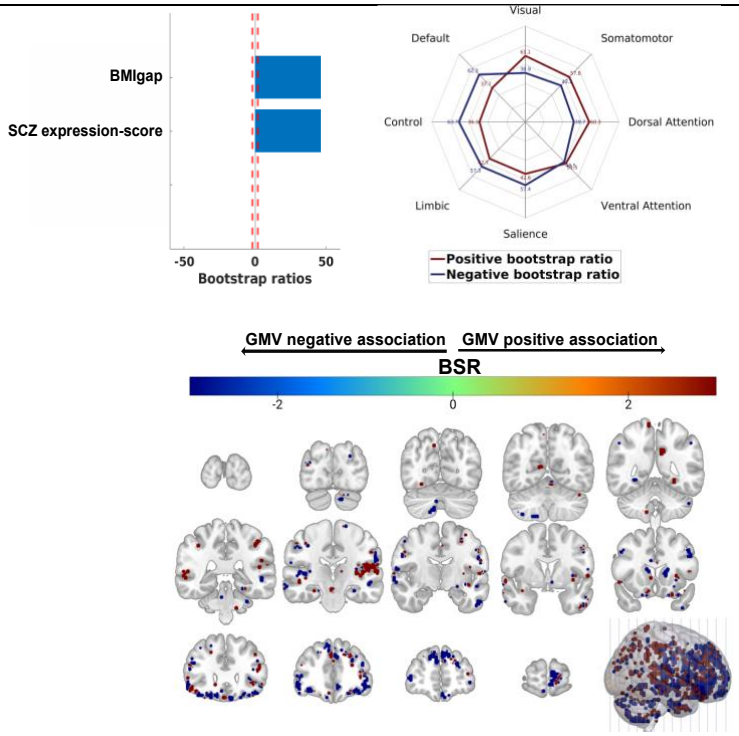

Figure 22. Obesity-SCZ expression signature. SPLS analysis results for LV4. Bar plots visualize the correlation of each variable with the LV, blue identifies variables significantly contributing to the LV. The x-axis denotes bootstrap ratios (BSR) (interpretable as z-scores) and the y-axis denotes BMIgap, SCZ expression-score and other clinical items. The red dotted line in the graph represents a BSR of 1.96 (equivalent to a 95% confidence interval). The contribution of individual voxels is shown using BSR in MNI space. Cool colors indicate voxels with a negative correlation of GMV and clinical items, whereas warm colors represent a positive correlation. The spider-plot illustrates the voxel contribution within the 17-network parcellation solution extracted using the Yeo-Buckner atlas (Thomas Yeo et al., 2011). The network names and the cerebral cortical regions that compose the 17 networks are from the supplementary video in Baker et al. (2014) (Baker et al., 2014). Abbreviations: LV= Latent variable, SCZ= Schizophrenia, BSR= Bootstrap ratios

3.4 Discussion

In this study, we conducted a comprehensive examination of BrainAGE across multiple dimensions. At first, we utilized extensive ROI data from the large, multi-site database of the newly established ECNP-NNADR and successfully developed a brain-age prediction model within a normative modelling framework from HC individuals with an MAE of 6.35 years. This brain-age predictor successfully generalized to an independent HC sample showing no significant differences. Next, we developed a separate BrainAGE model by using voxelized whole brain GMV images as features of the previously sampled HC individuals used in the BMIgap model to leverage the utility of the BMIgap tool to assess the brain alterations due to both obesity and ageing processes. The model demonstrated robust performance, achieving a MAE of 4.73 years, which surpasses the performance of the model using ROI data, even though a similar methodology was applied. In both cases, application of the brain-age models to psychiatric patients, particularly those with SCZ, revealed a positive BrainAGE deviation compared to HC samples. When the ROI-based model was applied to the MDD group, positive BrainAGE deviations were observed, but only with certain atlases. The second BrainAGE model was also applied to CHR and ROD individuals. The CHR group exhibited a positive deviation, though to a lesser extent than the SCZ group, while the ROD individuals did not show significant differences compared to HC individuals. We found that the BMI- and BrainAGE-predictive brain-regions overlap potentially suggesting that the somatic conditions may share underlying pathways specifically in the frontal regions. In fact, BrainAGE scores showed a substantial correlation with previously computed BMIgap scores across both HC individuals and patient groups, accounting for 15.22% of the variance computed for the entire sample. In addition, the predictive regions associated with obesity and brain-ageing overlapped with the SCZ-distinguishing patterns, further substantiating our initial hypothesis of a potential shared pathway. Moreover, the correlation between these ML-derived brain measures and clinical variables in SCZ patients enabled us to discern neuroanatomical-clinical signatures and elucidate these signatures at various levels. Certain signatures associated with obesity, ageing and SCZ expression whereas one signature was independent of BrainAGE effects. Over-all, these findings enhance the disentangle the neuroanatomical alterations associated with obesity and brain-ageing and their collective influence on psychiatric disorders.

3.4.1 ROI findings

The findings from ROI analysis showed that the models performed with MAE between 6.35-10 years which is comparable to previously reported age prediction models with MAE ranging between ~2.5-10 years (Dörfel et al., 2023; J. Han et al., 2022). The application of the model to the left-out HC sample unveiled BrainAGE scores that did not exhibit statistically significant differences from those of the HC normative individuals, thereby confirming the model's robustness and its ability to generalize across heterogeneous HC populations. Notably, we found accelerated brain-ageing in SZ patients relative to the norm, which is a consistent finding in the literature

(Constantinides et al., 2023; Koutsouleris et al., 2021; Nenadić et al., 2017). Additionally, the BrainAGE scores for the MDD patients aligned with the conflicting literature findings, where researchers remain inconclusive regarding evidence of accelerated ageing in this patient group. It's worth noting that this specific analysis served as a proof-of-concept to demonstrate the analytical potential and strengths of the data repository. We didn't employ complex ML approaches or site-correction methods. Despite this, the model estimates were comparable to existing literature findings, specifically those from ROI-based studies, potentially offering further insights into the occurrence of brain-ageing (Baecker et al., 2021; Constantinides et al., 2023; Gutierrez Becker et al., 2018). To summarize, our findings align with previous research, emphasizing the practicality of utilizing ROI as features, particularly in clinical settings with limited computational power and time constraints for computation.

3.4.2 Voxelized GMV approach

Given the curse of dimensionality and the high degree of redundancy inherent in voxelized data, including the substantial spatial between voxels correlations, we found that the model's performance proved more robust while using voxelized data. While we did not directly compare the same studies, the data included in the ROI data model encompassed a larger number of sites. This dataset had a larger sample size, enabling us to select a normative group representative of participants distributed equally across all age groups. Therefore, we anticipated that this group would produce better model performance compared to model developed using voxelized data. This finding underscores the effectiveness of implementing robust dimensionality reduction methods such as PCA in mitigating these challenges and enhancing prediction accuracy. In our whole brain GMV approach, we observed significant positive BrainAGE scores, particularly among the SCZ group, which represents the most severe patients. Interestingly, CHR individuals also exhibited positive BrainAGE scores, although to a lesser extent compared to the SCZ group. This discrepancy in scores could potentially be attributed to the lower disease severity observed in CHR patients. Our findings are supported by existing literature, which suggests that longitudinal analyses reveal a progressive worsening of accelerated brain-ageing with increasing disease severity (Haas et al., 2022). The ROD group exhibited no significant differences in BrainAGE scores compared to the HC discovery sample. This aligns with the variable findings regarding brain-ageing in patients with depression, as reported in many studies (Bashyam et al., 2020; Besteher et al., 2019; Kuo et al., 2020). Additionally, upon comparing the BrainAGE findings of the ROD cohort with those of individuals diagnosed with MDD, the observed predictive scores are coherent. MDD patients commonly exhibit a more advanced trajectory of depressive illness. Therefore, the lack of statistically significant deviations in BrainAGE scores between the ROD cohort and healthy control individuals is consistent with the milder clinical manifestation observed in ROD relative to MDD. Further longitudinal assessment of BrainAGE in ROD patients is essential for establishing conclusive insights into whether BrainAGE increases over time with disease progression. It is noteworthy that the BrainAGE score functions across the entire brain system by integrating data from voxels throughout the brain to produce an individualized score.

This specific score encapsulates multivariate information from the entire brain. Consequently, accelerated ageing might still occur in specific regions rather than across multiple areas, as observed in disorders like SCZ, which has been demonstrated in multiple studies (Besteher et al., 2019; Hajek et al., 2019; Kolenic et al., 2018). Furthermore, from a neurobiological perspective, molecular studies have shown that telomere length, a hallmark of cellular ageing, changes specifically in the hippocampus of MDD patients, but not in other regions such as the amygdala or PFC, indicating region-specific brain changes (Mamdani et al., 2015). Therefore, while the voxel-based method might not capture significant alterations, the ROI approach using various atlases could detect these changes, explaining the variability.

3.4.3 Brain-age predictive brain regions

Our findings of the predictive brain-regions attributed to brain-ageing are in line with the previous findings showing region specific brain alterations specifically across temporal, frontal lobes, parietal areas as well as parahippocampus and cerebellum. Brain atrophy in the temporal lobe is crucial to memory function and has been associated to loss of memory during old age. Additionally, age has been identified as a significant risk factor for medial temporal lobe atrophy (Ejw et al., 2019). The finding of frontal atrophy is also a common occurrence as constantly associated in neurodegenerative diseases such as dementia, specifically fronto-temporal dementia as well as in Alzheimer's diseases. The common neuropathology of these occurrences is the synaptic pruning and accelerated myelination leading to GMV loss as also seen in other psychiatric disorders specifically in psychotic disorders. The observation of cerebellum has been also associated with mobility frailty and further related in cognitive impairment. Cognitive impairment has been a consistent observation both with ageing and psychiatric disorders (Arleo et al., 2024). Furthermore, the PFC has been associated with executive functions such as decision-making, problem-solving and regulation of social-behavior. As this region undergoes age-related atrophy, individuals often face declines in working memory and attention. The cerebellum plays a crucial role in coordinating voluntary movements, balance and motor learning. Atrophy in this area can lead to decreased coordination and balance, raising the risk of falls, and causing difficulties with fine motor tasks.

3.4.4 Association between BrainAGE and BMIgap

Multiple studies have implicated obesity as a contributing factor to brain-ageing, but definitive conclusions are still lacking. Interestingly, we found overlapping brain patterns between obesity and ageing-associated brain regions specifically in frontal lobe that are associated with cognitive control. Studies, including ours, have shown that obese individuals exhibit reduced cognitive control when anticipating food, along with increased activity in reward-related areas (Brooks et al., 2013). It is well established that cognitive control and GMV in these regions gradually decline with age (Brooks et al., 2013). Consequently, the reduced cognitive control observed in obese individuals regarding food intake may also generalize to other functioning domains (Bischof &

Park, 2015). Evidence supporting this hypothesis indicate that obese children have reduced executive function, including cognitive control, compared to normal-weight children, resembling the brain-alterations seen in older adults (Liang et al., 2014). Taken together obesity might be additive towards the accelerated GMV decline in brain regions associated with cognitive control, a common phenomenon in brain-ageing. Obese adults may show added functional deterioration earlier in the lifespan than normal weight adults which should be addressed in lifespan studies. We also identified other regions that do not overlap, indicating distinct neuroanatomical changes uniquely associated with either obesity or ageing, instance, areas in the occipital lobe, which are typically responsible for visual and gustatory encoding of food.

Neurobiologically one possible underlying mechanism is that obesity may heighten the risk of neurodegeneration, leading to GMV loss similar to findings in the brain-ageing (Ronan et al., 2016). This is evidenced by findings that chronic inflammation related to obesity is associated with disruptions in integrity of gray matter, a condition also common for brain-ageing associated processes (Moreno-Navarrete et al., 2017). While certain research indicates that weight loss and calorie-restricted diets may reverse ageing-related biological processes, there remains uncertainty regarding whether changes in the brain can also be reversed (Colman et al., 2014). In this context, our established BMIgap tool can serve to evaluate and quantify brain changes linked to obesity, akin to BrainAGE's role in assessing brain health. Unlike the BMI score, the BMI-gap tool directly quantifies obesity-associated brain changes.

3.4.5 Association between BrainAGE, BMIgap and SCZ-expression

The finding of a high correlation between BMIgap and BrainAGE scores in both HC and patient groups suggests that this interplay persists in psychiatric conditions as well. Notably, the correlation is more pronounced in psychiatric groups, suggesting that obesity may contribute to brain-ageing even in high-risk states (CHR), at the onset of the disease (ROD) or as the condition progresses (SCZ). This is supported by the observation that obese patients with psychiatric disorders tend to show higher BrainAGE compared to non-obese patients. Additionally, we found a strong correlation between BrainAGE score and SCZ-expression score as well as between BMIgap and SCZ-expression score in patients with SCZ, reinforcing the idea that obesity accelerates brain-ageing process is indeed more pronounced in psychiatric patients. The findings align with previous literature indicating that psychiatric groups, such as first-episode psychosis and SCZ patients, who are obese exhibit higher BrainAGE compared to their normal-weight counterparts suggesting obesity has additive effects on brain structure was additive to disease effect (Colman et al., 2014). From a neurobiological perspective, the adverse effects of obesity on the brain might be connected to elevated cortisol levels or reduced brain-derived neurotrophic factor levels, similar to the pathophysiological mechanisms observed in psychiatric conditions, especially psychosis (Gubert et al., 2013; Kolenic et al., 2018; Minichino et al., 2017).Therefore, recognizing overweight and obesity as potential risk factors for neurostructural alterations in psychosis could be the initial step in managing these changes.

3.4.6 Association between BrainAGE, BMIgap, SCZ-expression and clinical variables

Our analysis revealed LV exhibiting varying degrees of association between structural brain derivatives quantifying obesity, ageing, SCZ diagnostic patterns, and other clinically relevant variables, all of which demonstrated patterns of comorbidity. Specifically, LV1 and LV3 reflected comorbid patterns linking brain-ageing and brain obesity, while LV2 and LV5 were associated with variables commonly linked to SCZ diagnosis. Additionally, LV4 displayed a unique comorbid pattern associated solely with brain-ageing and SCZ diagnostic separability. Overall, our analysis revealed that most LVs demonstrated comorbid patterns linking BMIgap, SCZ expression-score and brain-ageing. These patterns were primarily governed by predominant associations with control networks and especially, with reward regions in the LV exclusively showing an association between BMI gap and SCZ expression asserting our previously established hypothesis regarding the association between brain-obesity and psychiatric disorders, particularly across frontal regions. Furthermore, our analysis revealed both positive associations and negative associations of the variables across different brain regions. Specifically, we observed positive associations between BMI gap and BrainAGE in (LV1 and LV3), between BMI gap and SCZ expression score in (LV3 and LV4), and between BrainAGE and SCZ expression score in (LV2 and LV3). Conversely, negative associations were found between BMI gap and BrainAGE in (LV2 and LV5), between BMI gap and SCZ expression score in (LV2) and between BrainAGE and SCZ expression score in (LV5). These findings suggest that these associations may be region-specific or potentially indicative of the presence of subtypes governing these relationships.

Comorbid signature of brain-ageing and obesity

We found two LVs reflecting the comorbid signature of brain-ageing and obesity. Herein, positive associations between high BMIgap, BrainAGE, SCZ expression-score were associated with high clinical loading for variables indicating higher hospitalization frequency and later disease onset implicating a strong somatic comorbidity. This indicates the prevalence of disease severity due to the presence of obesity and brain-ageing effects. Since it has been shown that SCZ obese individuals experiencing psychotic episodes demonstrate higher brain-ageing than their normal-weight counterparts, the predominant negative association of GMV within this signature, including control and attention networks, suggests the potential for GMV loss due to brain-ageing, exacerbated by obesity (S. R. McWhinney et al., 2022). This additive effect may contribute to the onset or exacerbation of psychiatric disorders, as well as a decline in cognitive control functioning, thereby complicating the disease condition further.

SCZ defining signature

Across LV2 and LV8 we saw patterns where mostly the clinical variables were associated positively with SCZ-expression scores implying that strong severity of disease. BrainAGE and BMIgap were each shown positively associated with SCZ-expression in alternate LVs while they

did show negative loading as well. The negative BMIgap could mean that albeit having SCZ, individuals did not show obesity associated brain changes. We observe certain discrepancies, such as a negative loading for SCZ expression-score associated with a high PANSS total score. This may indicate specific brain regions in a subtype of individuals who, despite exhibiting high BrainAGE and obesity, show resilience towards developing psychotic symptoms. Alternatively, it could reflect brain pattern observed in patients experiencing reversible effects of brain changes, potentially due to effective treatment, resulting in less discriminative brain patterns compared to those who did not receive effective treatment. The negative loading in the PANSS item may predominantly reflect specific symptom profiles strongly associated with higher BMI or metabolic dysregulation but independent from brain-ageing.

Obesity-SCZ expression signature

This signature may imply neurobiological processes distinct from those associated with brain-ageing. It stands to reason that individuals exhibiting elevated brain obesity measures would manifest similarities with SCZ diagnostic profiles, potentially exacerbating the condition. This suggests that obesity may precipitate neurophysiological alterations exacerbating the SCZ phenotype.

In summary, these findings substantiate our claim regarding the existence of both shared and distinct pathways contributing to the alterations in brain structure associated with psychiatric disorders and obesity, further influenced by the effects of brain-ageing. This underscores the potential for investigating the characterization of psychiatric sub-types and elucidating the precise neurobiological mechanisms underlying each condition. Further analysis, including longitudinal studies and the incorporation of blood markers such as inflammatory markers, is necessary to comprehensively understand the neurobiological underpinnings of these comorbid conditions. Additionally, examining the same subjects at later time points may provide insight into the potential reversibility of these brain changes, particularly through therapeutic interventions.

3.4.7 Limitations

Nonetheless, several limitations and avenues are prevailed which can be addressed in the future. First, although the ROI data used is from a large sample size, the use of other imaging modalities is currently restrictive due to the limitations of the virtual data-sharing platform, which restricts the entry of higher metric datasets including use of voxelized datasets. Currently we do not support the findings with longitudinal assessments which is essential to conclusively tell that whether the obesity-brain changes sustain with the disease trajectory. Furthermore, blood-based markers such as neuroinflammatory markers should be assessed which implicated in ageing, obesity as well as disease conditions should be addressed as well. Furthermore, the BrainAGE model although uses large cohort multi-site data but the sample selection is not uniformly distributed. However, we retained the usage of same sample as used previously for the BMIgap model for

better comparability of the ML model estimates and interpretation to ensure that the results are due to the implicated conditions and not due to the change in sample characteristics.

3.4.8 Conclusion

In conclusion, our study highlights the intricate relationships between brain-ageing, obesity and psychiatric disorders. We observed that obesity is potentially a contributing factor to abnormalities associated with brain-ageing, with overlapping patterns in the frontal brain regions specifically across the control areas aligning with our hypothesis. We used our previously established BMIgap tool as a utility to deepen our understanding of obesity, brain-ageing processing across different psychiatric stages and implicated that obesity might indeed worsen the brain-ageing alterations observed in psychiatric patients, thereby requiring urgency of timely and early intervention specifically targeted to decrease the brain-obesity measures which can be quantified by the newly established BMIgap tool. Thereby, these insights deepen our understanding of the complex interactions between neuroanatomical changes, obesity and psychiatric disorders, highlighting the need for integrated approaches in diagnosis and treatment.

4. Discussion

The goal of this dissertation was to identify the neural underpinning of somatic comorbidities in psychiatric disorders specifically occurring due to obesity and ageing. In pursuit of this objective, we employed a comprehensive approach, combining multiscale, multi-site to understand the intricate interplay somatic comorbidities including obesity measured by BMI, ageing commonly found in common psychiatric disorders. Two separate studies were performed. First, we introduced the novel 'BMIgap' tool to assess obesity-related brain changes in both psychiatric and non-psychiatric populations. This tool enabled us to identify patterns of BMI-associated brain alterations specifically in reward and control regions, providing insights into the complex relationship between obesity and brain structure. The second study focused on understanding the process of brain-ageing related complexities using different neuroimaging modalities. Overall, some of our proposed hypotheses proved to be correct. We found that brain-obesity estimated using BMIgap score differed between HC individuals and psychiatric patients. We observed pronounced BMI-predictive regions showing negative GMV associations, mainly in lower fronto-temporal regions associated with negative GMV associations especially. The reward and control networks are particularly altered. In the second study, as expected, we observed higher BrainAGE values for patients with SCZ and MDD, with SCZ showing the highest positive values compared to CHR and ROD groups. However, we observed positive deviations for SCZ and CHR, with SCZ showing more positive values, whereas the ROD group did not show statistically different BrainAGE scores compared to norms, and although the MDD group did show changes, the findings were limited to specific atlases only. Additionally, while comparing the overlapping brain regions showing comorbidity for obesity, ageing, and SCZ expression, we indeed found predictive regions localized across frontal regions, specifically in the control network. Furthermore, while our initial hypothesis was that ROI data should have better model performance than the model using voxelized data, the findings were opposite.

By developing brain-age prediction models within a normative framework, we aimed to understand accelerated brain-ageing in patients with psychotic disorders. Furthermore, to leverage the utility of the BMIgap tool to understand BrainAGE and BMIgap association, we developed a BrainAGE model using the same voxelized dataset as previously used for the BMIgap model. Despite this data having a smaller sample size, being very high dimensional, and not following a normative modeling framework, it outperformed the performance of the ROI-based BrainAGE predictor, demonstrating robust performance in predicting brain age and emphasizing that the use of dimensionality reduction methods proves to eliminate the challenge of the 'curse of dimensionality'. Nevertheless, one should not forget the practicality of using ROI data, which is simpler, quicker and computationally less expensive targeting the clinical settings. Nevertheless, our model performed comparably with the existing literature despite using simpler ML method, due to restrictive computational resources, by focusing more on data selection and mitigating the site-effects. Hence further asserting the usage of normative modelling framework within the

clinical settings. Furthermore, applicability of DL methods such as neural networks can has been used to improve the model performances using the ROI datasets (Bashyam et al., 2020).

The negative relationship observed between BMI and GMV within the reward and salience regions has been implicated in regulating eating behavior (Li et al., 2022). This negative association suggests that alterations in these brain regions may influence how individuals respond to food cues and rewards, potentially contributing to overeating and weight gain. Additionally, negative GMV associations were found in taste perception, reward processing and inhibitory control areas. These changes collectively may contribute to the development of maladaptive eating patterns, thereby fostering obesity. Specifically, reductions in GMV in prefrontal regions have been associated with reduction inhibitory control and hence increasing vulnerability to consuming excessive calories. The presence of psychiatric disorders may exacerbate the condition. Psychiatric disorders specifically within the SCZ spectrum have shown prefrontal deficits, characterized by reduced cognitive drive. The reduced control coupled with impairments in inhibitory control, may worsen the susceptibility of the patients to engage in addictive behaviors, thereby fostering obesity. Interestingly, BrainAGE findings also revealed that age-associated alterations mostly overlapped in the frontal regions, specifically implicated in control regions as has been shown in our study as well. In summary, the ageing process and obesity both have negative implications for GMV, with the conditions showing additive effects (S. McWhinney et al., 2021). Furthermore, in combination with psychiatric disorders, they exacerbate the brain changes. Obesity-related alterations cause deficits across reward and inhibitory control-related regions. Loss of GMV in inhibitory control leads to a loss of control leading to overeating and causing maladaptive eating habits. Additionally, deficits in reward regions may increase vulnerability to consuming high-caloric foods, thereby contributing to obesity. Psychotic disorders, known for GMV loss in control regions, create a feed-forward loop for patients, as the already impaired control regions facilitate the cycle leading to overeating and obesity. Moreover, ageing is associated with GMV decline across control regions such as cognitive control. Therefore, ageing, when comorbid with obesity and psychotic symptoms, leads to more GMV loss, specifically due to cellular damage, demyelination, synaptic pruning, and telomere length shortening, all causing additive influence on loss of control and thereby worsening the conditions of obesity and psychotic symptoms such cognitive decline, as well as the disease status. Although, in our study we did not observe significant association between the medication usage and the brain-measure, we need to address them. Specific anti-depressants targeting weight loss have been implicated to improve brain health by showing improvements in cognitive functioning. Therefore, therapeutics targeting, and potentially reversing obesity specific alterations is needed. Additionally incorporating physical activities for patients may be helpful in reducing obesity associated brain-changes.

5. Future directions and conclusions

5.1 Future directions

The broader perspective of our research will be realized through longitudinal analysis, encompassing multiple data domains including clinical, genetics, blood markers and metabolic markers data. This comprehensive approach will allow us to accurately assess the clinical utility of the brain-obesity estimator 'BMIgap tool'. By including different subtypes of patients across a wider spectrum, we can facilitate the application and validation of transdiagnostic approaches. Moreover, it is crucial to investigate whether these observed brain changes are modifiable, thereby enhancing therapeutic efficacy. For instance, estimating BMIgap both before and after the initiation of treatment can elucidate whether the brain alterations persist over time. As research increasingly focuses on developing medications targeting weight loss, it will be intriguing to explore whether these interventions influence BMIgap values. Similarly, examining therapeutic interventions such as physical activity can provide valuable insights into their impact on brain-obesity relationships.

5.2 Conclusions

This holistic approach, combining multiscale, multi-modal datasets by incorporating stratification methods using ML methods, allowed us to address somatic comorbidities, particularly obesity and brain-ageing, in HC individuals as well as multiple psychiatric groups. We aimed to disentangle the brain structural alterations implicated due to their comorbidity with psychiatric disorders and to demonstrate associations with clinically relevant variables. We introduced 'BMIgap' as an innovative tool for assessing obesity-related brain changes in both psychiatric and non-psychiatric populations and further showed its associations with brain-ageing signatures. Although we demonstrate the existence of commonalities across the three conditions, the broader neurobiological underpinnings are yet to be fully understood.

6. References

Abdullah, H. M., Shahul, H. A., Hwang, M. Y., & Ferrando, S. (2020). Comorbidity in Schizophrenia: Conceptual Issues and Clinical Management. *Focus: Journal of Life Long Learning in Psychiatry*, *18*(4), 386. https://doi.org/10.1176/appi.focus.20200026

Afzal, M., Siddiqi, N., Ahmad, B., Afsheen, N., Aslam, F., Ali, A., Ayesha, R., Bryant, M., Holt, R., Khalid, H., Ishaq, K., Koly, K. N., Rajan, S., Saba, J., Tirbhowan, N., & Zavala, G. A. (2021). Prevalence of Overweight and Obesity in People With Severe Mental Illness: Systematic Review and Meta-Analysis. *Frontiers in Endocrinology*, *12*, 769309. https://doi.org/10.3389/fendo.2021.769309

Amidfar, M., Quevedo, J., Z. Réus, G., & Kim, Y.-K. (2021). Grey matter volume abnormalities in the first depressive episode of medication-naïve adult individuals: A systematic review of voxel based morphometric studies. *International Journal of Psychiatry in Clinical Practice*, *25*(4), 407–420. https://doi.org/10.1080/13651501.2020.1861632

Andreassen, O. A., Hindley, G. F. L., Frei, O., & Smeland, O. B. (2023). New insights from the last decade of research in psychiatric genetics: Discoveries, challenges and clinical implications. *World Psychiatry*, *22*(1), 4. https://doi.org/10.1002/wps.21034

Ang, M. Y., Takeuchi, F., & Kato, N. (2023). Deciphering the genetic landscape of obesity: A data-driven approach to identifying plausible causal genes and therapeutic targets. *Journal of Human Genetics*, *68*(12), 823–833. https://doi.org/10.1038/s10038-023-01189-3

Angebrandt, A., Abulseoud, O. A., Kisner, M., Diazgranados, N., Momenan, R., Yang, Y., Stein, E. A., & Ross, T. J. (2022). Dose-dependent relationship between social drinking and brain aging. *Neurobiology of Aging*, *111*, 71–81. https://doi.org/10.1016/j.neurobiolaging.2021.11.008

Annamalai, A., Kosir, U., & Tek, C. (2017). Prevalence of obesity and diabetes in patients with schizophrenia. *World Journal of Diabetes*, *8*(8), 390–396. https://doi.org/10.4239/wjd.v8.i8.390

Anticevic, A., Schleifer, C., & T. Cho, Y. (2015). Emotional and cognitive dysregulation in schizophrenia and depression: Understanding common and distinct behavioral and neural mechanisms. *Dialogues in Clinical Neuroscience*, *17*(4), 421–434.

Arleo, A., Bareš, M., Bernard, J. A., Bogoian, H. R., Bruchhage, M. M. K., Bryant, P., Carlson, E. S., Chan, C. C. H., Chen, L.-K., Chung, C.-P., Dotson, V. M., Filip, P., Guell, X., Habas, C., Jacobs, H. I. L., Kakei, S., Lee, T. M. C., Leggio, M., Misiura, M., … Manto, M. (2024). Consensus Paper: Cerebellum and Ageing. *Cerebellum (London, England)*, *23*(2), 802–832. https://doi.org/10.1007/s12311-023-01577-7

Arnone, D., Job, D., Selvaraj, S., Abe, O., Amico, F., Cheng, Y., Colloby, S. J., O'Brien, J. T., Frodl, T., Gotlib, I. H., Ham, B.-J., Kim, M. J., Koolschijn, P. C. M. P., Périco, C. A.-M., Salvadore, G., Thomas, A. J., Van Tol, M.-J., van der Wee, N. J. A., Veltman, D. J., … McIntosh, A. M. (2016). Computational meta-analysis of statistical parametric maps in major depression. *Human Brain Mapping*, *37*(4), 1393–1404. https://doi.org/10.1002/hbm.23108

Arnone, D., McKie, S., Elliott, R., Thomas, E. J., Downey, D., Juhasz, G., Williams, S. R., Deakin, J. F. W., & Anderson, I. M. (2012). Increased amygdala responses to sad but not fearful faces in major depression: Relation to mood state and pharmacological treatment. *The American Journal of Psychiatry*, *169*(8), 841–850. https://doi.org/10.1176/appi.ajp.2012.11121774

Arulanandam, B., Beladi, H., & Chakrabarti, A. (2023). Obesity and COVID-19 mortality are correlated. *Scientific Reports*, *13*(1), 5895. https://doi.org/10.1038/s41598-023-33093-3

Avery, J. A., Powell, J. N., Breslin, F. J., Lepping, R. J., Martin, L. E., Patrician, T. M., Donnelly, J. E., Savage, C. R., & Simmons, W. K. (2017). Obesity is associated with altered mid-insula functional connectivity to limbic regions underlying appetitive responses to foods. *Journal of Psychopharmacology (Oxford, England)*, *31*(11), 1475–1484. https://doi.org/10.1177/0269881117728429

Aycheh, H. M., Seong, J.-K., Shin, J.-H., Na, D. L., Kang, B., Seo, S. W., & Sohn, K.-A. (2018). Biological Brain Age Prediction Using Cortical Thickness Data: A Large Scale Cohort

Study. *Frontiers in Aging Neuroscience*, *10*, 252. https://doi.org/10.3389/fnagi.2018.00252

Bäckhed, F., Ding, H., Wang, T., Hooper, L. V., Koh, G. Y., Nagy, A., Semenkovich, C. F., & Gordon, J. I. (2004). The gut microbiota as an environmental factor that regulates fat storage. *Proceedings of the National Academy of Sciences of the United States of America*, *101*(44), 15718–15723. https://doi.org/10.1073/pnas.0407076101

Baecker, L., Dafflon, J., da Costa, P. F., Garcia-Dias, R., Vieira, S., Scarpazza, C., Calhoun, V. D., Sato, J. R., Mechelli, A., & Pinaya, W. H. L. (2021). Brain age prediction: A comparison between machine learning models using region- and voxel-based morphometric data. *Human Brain Mapping*, *42*(8), 2332–2346. https://doi.org/10.1002/hbm.25368

Bains, N., & Abdijadid, S. (2024). Major Depressive Disorder. In *StatPearls*. StatPearls Publishing. http://www.ncbi.nlm.nih.gov/books/NBK559078/

Baker, J. T., Holmes, A. J., Masters, G. A., Yeo, B. T. T., Krienen, F., Buckner, R. L., & Öngür, D. (2014). Disruption of cortical association networks in schizophrenia and psychotic bipolar disorder. *JAMA Psychiatry*, *71*(2), 109–118. https://doi.org/10.1001/jamapsychiatry.2013.3469

Ballester, P. L., Romano, M. T., de Azevedo Cardoso, T., Hassel, S., Strother, S. C., Kennedy, S. H., & Frey, B. N. (2022). Brain age in mood and psychotic disorders: A systematic review and meta-analysis. *Acta Psychiatrica Scandinavica*, *145*(1), 42–55. https://doi.org/10.1111/acps.13371

Baothman, O. A., Zamzami, M. A., Taher, I., Abubaker, J., & Abu-Farha, M. (2016). The role of Gut Microbiota in the development of obesity and Diabetes. *Lipids in Health and Disease*, *15*, 108. https://doi.org/10.1186/s12944-016-0278-4

Bashyam, V. M., Erus, G., Doshi, J., Habes, M., Nasrallah, I., Truelove-Hill, M., Srinivasan, D., Mamourian, L., Pomponio, R., Fan, Y., Launer, L. J., Masters, C. L., Maruff, P., Zhuo, C., Völzke, H., Johnson, S. C., Fripp, J., Koutsouleris, N., Satterthwaite, T. D., … Davatzikos, C. (2020). MRI signatures of brain age and disease over the lifespan based

on a deep brain network and 14 468 individuals worldwide. *Brain: A Journal of Neurology*, *143*(7), 2312–2324. https://doi.org/10.1093/brain/awaa160

Beck, L. C., Masi, A. C., Young, G. R., Vatanen, T., Lamb, C. A., Smith, R., Coxhead, J., Butler, A., Marsland, B. J., Embleton, N. D., Berrington, J. E., & Stewart, C. J. (2022). Strain-specific impacts of probiotics are a significant driver of gut microbiome development in very preterm infants. *Nature Microbiology*, *7*(10), 1525–1535. https://doi.org/10.1038/s41564-022-01213-w

Beheshti, I., Maikusa, N., & Matsuda, H. (2018). The association between "Brain-Age Score" (BAS) and traditional neuropsychological screening tools in Alzheimer's disease. *Brain and Behavior*, *8*(8), e01020. https://doi.org/10.1002/brb3.1020

Bellass, S., Lister, J., Kitchen, C. E. W., Kramer, L., Alderson, S. L., Doran, T., Gilbody, S., Han, L., Hewitt, C., Holt, R. I. G., Jacobs, R., Prady, S. L., Shiers, D., Siddiqi, N., & Taylor, J. (2021). Living with diabetes alongside a severe mental illness: A qualitative exploration with people with severe mental illness, family members and healthcare staff. *Diabetic Medicine*, *38*(7), e14562. https://doi.org/10.1111/dme.14562

Belov, V., Erwin-Grabner, T., Aghajani, M., Aleman, A., Amod, A. R., Basgoze, Z., Benedetti, F., Besteher, B., Bülow, R., Ching, C. R. K., Connolly, C. G., Cullen, K., Davey, C. G., Dima, D., Dols, A., Evans, J. W., Fu, C. H. Y., Gonul, A. S., Gotlib, I. H., … Goya-Maldonado, R. (2024). Multi-site benchmark classification of major depressive disorder using machine learning on cortical and subcortical measures. *Scientific Reports*, *14*(1), 1084. https://doi.org/10.1038/s41598-023-47934-8

Besteher, B., Gaser, C., & Nenadić, I. (2019). Machine-learning based brain age estimation in major depression showing no evidence of accelerated aging. *Psychiatry Research. Neuroimaging*, *290*, 1–4. https://doi.org/10.1016/j.pscychresns.2019.06.001

Bischof, G. N., & Park, D. C. (2015). Obesity and Aging: Consequences for Cognition, Brain Structure and Brain Function. *Psychosomatic Medicine*, *77*(6), 697–709. https://doi.org/10.1097/PSY.0000000000000212

Blasco, B. V., García-Jiménez, J., Bodoano, I., & Gutiérrez-Rojas, L. (2020). Obesity and Depression: Its Prevalence and Influence as a Prognostic Factor: A Systematic Review. *Psychiatry Investigation*, *17*(8), 715–724. https://doi.org/10.30773/pi.2020.0099

Bleuler, E. (1950). *Dementia praecox or the group of schizophrenias* (p. 548). International Universities Press.

Blier, P., Piñeyro, G., el Mansari, M., Bergeron, R., & de Montigny, C. (1998). Role of somatodendritic 5-HT autoreceptors in modulating 5-HT neurotransmission. *Annals of the New York Academy of Sciences*, *861*, 204–216. https://doi.org/10.1111/j.1749-6632.1998.tb10192.x

Bocklandt, S., Lin, W., Sehl, M. E., Sánchez, F. J., Sinsheimer, J. S., Horvath, S., & Vilain, E. (2011). Epigenetic Predictor of Age. *PLoS ONE*, *6*(6), e14821. https://doi.org/10.1371/journal.pone.0014821

Bohon, C., & Welch, H. (2021). Quadratic relations of BMI with depression and brain volume in children: Analysis of data from the ABCD study. *Journal of Psychiatric Research*, *136*, 421–427. https://doi.org/10.1016/j.jpsychires.2021.02.038

Bora, E., Akdede, B. B., & Alptekin, K. (2017). The relationship between cognitive impairment in schizophrenia and metabolic syndrome: A systematic review and meta-analysis. *Psychological Medicine*, *47*(6), 1030–1040. https://doi.org/10.1017/S0033291716003366

Bora, E., Fornito, A., Radua, J., Walterfang, M., Seal, M., Wood, S. J., Yücel, M., Velakoulis, D., & Pantelis, C. (2011). Neuroanatomical abnormalities in schizophrenia: A multimodal voxelwise meta-analysis and meta-regression analysis. *Schizophrenia Research*, *127*(1–3), 46–57. https://doi.org/10.1016/j.schres.2010.12.020

Borgwardt, S. J., McGuire, P. K., Aston, J., Gschwandtner, U., Pflüger, M. O., Stieglitz, R.-D., Radue, E.-W., & Riecher-Rössler, A. (2008). Reductions in frontal, temporal and parietal volume associated with the onset of psychosis. *Schizophrenia Research*, *106*(2), 108–114. https://doi.org/10.1016/j.schres.2008.08.007

Bornstein, S. R., Schuppenies, A., Wong, M.-L., & Licinio, J. (2006). Approaching the shared biology of obesity and depression: The stress axis as the locus of gene–environment interactions. *Molecular Psychiatry*, *11*(10), 892–902. https://doi.org/10.1038/sj.mp.4001873

Brenes, G. A. (2007). Anxiety, Depression, and Quality of Life in Primary Care Patients. *Primary Care Companion to The Journal of Clinical Psychiatry*, *9*(6), 437–443.

Brisch, R., Saniotis, A., Wolf, R., Bielau, H., Bernstein, H.-G., Steiner, J., Bogerts, B., Braun, K., Jankowski, Z., Kumaratilake, J., Henneberg, M., & Gos, T. (2014). The Role of Dopamine in Schizophrenia from a Neurobiological and Evolutionary Perspective: Old Fashioned, but Still in Vogue. *Frontiers in Psychiatry*, *5*, 47. https://doi.org/10.3389/fpsyt.2014.00047

Brooks, S. J., Cedernaes, J., & Schiöth, H. B. (2013). Increased Prefrontal and Parahippocampal Activation with Reduced Dorsolateral Prefrontal and Insular Cortex Activation to Food Images in Obesity: A Meta-Analysis of fMRI Studies. *PLoS ONE*, *8*(4), e60393. https://doi.org/10.1371/journal.pone.0060393

Burcusa, S. L., & Iacono, W. G. (2007). Risk for recurrence in depression. *Clinical Psychology Review*, *27*(8), 959–985. https://doi.org/10.1016/j.cpr.2007.02.005

Busatto, G. F. (2013). Structural and Functional Neuroimaging Studies in Major Depressive Disorder With Psychotic Features: A Critical Review. *Schizophrenia Bulletin*, *39*(4), 776–786. https://doi.org/10.1093/schbul/sbt054

Cannon, T. D. (2005). The inheritance of intermediate phenotypes for schizophrenia. *Current Opinion in Psychiatry*, *18*(2), 135–140. https://doi.org/10.1097/00001504-200503000-00005

Carney, R., Cotter, J., Bradshaw, T., Firth, J., & Yung, A. R. (2016). Cardiometabolic risk factors in young people at ultra-high risk for psychosis: A systematic review and meta-analysis. *Schizophrenia Research*, *170*(2), 290–300. https://doi.org/10.1016/j.schres.2016.01.010

Castanon, N., Luheshi, G., & Laye, S. (2015). Role of neuroinflammation in the emotional and cognitive alterations displayed by animal models of obesity. *Frontiers in Neuroscience*, *9*. https://doi.org/10.3389/fnins.2015.00229

Cazacu, I. M., Udristoiu, A., Gruionu, L. G., Iacob, A., Gruionu, G., & Saftoiu, A. (2019). Artificial intelligence in pancreatic cancer: Toward precision diagnosis. *Endoscopic Ultrasound*, *8*(6), 357–359. https://doi.org/10.4103/eus.eus_76_19

Chao, A. M., Wadden, T. A., & Berkowitz, R. I. (2019). Obesity in Adolescents with Psychiatric Disorders. *Current Psychiatry Reports*, *21*(1), 3. https://doi.org/10.1007/s11920-019-0990-7

Chekroud, A. M., Bondar, J., Delgadillo, J., Doherty, G., Wasil, A., Fokkema, M., Cohen, Z., Belgrave, D., DeRubeis, R., Iniesta, R., Dwyer, D., & Choi, K. (2021). The promise of machine learning in predicting treatment outcomes in psychiatry. *World Psychiatry*, *20*(2), 154–170. https://doi.org/10.1002/wps.20882

Christman, S., Bermudez, C., Hao, L., Landman, B. A., Boyd, B., Albert, K., Woodward, N., Shokouhi, S., Vega, J., Andrews, P., & Taylor, W. D. (2020). Accelerated brain aging predicts impaired cognitive performance and greater disability in geriatric but not midlife adult depression. *Translational Psychiatry*, *10*(1), 317. https://doi.org/10.1038/s41398-020-01004-z

Chung, Y., Addington, J., Bearden, C. E., Cadenhead, K., Cornblatt, B., Mathalon, D. H., McGlashan, T., Perkins, D., Seidman, L. J., Tsuang, M., Walker, E., Woods, S. W., McEwen, S., van Erp, T. G. M., Cannon, T. D., & North American Prodrome Longitudinal Study (NAPLS) Consortium and the Pediatric Imaging, Neurocognition, and Genetics (PING) Study Consortium. (2018). Use of Machine Learning to Determine Deviance in Neuroanatomical Maturity Associated With Future Psychosis in Youths at Clinically High Risk. *JAMA Psychiatry*, *75*(9), 960–968. https://doi.org/10.1001/jamapsychiatry.2018.1543

Cole, J. H., & Franke, K. (2017). Predicting Age Using Neuroimaging: Innovative Brain-ageing Biomarkers. *Trends in Neurosciences*, *40*(12), 681–690. https://doi.org/10.1016/j.tins.2017.10.001

Cole, J. H., Marioni, R. E., Harris, S. E., & Deary, I. J. (2019a). Brain age and other bodily 'ages': Implications for neuropsychiatry. *Molecular Psychiatry*, *24*(2), 266–281. https://doi.org/10.1038/s41380-018-0098-1

Cole, J. H., Marioni, R. E., Harris, S. E., & Deary, I. J. (2019b). Brain age and other bodily 'ages': Implications for neuropsychiatry. *Molecular Psychiatry*, *24*(2), 266–281. https://doi.org/10.1038/s41380-018-0098-1

Colman, R. J., Beasley, T. M., Kemnitz, J. W., Johnson, S. C., Weindruch, R., & Anderson, R. M. (2014). Caloric restriction reduces age-related and all-cause mortality in rhesus monkeys. *Nature Communications*, *5*(1), 3557. https://doi.org/10.1038/ncomms4557

Connell, J., O'Cathain, A., & Brazier, J. (2014). Measuring quality of life in mental health: Are we asking the right questions? *Social Science & Medicine (1982)*, *120*, 12–20. https://doi.org/10.1016/j.socscimed.2014.08.026

Constantinides, C., Han, L. K. M., Alloza, C., Antonucci, L. A., Arango, C., Ayesa-Arriola, R., Banaj, N., Bertolino, A., Borgwardt, S., Bruggemann, J., Bustillo, J., Bykhovski, O., Calhoun, V., Carr, V., Catts, S., Chung, Y.-C., Crespo-Facorro, B., Díaz-Caneja, C. M., Donohoe, G., … Walton, E. (2023). Brain-ageing in schizophrenia: Evidence from 26 international cohorts via the ENIGMA Schizophrenia consortium. *Molecular Psychiatry*, *28*(3), 1201–1209. https://doi.org/10.1038/s41380-022-01897-w

Corica, D., Aversa, T., Valenzise, M., Messina, M. F., Alibrandi, A., De Luca, F., & Wasniewska, M. (2018). Does Family History of Obesity, Cardiovascular, and Metabolic Diseases Influence Onset and Severity of Childhood Obesity? *Frontiers in Endocrinology*, *9*, 187. https://doi.org/10.3389/fendo.2018.00187

Cortes-Briones, J. A., Tapia-Rivas, N. I., D'Souza, D. C., & Estevez, P. A. (2022). Going deep into schizophrenia with artificial intelligence. *Schizophrenia Research*, *245*, 122–140. https://doi.org/10.1016/j.schres.2021.05.018

COVID-19 Mental Disorders Collaborators. (2021). Global prevalence and burden of depressive and anxiety disorders in 204 countries and territories in 2020 due to the COVID-19

pandemic. *Lancet (London, England)*, *398*(10312), 1700–1712. https://doi.org/10.1016/S0140-6736(21)02143-7

Damme, K. S. F., Vargas, T., Calhoun, V., Turner, J., & Mittal, V. A. (2020). Global and Specific Cortical Volume Asymmetries in Individuals With Psychosis Risk Syndrome and Schizophrenia: A Mixed Cross-sectional and Longitudinal Perspective. *Schizophrenia Bulletin*, *46*(3), 713–721. https://doi.org/10.1093/schbul/sbz096

Dantzer, R., O'Connor, J. C., Freund, G. G., Johnson, R. W., & Kelley, K. W. (2008). From inflammation to sickness and depression: When the immune system subjugates the brain. *Nature Reviews Neuroscience*, *9*(1), 46–56. https://doi.org/10.1038/nrn2297

DE HERT, M., SCHREURS, V., VANCAMPFORT, D., & VAN WINKEL, R. (2009). Metabolic syndrome in people with schizophrenia: A review. *World Psychiatry*, *8*(1), 15–22.

de Lange, A. H., Pak, K., Osagie, E., van Dam, K., Christensen, M., Furunes, T., Løvseth, L. T., & Detaille, S. (2020). An Open Time Perspective and Social Support to Sustain in Healthcare Work: Results of a Two-Wave Complete Panel Study. *Frontiers in Psychology*, *11*. https://doi.org/10.3389/fpsyg.2020.01308

De Micheli, A., Provenzani, U., Krakowski, K., Oliver, D., Damiani, S., Brondino, N., McGuire, P., & Fusar-Poli, P. (2024). Physical Health and Transition to Psychosis in People at Clinical High Risk. *Biomedicines*, *12*(3), Article 3. https://doi.org/10.3390/biomedicines12030523

de Nijs, J., Schnack, H. G., Koevoets, M. G. J. C., Kubota, M., Kahn, R. S., van Haren, N. E. M., & Cahn, W. (2018). Reward-related brain structures are smaller in patients with schizophrenia and comorbid metabolic syndrome. *Acta Psychiatrica Scandinavica*, *138*(6), 581–590. https://doi.org/10.1111/acps.12955

Dean, J., & Keshavan, M. (2017). The neurobiology of depression: An integrated view. *Asian Journal of Psychiatry*, *27*, 101–111. https://doi.org/10.1016/j.ajp.2017.01.025

Dementia Praecox and Paraphrenia. (1972). *Annals of Internal Medicine*, *76*(6), 1058. https://doi.org/10.7326/0003-4819-76-6-1058_8

Demro, C., Shen, C., Hendrickson, T. J., Arend, J. L., Disner, S. G., & Sponheim, S. R. (2022). Advanced Brain-Age in Psychotic Psychopathology: Evidence for Transdiagnostic Neurodevelopmental Origins. *Frontiers in Aging Neuroscience*, *14*. https://doi.org/10.3389/fnagi.2022.872867

Dieset, I., Andreassen, O. A., & Haukvik, U. K. (2016). Somatic Comorbidity in Schizophrenia: Some Possible Biological Mechanisms Across the Life Span. *Schizophrenia Bulletin*, *42*(6), 1316–1319. https://doi.org/10.1093/schbul/sbw028

Dörfel, R. P., Arenas-Gomez, J. M., Fisher, P. M., Ganz, M., Knudsen, G. M., Svensson, J. E., & Plavén-Sigray, P. (2023). Prediction of brain age using structural magnetic resonance imaging: A comparison of accuracy and test–retest reliability of publicly available software packages. *Human Brain Mapping*, *44*(17), 6139–6148. https://doi.org/10.1002/hbm.26502

Dornquast, C., Tomzik, J., Reinhold, T., Walle, M., Mönter, N., & Berghöfer, A. (2017). To what extent are psychiatrists aware of the comorbid somatic illnesses of their patients with serious mental illnesses? – A cross-sectional secondary data analysis. *BMC Health Services Research*, *17*(1), 162. https://doi.org/10.1186/s12913-017-2106-6

Drobinin, V., Van Gestel, H., Helmick, C. A., Schmidt, M. H., Bowen, C. V., & Uher, R. (2022). The Developmental Brain Age Is Associated With Adversity, Depression, and Functional Outcomes Among Adolescents. *Biological Psychiatry: Cognitive Neuroscience and Neuroimaging*, *7*(4), 406–414. https://doi.org/10.1016/j.bpsc.2021.09.004

Dugré, J. R., Bitar, N., Dumais, A., & Potvin, S. (2019). Limbic Hyperactivity in Response to Emotionally Neutral Stimuli in Schizophrenia: A Neuroimaging Meta-Analysis of the Hypervigilant Mind. *The American Journal of Psychiatry*, *176*(12), 1021–1029. https://doi.org/10.1176/appi.ajp.2019.19030247

Dunlop, K., Victoria, L. W., Downar, J., Gunning, F. M., & Liston, C. (2021). Accelerated brain aging predicts impulsivity and symptom severity in depression. *Neuropsychopharmacology*, *46*(5), 911–919. https://doi.org/10.1038/s41386-021-00967-x

Dwyer, D. B., Falkai, P., & Koutsouleris, N. (2018). Machine Learning Approaches for Clinical Psychology and Psychiatry. *Annual Review of Clinical Psychology*, *14*(Volume 14, 2018), 91–118. https://doi.org/10.1146/annurev-clinpsy-032816-045037

Ejw, V. S., Jm, O., B, V. H., Rl, V., Aa, G., Hc, W., A, P., P, S., & Eja, S. (2019). Medial temporal lobe atrophy relates more strongly to sleep-wake rhythm fragmentation than to age or any other known risk. *Neurobiology of Learning and Memory*, *160*. https://doi.org/10.1016/j.nlm.2018.05.017

Eknoyan, G. (2008). Adolphe Quetelet (1796–1874)—The average man and indices of obesity. *Nephrology Dialysis Transplantation*, *23*(1), 47–51. https://doi.org/10.1093/ndt/gfm517

Everwijn, S. M. P., Namburete, A. I. L., van Geloven, N., Jansen, F. A. R., Papageorghiou, A. T., Noble, A. J., Teunissen, A. K. K., Rozendaal, L., Blom, N. A., van Lith, J. M. M., & Haak, M. C. (2019). Cortical development in fetuses with congenital heart defects using an automated brain-age prediction algorithm. *Acta Obstetricia et Gynecologica Scandinavica*, *98*(12), 1595–1602. https://doi.org/10.1111/aogs.13687

Falkai, P., Schmitt, A., & Andreasen, N. (2018). Forty years of structural brain imaging in mental disorders: Is it clinically useful or not? *Dialogues in Clinical Neuroscience*, *20*(3), 179–186.

Fava, M. (2000). Weight gain and antidepressants. *The Journal of Clinical Psychiatry*, *61 Suppl 11*, 37–41.

Flint, J. (2023). The genetic basis of major depressive disorder. *Molecular Psychiatry*, *28*(6), 2254–2265. https://doi.org/10.1038/s41380-023-01957-9

Folsom, D. P., Lebowitz, B. D., Lindamer, L. A., Palmer, B. W., Patterson, T. L., & Jeste, D. V. (2006). Schizophrenia in late life: Emerging issues. *Dialogues in Clinical Neuroscience*, *8*(1), 45–52. https://doi.org/10.31887/DCNS.2006.8.1/dfolsom

Fornito, A., Yücel, M., Dean, B., Wood, S. J., & Pantelis, C. (2009). Anatomical abnormalities of the anterior cingulate cortex in schizophrenia: Bridging the gap between neuroimaging and neuropathology. *Schizophrenia Bulletin*, *35*(5), 973–993. https://doi.org/10.1093/schbul/sbn025

Franke, K., Bublak, P., Hoyer, D., Billiet, T., Gaser, C., Witte, O. W., & Schwab, M. (2020). In vivo biomarkers of structural and functional brain development and aging in humans. *Neuroscience and Biobehavioral Reviews*, *117*, 142–164. https://doi.org/10.1016/j.neubiorev.2017.11.002

Franke, K., & Gaser, C. (2019). Ten Years of BrainAGE as a Neuroimaging Biomarker of Brain Aging: What Insights Have We Gained? *Frontiers in Neurology*, *10*. https://doi.org/10.3389/fneur.2019.00789

Franke, K., Ziegler, G., Klöppel, S., & Gaser, C. (2010). Estimating the age of healthy subjects from T1-weighted MRI scans using kernel methods: Exploring the influence of various parameters. *NeuroImage*, *50*(3), 883–892. https://doi.org/10.1016/j.neuroimage.2010.01.005

Friston, K. J., & Frith, C. D. (1995). Schizophrenia: A disconnection syndrome? *Clinical Neuroscience (New York, N.Y.)*, *3*(2), 89–97.

Fusar-Poli, P. (2017). The Clinical High-Risk State for Psychosis (CHR-P), Version II. *Schizophrenia Bulletin*, *43*(1), 44–47. https://doi.org/10.1093/schbul/sbw158

Fusar-Poli, P., Borgwardt, S., Bechdolf, A., Addington, J., Riecher-Rössler, A., Schultze-Lutter, F., Keshavan, M., Wood, S., Ruhrmann, S., Seidman, L. J., Valmaggia, L., Cannon, T., Velthorst, E., De Haan, L., Cornblatt, B., Bonoldi, I., Birchwood, M., McGlashan, T., Carpenter, W., … Yung, A. (2013). The Psychosis High-Risk State. *JAMA Psychiatry*, *70*(1), 107–120. https://doi.org/10.1001/jamapsychiatry.2013.269

Gao, S., Calhoun, V. D., & Sui, J. (2018). Machine learning in major depression: From classification to treatment outcome prediction. *CNS Neuroscience & Therapeutics*, *24*(11), 1037–1052. https://doi.org/10.1111/cns.13048

Gaser, C., Franke, K., Klöppel, S., Koutsouleris, N., Sauer, H., & Initiative, A. D. N. (2013). BrainAGE in Mild Cognitive Impaired Patients: Predicting the Conversion to Alzheimer's Disease. *PLOS ONE*, *8*(6), e67346. https://doi.org/10.1371/journal.pone.0067346

GBD 2017 Causes of Death Collaborators. (2018). Global, regional, and national age-sex-specific mortality for 282 causes of death in 195 countries and territories, 1980-2017: A

systematic analysis for the Global Burden of Disease Study 2017. *Lancet (London, England)*, *392*(10159), 1736–1788. https://doi.org/10.1016/S0140-6736(18)32203-7

GBD Results. (n.d.). Institute for Health Metrics and Evaluation. Retrieved May 19, 2024, from https://vizhub.healthdata.org/gbd-results

Gill, H., Gill, B., El-Halabi, S., Chen-Li, D., Lipsitz, O., Rosenblat, J. D., Van Rheenen, T. E., Rodrigues, N. B., Mansur, R. B., Majeed, A., Lui, L. M. W., Nasri, F., Lee, Y., & Mcintyre, R. S. (2020). Antidepressant Medications and Weight Change: A Narrative Review. *Obesity*, *28*(11), 2064–2072. https://doi.org/10.1002/oby.22969

Gómez-Verdejo, V., Parrado-Hernandez, E., & Tohka, J. (2019). Sign-Consistency Based Variable Importance for Machine Learning in Brain Imaging. *Neuroinformatics*, *17*. https://doi.org/10.1007/s12021-019-9415-3

Good, C. D., Johnsrude, I. S., Ashburner, J., Henson, R. N., Friston, K. J., & Frackowiak, R. S. (2001). A voxel-based morphometric study of ageing in 465 normal adult human brains. *NeuroImage*, *14*(1 Pt 1), 21–36. https://doi.org/10.1006/nimg.2001.0786

Gregor, M. F., & Hotamisligil, G. S. (2011). Inflammatory Mechanisms in Obesity. *Annual Review of Immunology*, *29*(Volume 29, 2011), 415–445. https://doi.org/10.1146/annurev-immunol-031210-101322

Grosu, C., Klauser, P., Dwir, D., Khadimallah, I., Alemán-Gómez, Y., Laaboub, N., Piras, M., Fournier, M., Preisig, M., Conus, P., Draganski, B., & Eap, C. B. (2024). Associations between antipsychotics-induced weight gain and brain networks of impulsivity. *Translational Psychiatry*, *14*(1), 1–9. https://doi.org/10.1038/s41398-024-02881-4

Gubert, C., Stertz, L., Pfaffenseller, B., Panizzutti, B. S., Rezin, G. T., Massuda, R., Streck, E. L., Gama, C. S., Kapczinski, F., & Kunz, M. (2013). Mitochondrial activity and oxidative stress markers in peripheral blood mononuclear cells of patients with bipolar disorder, schizophrenia, and healthy subjects. *Journal of Psychiatric Research*, *47*(10), 1396–1402. https://doi.org/10.1016/j.jpsychires.2013.06.018

Gutierrez Becker, B., Klein, T., & Wachinger, C. (2018). Gaussian process uncertainty in age estimation as a measure of brain abnormality. *NeuroImage*, *175*, 246–258. https://doi.org/10.1016/j.neuroimage.2018.03.075

Haas, S. S., Ge, R., Sanford, N., Modabbernia, A., Reichenberg, A., Whalley, H. C., Kahn, R. S., & Frangou, S. (2022). Accelerated Global and Local Brain Aging Differentiate Cognitively Impaired From Cognitively Spared Patients With Schizophrenia. *Frontiers in Psychiatry*, *13*, 913470. https://doi.org/10.3389/fpsyt.2022.913470

Hahn, T., Ernsting, J., Winter, N. R., Holstein, V., Leenings, R., Beisemann, M., Fisch, L., Sarink, K., Emden, D., Opel, N., Redlich, R., Repple, J., Grotegerd, D., Meinert, S., Hirsch, J. G., Niendorf, T., Endemann, B., Bamberg, F., Kröncke, T., … Berger, K. (2022). An uncertainty-aware, shareable, and transparent neural network architecture for brain-age modeling. *Science Advances*, *8*(1), eabg9471. https://doi.org/10.1126/sciadv.abg9471

Hajek, T., Franke, K., Kolenic, M., Capkova, J., Matejka, M., Propper, L., Uher, R., Stopkova, P., Novak, T., Paus, T., Kopecek, M., Spaniel, F., & Alda, M. (2019). Brain Age in Early Stages of Bipolar Disorders or Schizophrenia. *Schizophrenia Bulletin*, *45*(1), 190–198. https://doi.org/10.1093/schbul/sbx172

Hammers, A., Allom, R., Koepp, M. J., Free, S. L., Myers, R., Lemieux, L., Mitchell, T. N., Brooks, D. J., & Duncan, J. S. (2003). Three-dimensional maximum probability atlas of the human brain, with particular reference to the temporal lobe. *Human Brain Mapping*, *19*(4), 224–247. https://doi.org/10.1002/hbm.10123

Han, J., Kim, S. Y., Lee, J., & Lee, W. H. (2022). Brain Age Prediction: A Comparison between Machine Learning Models Using Brain Morphometric Data. *Sensors*, *22*(20), Article 20. https://doi.org/10.3390/s22208077

Han, L. K. M., Dinga, R., Hahn, T., Ching, C. R. K., Eyler, L. T., Aftanas, L., Aghajani, M., Aleman, A., Baune, B. T., Berger, K., Brak, I., Filho, G. B., Carballedo, A., Connolly, C. G., Couvy-Duchesne, B., Cullen, K. R., Dannlowski, U., Davey, C. G., Dima, D., … Schmaal, L. (2021). Brain aging in major depressive disorder: Results from the

ENIGMA major depressive disorder working group. *Molecular Psychiatry*, *26*(9), 5124–5139. https://doi.org/10.1038/s41380-020-0754-0

Hasher, L., & Zacks, R. T. (1988). Working Memory, Comprehension, and Aging: A Review and a New View. In G. H. Bower (Ed.), *Psychology of Learning and Motivation* (Vol. 22, pp. 193–225). Academic Press. https://doi.org/10.1016/S0079-7421(08)60041-9

Hebb, D. O. (1949). *The organization of behavior; a neuropsychological theory* (pp. xix, 335). Wiley.

Heckers, S., Engstrom, E. J., & Kendler, K. S. (2022). “Manifestations of insanity”: Kraepelin’s final views on psychiatric nosology in their historical context. *Molecular Psychiatry*, *27*(1), 328–334. https://doi.org/10.1038/s41380-021-01232-9

Hedden, T., & Gabrieli, J. D. E. (2004). Insights into the ageing mind: A view from cognitive neuroscience. *Nature Reviews. Neuroscience*, *5*(2), 87–96. https://doi.org/10.1038/nrn1323

Herrera, B. M., Keildson, S., & Lindgren, C. M. (2011). Genetics and epigenetics of obesity. *Maturitas*, *69*(1), 41–49. https://doi.org/10.1016/j.maturitas.2011.02.018

Herrmann, M. J., Tesar, A.-K., Beier, J., Berg, M., & Warrings, B. (2019). Grey matter alterations in obesity: A meta-analysis of whole-brain studies. *Obesity Reviews: An Official Journal of the International Association for the Study of Obesity*, *20*(3), 464–471. https://doi.org/10.1111/obr.12799

Horn, J. L., & Donaldson, G. (1976). On the myth of intellectual decline in adulthood. *American Psychologist*, *31*(10), 701–719. https://doi.org/10.1037/0003-066X.31.10.701

Howes, O. D., Cummings, C., Chapman, G. E., & Shatalina, E. (2023). Neuroimaging in schizophrenia: An overview of findings and their implications for synaptic changes. *Neuropsychopharmacology*, *48*(1), 151–167. https://doi.org/10.1038/s41386-022-01426-x

Huber, G., & Gross, G. (1989). The concept of basic symptoms in schizophrenic and schizoaffective psychoses. *Recenti Progressi in Medicina*, *80*(12), 646–652.

Iyortsuun, N. K., Kim, S.-H., Jhon, M., Yang, H.-J., & Pant, S. (2023). A Review of Machine Learning and Deep Learning Approaches on Mental Health Diagnosis. *Healthcare*, *11*(3). https://doi.org/10.3390/healthcare11030285

Jackson, S. H. D., Weale, M. R., & Weale, R. A. (2003). Biological age—What is it and can it be measured? *Archives of Gerontology and Geriatrics*, *36*(2), 103–115. https://doi.org/10.1016/S0167-4943(02)00060-2

Jamea, A. A., Alblowi, M., Alghamdi, J., Alosaimi, F. D., Albadr, F., Abualait, T., & Bashir, S. (2021). Altered default mode network activity and cortical thickness as vulnerability indicators for SCZ: A preliminary resting state MRI study. *European Review for Medical and Pharmacological Sciences*, *25*(2), 669–677. https://doi.org/10.26355/eurrev_202101_24628

Kahn, R. S., Sommer, I. E., Murray, R. M., Meyer-Lindenberg, A., Weinberger, D. R., Cannon, T. D., O'Donovan, M., Correll, C. U., Kane, J. M., van Os, J., & Insel, T. R. (2015). Schizophrenia. *Nature Reviews. Disease Primers*, *1*, 15067. https://doi.org/10.1038/nrdp.2015.67

Kambeitz, J., Cabral, C., Sacchet, M. D., Gotlib, I. H., Zahn, R., Serpa, M. H., Walter, M., Falkai, P., & Koutsouleris, N. (2017). Detecting Neuroimaging Biomarkers for Depression: A Meta-analysis of Multivariate Pattern Recognition Studies. *Biological Psychiatry*, *82*(5), 330–338. https://doi.org/10.1016/j.biopsych.2016.10.028

Kaufman, J., DeLorenzo, C., Choudhury, S., & Parsey, R. V. (2016). The 5-HT1A receptor in Major Depressive Disorder. *European Neuropsychopharmacology : The Journal of the European College of Neuropsychopharmacology*, *26*(3), 397–410. https://doi.org/10.1016/j.euroneuro.2015.12.039

Kaufmann, T., van der Meer, D., Doan, N. T., Schwarz, E., Lund, M. J., Agartz, I., Alnæs, D., Barch, D. M., Baur-Streubel, R., Bertolino, A., Bettella, F., Beyer, M. K., Bøen, E., Borgwardt, S., Brandt, C. L., Buitelaar, J., Celius, E. G., Cervenka, S., Conzelmann, A., … Westlye, L. T. (2019). Common brain disorders are associated with heritable patterns of apparent aging of the brain. *Nature Neuroscience*, *22*(10), 1617–1623. https://doi.org/10.1038/s41593-019-0471-7

Kaul, V., Enslin, S., & Gross, S. A. (2020). History of artificial intelligence in medicine. *Gastrointestinal Endoscopy*, *92*(4), 807–812. https://doi.org/10.1016/j.gie.2020.06.040

Keys, A., Fidanza, F., Karvonen, M. J., Kimura, N., & Taylor, H. L. (1972). Indices of relative weight and obesity. *Journal of Chronic Diseases*, *25*(6), 329–343. https://doi.org/10.1016/0021-9681(72)90027-6

Kolenic, M., Franke, K., Hlinka, J., Matejka, M., Capkova, J., Pausova, Z., Uher, R., Alda, M., Spaniel, F., & Hajek, T. (2018). Obesity, dyslipidemia and brain age in first-episode psychosis. *Journal of Psychiatric Research*, *99*, 151–158. https://doi.org/10.1016/j.jpsychires.2018.02.012

Kononenko, I. (2001). Machine learning for medical diagnosis: History, state of the art and perspective. *Artificial Intelligence in Medicine*, *23*(1), 89–109. https://doi.org/10.1016/s0933-3657(01)00077-x

Koochakpour, G., Esfandiar, Z., Hosseini-Esfahani, F., Mirmiran, P., Daneshpour, M. S., Sedaghati-Khayat, B., & Azizi, F. (2019). Evaluating the interaction of common FTO genetic variants, added sugar, and trans-fatty acid intakes in altering obesity phenotypes. *Nutrition, Metabolism, and Cardiovascular Diseases: NMCD*, *29*(5), 474–480. https://doi.org/10.1016/j.numecd.2019.01.005

Koutsouleris, N., Davatzikos, C., Borgwardt, S., Gaser, C., Bottlender, R., Frodl, T., Falkai, P., Riecher-Rössler, A., Möller, H.-J., Reiser, M., Pantelis, C., & Meisenzahl, E. (2014). Accelerated brain aging in schizophrenia and beyond: A neuroanatomical marker of psychiatric disorders. *Schizophrenia Bulletin*, *40*(5), 1140–1153. https://doi.org/10.1093/schbul/sbt142

Koutsouleris, N., Dwyer, D. B., Degenhardt, F., Maj, C., Urquijo-Castro, M. F., Sanfelici, R., Popovic, D., Oeztuerk, O., Haas, S. S., Weiske, J., Ruef, A., Kambeitz-Ilankovic, L., Antonucci, L. A., Neufang, S., Schmidt-Kraepelin, C., Ruhrmann, S., Penzel, N., Kambeitz, J., Haidl, T. K., … PRONIA Consortium. (2021). Multimodal Machine Learning Workflows for Prediction of Psychosis in Patients With Clinical High-Risk Syndromes and Recent-Onset Depression. *JAMA Psychiatry*, *78*(2), 195–209. https://doi.org/10.1001/jamapsychiatry.2020.3604

Koutsouleris, N., Kambeitz-Ilankovic, L., Ruhrmann, S., Rosen, M., Ruef, A., Dwyer, D. B., Paolini, M., Chisholm, K., Kambeitz, J., Haidl, T., Schmidt, A., Gillam, J., Schultze-Lutter, F., Falkai, P., Reiser, M., Riecher-Rössler, A., Upthegrove, R., Hietala, J., Salokangas, R. K. R., … PRONIA Consortium. (2018). Prediction Models of Functional Outcomes for Individuals in the Clinical High-Risk State for Psychosis or With Recent-Onset Depression: A Multimodal, Multisite Machine Learning Analysis. *JAMA Psychiatry*, *75*(11), 1156–1172. https://doi.org/10.1001/jamapsychiatry.2018.2165

Koutsouleris, N., Riecher-Rössler, A., Meisenzahl, E. M., Smieskova, R., Studerus, E., Kambeitz-Ilankovic, L., von Saldern, S., Cabral, C., Reiser, M., Falkai, P., & Borgwardt, S. (2015). Detecting the psychosis prodrome across high-risk populations using neuroanatomical biomarkers. *Schizophrenia Bulletin*, *41*(2), 471–482. https://doi.org/10.1093/schbul/sbu078

Kraepelin, E., & Beer, D. (1992). The manifestations of insanity. *History of Psychiatry*, *3*(12), 504–508. https://doi.org/10.1177/0957154X9200301207

Krishnan, A., Williams, L. J., McIntosh, A. R., & Abdi, H. (2011). Partial Least Squares (PLS) methods for neuroimaging: A tutorial and review. *NeuroImage*, *56*(2), 455–475. https://doi.org/10.1016/j.neuroimage.2010.07.034

Kubicki, M., Shenton, M. E., Salisbury, D. F., Hirayasu, Y., Kasai, K., Kikinis, R., Jolesz, F. A., & McCarley, R. W. (2002). Voxel-Based Morphometric Analysis of Gray Matter in First Episode Schizophrenia. *NeuroImage*, *17*(4), 1711–1719. https://doi.org/10.1006/nimg.2002.1296

Kucukgoncu, S., Kosir, U., Zhou, E., Sullivan, E., Srihari, V. H., & Tek, C. (2019). Glucose metabolism dysregulation at the onset of mental illness is not limited to first episode psychosis: A systematic review and meta-analysis. *Early Intervention in Psychiatry*, *13*(5), 1021–1031. https://doi.org/10.1111/eip.12749

Kuo, C.-Y., Lee, P.-L., Hung, S.-C., Liu, L.-K., Lee, W.-J., Chung, C.-P., Yang, A. C., Tsai, S.-J., Wang, P.-N., Chen, L.-K., Chou, K.-H., & Lin, C.-P. (2020). Large-Scale Structural Covariance Networks Predict Age in Middle-to-Late Adulthood: A Novel Brain Aging

Biomarker. *Cerebral Cortex (New York, N.Y.: 1991)*, *30*(11), 5844–5862. https://doi.org/10.1093/cercor/bhaa161

Kupfer, D. J., & Frank, E. (2003). Comorbidity in depression. *Acta Psychiatrica Scandinavica. Supplementum*, *418*, 57–60. https://doi.org/10.1034/j.1600-0447.108.s418.12.x

Lalousis, P. A., Schmaal, L., Wood, S. J., Reniers, R. L. E. P., Barnes, N. M., Chisholm, K., Griffiths, S. L., Stainton, A., Wen, J., Hwang, G., Davatzikos, C., Wenzel, J., Kambeitz-Ilankovic, L., Andreou, C., Bonivento, C., Dannlowski, U., Ferro, A., Lichtenstein, T., Riecher-Rössler, A., … PRONIA Consortium. (2022). Neurobiologically Based Stratification of Recent-Onset Depression and Psychosis: Identification of Two Distinct Transdiagnostic Phenotypes. *Biological Psychiatry*, *92*(7), 552–562. https://doi.org/10.1016/j.biopsych.2022.03.021

Lê Cao, K.-A., Rossouw, D., Robert-Granié, C., & Besse, P. (2008). A sparse PLS for variable selection when integrating omics data. *Statistical Applications in Genetics and Molecular Biology*, *7*(1), Article 35. https://doi.org/10.2202/1544-6115.1390

Leutner, M., Dervic, E., Bellach, L., Klimek, P., Thurner, S., & Kautzky, A. (2023). Obesity as pleiotropic risk state for metabolic and mental health throughout life. *Translational Psychiatry*, *13*, 175. https://doi.org/10.1038/s41398-023-02447-w

Li, L., Yu, H., Zhong, M., Liu, S., Wei, W., Meng, Y., Li, M.-L., Li, T., & Wang, Q. (2022). Gray matter volume alterations in subjects with overweight and obesity: Evidence from a voxel-based meta-analysis. *Frontiers in Psychiatry*, *13*, 955741. https://doi.org/10.3389/fpsyt.2022.955741

Liang, J., Matheson, BE., Kaye, WH., & Boutelle, KN. (2014). Neurocognitive correlates of obesity and obesity-related behaviors in children and adolescents. *International Journal of Obesity (2005)*, *38*(4), 494–506. https://doi.org/10.1038/ijo.2013.142

Limosin, F., Gasquet, I., Leguay, D., Azorin, J.-M., & Rouillon, F. (2008). Body mass index and prevalence of obesity in a French cohort of patients with schizophrenia. *Acta Psychiatrica Scandinavica*, *118*(1), 19–25. https://doi.org/10.1111/j.1600-0447.2008.01208.x

Lin, S.-H., Tseng, H.-H., Tsai, H. C., Chi, M. H., Lee, I. H., Chen, P. S., Chen, K. C., & Yang, Y. K. (2021). Positive Symptoms in Antipsychotic-naïve Schizophrenia are Associated with Increased Body Mass Index after Treatment. *Clinical Psychopharmacology and Neuroscience*, *19*(1), 155–159. https://doi.org/10.9758/cpn.2021.19.1.155

Lin, X., & Li, H. (2021). Obesity: Epidemiology, Pathophysiology, and Therapeutics. *Frontiers in Endocrinology*, *12*, 706978. https://doi.org/10.3389/fendo.2021.706978

Loch, A. A., Gondim, J. M., Argolo, F. C., Lopes-Rocha, A. C., Andrade, J. C., van de Bilt, M. T., de Jesus, L. P., Haddad, N. M., Cecchi, G. A., Mota, N. B., Gattaz, W. F., Corcoran, C. M., & Ara, A. (2023). Detecting at-risk mental states for psychosis (ARMS) using machine learning ensembles and facial features. *Schizophrenia Research*, *258*, 45–52. https://doi.org/10.1016/j.schres.2023.07.011

López-Otín, C., Blasco, M. A., Partridge, L., Serrano, M., & Kroemer, G. (2013). The Hallmarks of Aging. *Cell*, *153*(6), 1194. https://doi.org/10.1016/j.cell.2013.05.039

Lopresti, A., & Drummond, P. (2013). Obesity and psychiatric disorders: Commonalities in dysregulated biological pathways and their implications for treatment. *Progress in Neuro-Psychopharmacology & Biological Psychiatry*, *45*. https://doi.org/10.1016/j.pnpbp.2013.05.005

Luckhoff, H. K., Asmal, L., Scheffler, F., Phahladira, L., Smit, R., van den Heuvel, L., Fouche, J. P., Seedat, S., Emsley, R., & du Plessis, S. (2022). Associations between BMI and brain structures involved in food intake regulation in first-episode schizophrenia spectrum disorders and healthy controls. *Journal of Psychiatric Research*, *152*, 250–259. https://doi.org/10.1016/j.jpsychires.2022.06.024

Luppino, F. S., de Wit, L. M., Bouvy, P. F., Stijnen, T., Cuijpers, P., Penninx, B. W. J. H., & Zitman, F. G. (2010). Overweight, Obesity, and Depression: A Systematic Review and Meta-analysis of Longitudinal Studies. *Archives of General Psychiatry*, *67*(3), 220–229. https://doi.org/10.1001/archgenpsychiatry.2010.2

Luvsannyam, E., Jain, M. S., Pormento, M. K. L., Siddiqui, H., Balagtas, A. R. A., Emuze, B. O., & Poprawski, T. (2022). Neurobiology of Schizophrenia: A Comprehensive Review. *Cureus*, *14*(4), e23959. https://doi.org/10.7759/cureus.23959

Mahfoud, D., Fekih-Romdhane, F., Abou Zeid, J., Rustom, L., Mouez, C., Haddad, G., & Hallit, S. (2023). Functionality appreciation is inversely associated with positive psychotic symptoms in overweight/obese patients with schizophrenia. *BMC Psychiatry*, *23*(1), 306. https://doi.org/10.1186/s12888-023-04795-9

Maj, M. (2005). 'Psychiatric comorbidity': An artefact of current diagnostic systems? *The British Journal of Psychiatry*, *186*(3), 182–184. https://doi.org/10.1192/bjp.186.3.182

Mamdani, F., Rollins, B., Morgan, L., Myers, R. M., Barchas, J. D., Schatzberg, A. F., Watson, S. J., Akil, H., Potkin, S. G., Bunney, W. E., Vawter, M. P., & Sequeira, P. A. (2015). Variable telomere length across post-mortem human brain regions and specific reduction in the hippocampus of major depressive disorder. *Translational Psychiatry*, *5*(9), e636–e636. https://doi.org/10.1038/tp.2015.134

Mangurian, C., Newcomer, J. W., Modlin, C., & Schillinger, D. (2016). Diabetes and Cardiovascular Care Among People with Severe Mental Illness: A Literature Review. *Journal of General Internal Medicine*, *31*(9), 1083–1091. https://doi.org/10.1007/s11606-016-3712-4

Marquand, A. F., Kia, S. M., Zabihi, M., Wolfers, T., Buitelaar, J. K., & Beckmann, C. F. (2019). Conceptualizing mental disorders as deviations from normative functioning. *Molecular Psychiatry*, *24*(10), 1415–1424. https://doi.org/10.1038/s41380-019-0441-1

Martins, L. B., Monteze, N. M., Calarge, C., Ferreira, A. V. M., & Teixeira, A. L. (2019). Pathways linking obesity to neuropsychiatric disorders. *Nutrition*, *66*, 16–21. https://doi.org/10.1016/j.nut.2019.03.017

Marx, W., Lane, M., Hockey, M., Aslam, H., Berk, M., Walder, K., Borsini, A., Firth, J., Pariante, C. M., Berding, K., Cryan, J. F., Clarke, G., Craig, J. M., Su, K.-P., Mischoulon, D., Gomez-Pinilla, F., Foster, J. A., Cani, P. D., Thuret, S., … Jacka, F. N. (2021). Diet and

depression: Exploring the biological mechanisms of action. *Molecular Psychiatry*, *26*(1), 134–150. https://doi.org/10.1038/s41380-020-00925-x

McElroy, S. L. (2009). Obesity in patients with severe mental illness: Overview and management. *The Journal of Clinical Psychiatry*, *70 Suppl 3*, 12–21. https://doi.org/10.4088/JCP.7075su1c.03

McGrath, J. J., Lim, C. C. W., Plana-Ripoll, O., Holtz, Y., Agerbo, E., Momen, N. C., Mortensen, P. B., Pedersen, C. B., Abdulmalik, J., Aguilar-Gaxiola, S., Al-Hamzawi, A., Alonso, J., Bromet, E. J., Bruffaerts, R., Bunting, B., de Almeida, J. M. C., de Girolamo, G., De Vries, Y. A., Florescu, S., … de Jonge, P. (2020). Comorbidity within mental disorders: A comprehensive analysis based on 145 990 survey respondents from 27 countries. *Epidemiology and Psychiatric Sciences*, *29*, e153. https://doi.org/10.1017/S2045796020000633

McWhinney, S., Kolenic, M., Franke, K., Fialova, M., Knytl, P., Matejka, M., Spaniel, F., & Hajek, T. (2021). Obesity as a Risk Factor for Accelerated Brain-ageing in First-Episode Psychosis—A Longitudinal Study. *Schizophrenia Bulletin*, *47*(6), 1772–1781. https://doi.org/10.1093/schbul/sbab064

McWhinney, S. R., Brosch, K., Calhoun, V. D., Crespo-Facorro, B., Crossley, N. A., Dannlowski, U., Dickie, E., Dietze, L. M. F., Donohoe, G., Du Plessis, S., Ehrlich, S., Emsley, R., Furstova, P., Glahn, D. C., Gonzalez- Valderrama, A., Grotegerd, D., Holleran, L., Kircher, T. T. J., Knytl, P., … Hajek, T. (2022). Obesity and brain structure in schizophrenia – ENIGMA study in 3021 individuals. *Molecular Psychiatry*, *27*(9), 3731–3737. https://doi.org/10.1038/s41380-022-01616-5

Meyer, J. H., Cervenka, S., Kim, M.-J., Kreisl, W. C., Henter, I. D., & Innis, R. B. (2020). Neuroinflammation in psychiatric disorders: PET imaging and promising new targets. *The Lancet. Psychiatry*, *7*(12), 1064–1074. https://doi.org/10.1016/S2215-0366(20)30255-8

Mezquida, G., Savulich, G., Garcia-Rizo, C., Garcia-Portilla, M. P., Toll, A., Garcia-Alvarez, L., Bobes, J., Mané, A., Bernardo, M., & Fernandez-Egea, E. (2018). Inverse association

between negative symptoms and body mass index in chronic schizophrenia. *Schizophrenia Research*, *192*, 69–74. https://doi.org/10.1016/j.schres.2017.04.002

Michaud, M., Balardy, L., Moulis, G., Gaudin, C., Peyrot, C., Vellas, B., Cesari, M., & Nourhashemi, F. (2013). Proinflammatory cytokines, aging, and age-related diseases. *Journal of the American Medical Directors Association*, *14*(12), 877–882. https://doi.org/10.1016/j.jamda.2013.05.009

Mihalik, A., Chapman, J., Adams, R. A., Winter, N. R., Ferreira, F. S., Shawe-Taylor, J., & Mourão-Miranda, J. (2022). Canonical Correlation Analysis and Partial Least Squares for Identifying Brain–Behavior Associations: A Tutorial and a Comparative Study. *Biological Psychiatry: Cognitive Neuroscience and Neuroimaging*, *7*(11), 1055–1067. https://doi.org/10.1016/j.bpsc.2022.07.012

Miles, W. R. (1933). Age and human ability. *Psychological Review*, *40*(2), 99–123. https://doi.org/10.1037/h0075341

Minichino, A., Ando', A., Francesconi, M., Salatino, A., Delle Chiaie, R., & Cadenhead, K. (2017). Investigating the link between drug-naive first episode psychoses (FEPs), weight gain abnormalities and brain structural damages: Relevance and implications for therapy. *Progress in Neuro-Psychopharmacology and Biological Psychiatry*, *77*, 9–22. https://doi.org/10.1016/j.pnpbp.2017.03.020

Mitchell, R. (2013). Is physical activity in natural environments better for mental health than physical activity in other environments? *Social Science & Medicine*, *91*, 130–134. https://doi.org/10.1016/j.socscimed.2012.04.012

Monteiro, J. M., Rao, A., Shawe-Taylor, J., & Mourão-Miranda, J. (2016). A multiple hold-out framework for Sparse Partial Least Squares. *Journal of Neuroscience Methods*, *271*, 182–194. https://doi.org/10.1016/j.jneumeth.2016.06.011

Moreno-Navarrete, J. M., Blasco, G., Puig, J., Biarnés, C., Rivero, M., Gich, J., Fernández-Aranda, F., Garre-Olmo, J., Ramió-Torrentà, L., Alberich-Bayarri, Á., García-Castro, F., Pedraza, S., Ricart, W., & Fernández-Real, J. M. (2017). Neuroinflammation in obesity: Circulating lipopolysaccharide-binding protein associates with brain structure and

cognitive performance. *International Journal of Obesity*, *41*(11), 1627–1635. https://doi.org/10.1038/ijo.2017.162

Moskalev, A. A., Shaposhnikov, M. V., Plyusnina, E. N., Zhavoronkov, A., Budovsky, A., Yanai, H., & Fraifeld, V. E. (2013). The role of DNA damage and repair in aging through the prism of Koch-like criteria. *Ageing Research Reviews*, *12*(2), 661–684. https://doi.org/10.1016/j.arr.2012.02.001

Mulugeta, A., Zhou, A., Power, C., & Hyppönen, E. (2018). Obesity and depressive symptoms in mid-life: A population-based cohort study. *BMC Psychiatry*, *18*(1), 297. https://doi.org/10.1186/s12888-018-1877-6

Najjar, S., Pearlman, D. M., Alper, K., Najjar, A., & Devinsky, O. (2013). Neuroinflammation and psychiatric illness. *Journal of Neuroinflammation*, *10*, 43. https://doi.org/10.1186/1742-2094-10-43

Nenadić, I., Dietzek, M., Langbein, K., Sauer, H., & Gaser, C. (2017). BrainAGE score indicates accelerated brain aging in schizophrenia, but not bipolar disorder. *Psychiatry Research. Neuroimaging*, *266*, 86–89. https://doi.org/10.1016/j.pscychresns.2017.05.006

Nestler, E. J., & Carlezon, W. A. (2006). The Mesolimbic Dopamine Reward Circuit in Depression. *Biological Psychiatry*, *59*(12), 1151–1159. https://doi.org/10.1016/j.biopsych.2005.09.018

Opel, N., Redlich, R., Grotegerd, D., Dohm, K., Heindel, W., Kugel, H., Arolt, V., & Dannlowski, U. (2015). Obesity and major depression: Body-mass index (BMI) is associated with a severe course of disease and specific neurostructural alterations. *Psychoneuroendocrinology*, *51*, 219–226. https://doi.org/10.1016/j.psyneuen.2014.10.001

Opel, N., Redlich, R., Grotegerd, D., Dohm, K., Zaremba, D., Meinert, S., Bürger, C., Plümpe, L., Alferink, J., Heindel, W., Kugel, H., Zwanzger, P., Arolt, V., & Dannlowski, U. (2017). Prefrontal brain responsiveness to negative stimuli distinguishes familial risk for major depression from acute disorder. *Journal of Psychiatry & Neuroscience : JPN*, *42*(5), 343–352. https://doi.org/10.1503/jpn.160198

Organization, W. H. (2005). *Surveillance of chronic disease risk factors: Country level data and comparable estimates*. World Health Organization. https://iris.who.int/handle/10665/43190

Oswald, W. D. (2000). [Can age and aging be measured?]. *Zeitschrift Fur Gerontologie Und Geriatrie*, *33 Suppl 1*, 8–14. https://doi.org/10.1007/s003910070002

Panariello, F., De Luca, V., & de Bartolomeis, A. (2011). Weight gain, schizophrenia and antipsychotics: New findings from animal model and pharmacogenomic studies. *Schizophrenia Research and Treatment*, *2011*, 459284. https://doi.org/10.1155/2011/459284

Panuganti, K. K., Nguyen, M., & Kshirsagar, R. K. (2024). Obesity. In *StatPearls*. StatPearls Publishing. http://www.ncbi.nlm.nih.gov/books/NBK459357/

Park, D. C., Polk, T. A., Mikels, J. A., Taylor, S. F., & Marshuetz, C. (2001). Cerebral aging: Integration of brain and behavioral models of cognitive function. *Dialogues in Clinical Neuroscience*, *3*(3), 151–165. https://doi.org/10.31887/DCNS.2001.3.3/dcpark

Parvandeh, S., Yeh, H.-W., Paulus, M. P., & McKinney, B. A. (2020). Consensus features nested cross-validation. *Bioinformatics (Oxford, England)*, *36*(10), 3093–3098. https://doi.org/10.1093/bioinformatics/btaa046

Patel, V., & Saxena, S. (2014). Transforming lives, enhancing communities—Innovations in global mental health. *The New England Journal of Medicine*, *370*(6), 498–501. https://doi.org/10.1056/NEJMp1315214

Pearson, D. E., Eren, Ö., Ortega, Y. K., Hierro, J. L., Karakuş, B., Kala, S., Bullington, L., & Lekberg, Y. (2022). Combining biogeographical approaches to advance invasion ecology and methodology. *Journal of Ecology*, *110*(9), 2033–2045. https://doi.org/10.1111/1365-2745.13945

Penninx, B. W. J. H., & Lange, S. M. M. (2018). Metabolic syndrome in psychiatric patients: Overview, mechanisms, and implications. *Dialogues in Clinical Neuroscience*, *20*(1), 63–73.

Pettersson-Yeo, W., Allen, P., Benetti, S., McGuire, P., & Mechelli, A. (2011). Dysconnectivity in schizophrenia: Where are we now? *Neuroscience and Biobehavioral Reviews*, *35*(5), 1110–1124. https://doi.org/10.1016/j.neubiorev.2010.11.004

Pfefferbaum, A., Mathalon, D. H., Sullivan, E. V., Rawles, J. M., Zipursky, R. B., & Lim, K. O. (1994). A quantitative magnetic resonance imaging study of changes in brain morphology from infancy to late adulthood. *Archives of Neurology*, *51*(9), 874–887. https://doi.org/10.1001/archneur.1994.00540210046012

Phelps, N. H., Singleton, R. K., Zhou, B., Heap, R. A., Mishra, A., Bennett, J. E., Paciorek, C. J., Lhoste, V. P., Carrillo-Larco, R. M., Stevens, G. A., Rodriguez-Martinez, A., Bixby, H., Bentham, J., Cesare, M. D., Danaei, G., Rayner, A. W., Barradas-Pires, A., Cowan, M. J., Savin, S., … Ezzati, M. (2024). Worldwide trends in underweight and obesity from 1990 to 2022: A pooled analysis of 3663 population-representative studies with 222 million children, adolescents, and adults. *The Lancet*, *403*(10431), 1027–1050. https://doi.org/10.1016/S0140-6736(23)02750-2

Popovic, D., Ruef, A., Dwyer, D. B., Antonucci, L. A., Eder, J., Sanfelici, R., Kambeitz-Ilankovic, L., Oztuerk, O. F., Dong, M. S., Paul, R., Paolini, M., Hedderich, D., Haidl, T., Kambeitz, J., Ruhrmann, S., Chisholm, K., Schultze-Lutter, F., Falkai, P., Pergola, G., … Piccin, S. (2020). Traces of Trauma: A Multivariate Pattern Analysis of Childhood Trauma, Brain Structure, and Clinical Phenotypes. *Biological Psychiatry*, *88*(11), 829–842. https://doi.org/10.1016/j.biopsych.2020.05.020

Ranjbar, S., Pai, N., & Deng, C. (2013). The association of antidepressant medication and body weight gain. *Faculty of Science, Medicine and Health - Papers: Part A*, 1–9.

Remes, O., Mendes, J. F., & Templeton, P. (2021). Biological, Psychological, and Social Determinants of Depression: A Review of Recent Literature. *Brain Sciences*, *11*(12). https://doi.org/10.3390/brainsci11121633

Resnick, S. M., Pham, D. L., Kraut, M. A., Zonderman, A. B., & Davatzikos, C. (2003). Longitudinal Magnetic Resonance Imaging Studies of Older Adults: A Shrinking Brain. *The Journal of Neuroscience*, *23*(8), 3295–3301. https://doi.org/10.1523/JNEUROSCI.23-08-03295.2003

Rolls, E. T., Huang, C.-C., Lin, C.-P., Feng, J., & Joliot, M. (2020). Automated anatomical labelling atlas 3. *NeuroImage*, *206*, 116189. https://doi.org/10.1016/j.neuroimage.2019.116189

Ronan, L., Alexander-Bloch, A. F., Wagstyl, K., Farooqi, S., Brayne, C., Tyler, L. K., Cam-CAN, & Fletcher, P. C. (2016). Obesity associated with increased brain age from midlife. *Neurobiology of Aging*, *47*, 63–70. https://doi.org/10.1016/j.neurobiolaging.2016.07.010

Rutherford, S., Kia, S. M., Wolfers, T., Fraza, C., Zabihi, M., Dinga, R., Berthet, P., Worker, A., Verdi, S., Ruhe, H. G., Beckmann, C. F., & Marquand, A. F. (2022). The normative modeling framework for computational psychiatry. *Nature Protocols*, *17*(7), 1711–1734. https://doi.org/10.1038/s41596-022-00696-5

Ryan, M. C. M., Collins, P., & Thakore, J. H. (2003). Impaired fasting glucose tolerance in first-episode, drug-naive patients with schizophrenia. *The American Journal of Psychiatry*, *160*(2), 284–289. https://doi.org/10.1176/appi.ajp.160.2.284

Sadeghirad, B., Duhaney, T., Motaghipisheh, S., Campbell, N. R. C., & Johnston, B. C. (2016). Influence of unhealthy food and beverage marketing on children's dietary intake and preference: A systematic review and meta-analysis of randomized trials. *Obesity Reviews: An Official Journal of the International Association for the Study of Obesity*, *17*(10), 945–959. https://doi.org/10.1111/obr.12445

Sahpolat, M., Ayar, D., Ari, M., & Karaman, M. A. (2021). Elevated Monocyte to High-density Lipoprotein Ratios as an Inflammation Markers for Schizophrenia Patients. *Clinical Psychopharmacology and Neuroscience*, *19*(1), 112. https://doi.org/10.9758/cpn.2021.19.1.112

Salazar de Pablo, G., Woods, S. W., Drymonitou, G., de Diego, H., & Fusar-Poli, P. (2021). Prevalence of Individuals at Clinical High-Risk of Psychosis in the General Population and Clinical Samples: Systematic Review and Meta-Analysis. *Brain Sciences*, *11*(11), Article 11. https://doi.org/10.3390/brainsci11111544

Salthouse, T. A. (1996). The processing-speed theory of adult age differences in cognition. *Psychological Review*, *103*(3), 403–428. https://doi.org/10.1037/0033-295X.103.3.403

Saxena, A., Patel, D., Ayesha, I. E., Monson, N. R., Klair, N., Patel, U., & Khan, S. (2023). Metabolic Syndrome Causing Cognitive Impairment in Patients With Schizophrenia: A Systematic Review. *Cureus*, *15*(10). https://doi.org/10.7759/cureus.47587

Schaefer, A., Kong, R., Gordon, E. M., Laumann, T. O., Zuo, X.-N., Holmes, A. J., Eickhoff, S. B., & Yeo, B. T. T. (2018). Local-Global Parcellation of the Human Cerebral Cortex from Intrinsic Functional Connectivity MRI. *Cerebral Cortex*, *28*(9), 3095–3114. https://doi.org/10.1093/cercor/bhx179

Schmaal, L., Hibar, D. P., Sämann, P. G., Hall, G. B., Baune, B. T., Jahanshad, N., Cheung, J. W., van Erp, T. G. M., Bos, D., Ikram, M. A., Vernooij, M. W., Niessen, W. J., Tiemeier, H., Hofman, A., Wittfeld, K., Grabe, H. J., Janowitz, D., Bülow, R., Selonke, M., … Veltman, D. J. (2017). Cortical abnormalities in adults and adolescents with major depression based on brain scans from 20 cohorts worldwide in the ENIGMA Major Depressive Disorder Working Group. *Molecular Psychiatry*, *22*(6), 900–909. https://doi.org/10.1038/mp.2016.60

Schnack, H. G., van Haren, N. E. M., Nieuwenhuis, M., Hulshoff Pol, H. E., Cahn, W., & Kahn, R. S. (2016). Accelerated Brain Aging in Schizophrenia: A Longitudinal Pattern Recognition Study. *The American Journal of Psychiatry*, *173*(6), 607–616. https://doi.org/10.1176/appi.ajp.2015.15070922

Schneider-Thoma, J., Efthimiou, O., Bighelli, I., Dörries, C., Huhn, M., Krause, M., Reichelt, L., Röder, H., Furukawa, T. A., Davis, J. M., & Leucht, S. (2019). Second-generation antipsychotic drugs and short-term somatic serious adverse events: A systematic review and meta-analysis. *The Lancet. Psychiatry*, *6*(9), 753–765. https://doi.org/10.1016/S2215-0366(19)30223-8

Seitz-Holland, J., Haas, S. S., Penzel, N., Reichenberg, A., & Pasternak, O. (2024). BrainAGE, brain health, and mental disorders: A systematic review. *Neuroscience & Biobehavioral Reviews*, *159*, 105581. https://doi.org/10.1016/j.neubiorev.2024.105581

Shahab, S., Mulsant, B. H., Levesque, M. L., Calarco, N., Nazeri, A., Wheeler, A. L., Foussias, G., Rajji, T. K., & Voineskos, A. N. (2019). Brain structure, cognition, and brain age in schizophrenia, bipolar disorder, and healthy controls. *Neuropsychopharmacology:*

Official Publication of the American College of Neuropsychopharmacology, *44*(5), 898–906. https://doi.org/10.1038/s41386-018-0298-z

Shen, C.-L., Tsai, S.-J., Lin, C.-P., & Yang, A. C. (2023). Progressive brain abnormalities in schizophrenia across different illness periods: A structural and functional MRI study. *Schizophrenia*, *9*(1), 1–9. https://doi.org/10.1038/s41537-022-00328-7

Shenton, M. E., Dickey, C. C., Frumin, M., & McCarley, R. W. (2001). A review of MRI findings in schizophrenia. *Schizophrenia Research*, *49*(1–2), 1–52. https://doi.org/10.1016/s0920-9964(01)00163-3

Smith, S. M., Vidaurre, D., Alfaro-Almagro, F., Nichols, T. E., & Miller, K. L. (2019). Estimation of brain age delta from brain imaging. *NeuroImage*, *200*, 528–539. https://doi.org/10.1016/j.neuroimage.2019.06.017

Solmi, M., Soardo, L., Kaur, S., Azis, M., Cabras, A., Censori, M., Fausti, L., Besana, F., Salazar de Pablo, G., & Fusar-Poli, P. (2023). Meta-analytic prevalence of comorbid mental disorders in individuals at clinical high risk of psychosis: The case for transdiagnostic assessment. *Molecular Psychiatry*, *28*(6), 2291–2300. https://doi.org/10.1038/s41380-023-02029-8

Sowell, E. R., Thompson, P. M., Leonard, C. M., Welcome, S. E., Kan, E., & Toga, A. W. (2004). Longitudinal mapping of cortical thickness and brain growth in normal children. *The Journal of Neuroscience: The Official Journal of the Society for Neuroscience*, *24*(38), 8223–8231. https://doi.org/10.1523/JNEUROSCI.1798-04.2004

Spear, L. P. (2013). Adolescent Neurodevelopment. *The Journal of Adolescent Health : Official Publication of the Society for Adolescent Medicine*, *52*(2 0 2), S7-13. https://doi.org/10.1016/j.jadohealth.2012.05.006

Stadler, J. T., & Marsche, G. (2020). Obesity-Related Changes in High-Density Lipoprotein Metabolism and Function. *International Journal of Molecular Sciences*, *21*(23), 8985. https://doi.org/10.3390/ijms21238985

Steenblock, C., Hassanein, M., Khan, E. G., Yaman, M., Kamel, M., Barbir, M., Lorke, D. E., Everett, D., Bejtullah, S., Lohmann, T., Lindner, U., Tahirukaj, E., Jirjees, F. J., Soliman,

S. S. M., Quitter, F., & Bornstein, S. R. (2022). Obesity and COVID-19: What are the Consequences? *Hormone and Metabolic Research*, *54*(8), 496–502. https://doi.org/10.1055/a-1878-9757

Steffen, A., Nübel, J., Jacobi, F., Bätzing, J., & Holstiege, J. (2020). Mental and somatic comorbidity of depression: A comprehensive cross-sectional analysis of 202 diagnosis groups using German nationwide ambulatory claims data. *BMC Psychiatry*, *20*(1), 142. https://doi.org/10.1186/s12888-020-02546-8

Stein, D. J., Fernandes Medeiros, L., Caumo, W., & Torres, I. L. (2020). Transcranial Direct Current Stimulation in Patients with Anxiety: Current Perspectives. *Neuropsychiatric Disease and Treatment*, *16*, 161–169. https://doi.org/10.2147/NDT.S195840

Stunkard, A. J., Faith, M. S., & Allison, K. C. (2003). Depression and obesity. *Biological Psychiatry*, *54*(3), 330–337. https://doi.org/10.1016/S0006-3223(03)00608-5

Tamminga, C. A., Thaker, G. K., Buchanan, R., Kirkpatrick, B., Alphs, L. D., Chase, T. N., & Carpenter, W. T. (1992). Limbic system abnormalities identified in schizophrenia using positron emission tomography with fluorodeoxyglucose and neocortical alterations with deficit syndrome. *Archives of General Psychiatry*, *49*(7), 522–530. https://doi.org/10.1001/archpsyc.1992.01820070016003

Terribilli, D., Schaufelberger, M. S., Duran, F. L. S., Zanetti, M. V., Curiati, P. K., Menezes, P. R., Scazufca, M., Amaro, E., Leite, C. C., & Busatto, G. F. (2011). Age-related gray matter volume changes in the brain during non-elderly adulthood. *Neurobiology of Aging*, *32*(2–6), 354–368. https://doi.org/10.1016/j.neurobiolaging.2009.02.008

Thomas Yeo, B. T., Krienen, F. M., Sepulcre, J., Sabuncu, M. R., Lashkari, D., Hollinshead, M., Roffman, J. L., Smoller, J. W., Zöllei, L., Polimeni, J. R., Fischl, B., Liu, H., & Buckner, R. L. (2011). The organization of the human cerebral cortex estimated by intrinsic functional connectivity. *Journal of Neurophysiology*, *106*(3), 1125–1165. https://doi.org/10.1152/jn.00338.2011

Treur, J. L. (2022). Commentary on Whitsel et al.: Smoking, alcohol use and the brain- the challenge of answering causal questions. *Addiction*, *117*(4), 1060–1061. https://doi.org/10.1111/add.15802

Tsai, S.-Y., Sajatovic, M., Hsu, J.-L., Chung, K.-H., Chen, P.-H., & Huang, Y.-J. (2020). Body mass index, residual psychotic symptoms, and inflammation associated with brain volume reduction in older patients with schizophrenia. *International Journal of Geriatric Psychiatry*, *35*(7), 728–736. https://doi.org/10.1002/gps.5291

Ursu, S., Kring, A. M., Gard, M. G., Minzenberg, M. J., Yoon, J. H., Ragland, J. D., Solomon, M., & Carter, C. S. (2011). Prefrontal cortical deficits and impaired cognition-emotion interactions in schizophrenia. *The American Journal of Psychiatry*, *168*(3), 276–285. https://doi.org/10.1176/appi.ajp.2010.09081215

Vancampfort, D., Stubbs, B., Mitchell, A. J., De Hert, M., Wampers, M., Ward, P. B., Rosenbaum, S., & Correll, C. U. (2015). Risk of metabolic syndrome and its components in people with schizophrenia and related psychotic disorders, bipolar disorder and major depressive disorder: A systematic review and meta-analysis. *World Psychiatry: Official Journal of the World Psychiatric Association (WPA)*, *14*(3), 339–347. https://doi.org/10.1002/wps.20252

Vandermeer, M. R. J., Liu, P., Mohamed Ali, O., Daoust, A. R., Joanisse, M. F., Barch, D. M., & Hayden, E. P. (2020). Orbitofrontal cortex grey matter volume is related to children's depressive symptoms. *NeuroImage : Clinical*, *28*, 102395. https://doi.org/10.1016/j.nicl.2020.102395

Velloso, L. A. (2009). The brain is the conductor: Diet-induced inflammation overlapping physiological control of body mass and metabolism. *Arquivos Brasileiros De Endocrinologia E Metabologia*, *53*(2), 151–158. https://doi.org/10.1590/s0004-27302009000200006

Weiss, F., Barbuti, M., Carignani, G., Calderone, A., Santini, F., Maremmani, I., & Perugi, G. (2020). Psychiatric Aspects of Obesity: A Narrative Review of Pathophysiology and Psychopathology. *Journal of Clinical Medicine*, *9*(8), 2344. https://doi.org/10.3390/jcm9082344

Weizenbaum, J. (1966). ELIZA—a computer program for the study of natural language communication between man and machine. *Communications of the ACM*, *9*(1), 36–45. https://doi.org/10.1145/365153.365168

Wilson, P. W. F., D'Agostino, R. B., Parise, H., Sullivan, L., & Meigs, J. B. (2005). Metabolic syndrome as a precursor of cardiovascular disease and type 2 diabetes mellitus. *Circulation*, *112*(20), 3066–3072. https://doi.org/10.1161/CIRCULATIONAHA.105.539528

Wittchen, H. U., Jacobi, F., Rehm, J., Gustavsson, A., Svensson, M., Jönsson, B., Olesen, J., Allgulander, C., Alonso, J., Faravelli, C., Fratiglioni, L., Jennum, P., Lieb, R., Maercker, A., van Os, J., Preisig, M., Salvador-Carulla, L., Simon, R., & Steinhausen, H.-C. (2011). The size and burden of mental disorders and other disorders of the brain in Europe 2010. *European Neuropsychopharmacology: The Journal of the European College of Neuropsychopharmacology*, *21*(9), 655–679. https://doi.org/10.1016/j.euroneuro.2011.07.018

Wolfers, T., Doan, N. T., Kaufmann, T., Alnæs, D., Moberget, T., Agartz, I., Buitelaar, J. K., Ueland, T., Melle, I., Franke, B., Andreassen, O. A., Beckmann, C. F., Westlye, L. T., & Marquand, A. F. (2018). Mapping the Heterogeneous Phenotype of Schizophrenia and Bipolar Disorder Using Normative Models. *JAMA Psychiatry*, *75*(11), 1146–1155. https://doi.org/10.1001/jamapsychiatry.2018.2467

Wolin, K. Y. (2009). *Obesity / Kathleen Y. Wolin, and Jennifer M. Petrelli.* Greenwood Press/ABC-CLIO.

Xu, W., Wang, Z., Hong, L., He, L., & Chen, X. (2015). The uncertainty recovery analysis for interdependent infrastructure systems using the dynamic inoperability input–output model. *International Journal of Systems Science*. https://www.tandfonline.com/doi/abs/10.1080/00207721.2013.822121

Yan, H., Lau, W. K. W., Eickhoff, S. B., Long, J., Song, X., Wang, C., Zhao, J., Feng, X., Huang, R., Wang, M., Zhang, X., & Zhang, R. (2022). Charting the neural circuits disruption in inhibitory control and its subcomponents across psychiatric disorders: A neuroimaging

meta-analysis. *Progress in Neuro-Psychopharmacology & Biological Psychiatry*, *119*, 110618. https://doi.org/10.1016/j.pnpbp.2022.110618

Yen, C., Lin, C.-L., & Chiang, M.-C. (2023). Exploring the Frontiers of Neuroimaging: A Review of Recent Advances in Understanding Brain Functioning and Disorders. *Life*, *13*(7), 1472. https://doi.org/10.3390/life13071472

Yoo, S. (2018). Dynamic Energy Balance and Obesity Prevention. *Journal of Obesity & Metabolic Syndrome*, *27*(4), 203–212. https://doi.org/10.7570/jomes.2018.27.4.203

Zeighami, Y., Dadar, M., Daoust, J., Pelletier, M., Biertho, L., Bouvet-Bouchard, L., Fulton, S., Tchernof, A., Dagher, A., Richard, D., Evans, A., & Michaud, A. (2022). Impact of weight loss on brain age: Improved brain health following bariatric surgery. *NeuroImage*, *259*, 119415. https://doi.org/10.1016/j.neuroimage.2022.119415

Zhang, B., Zhang, S., Feng, J., & Zhang, S. (2023). Age-level bias correction in brain age prediction. *NeuroImage : Clinical*, *37*, 103319. https://doi.org/10.1016/j.nicl.2023.103319

7. Acknowledgements

I would like to express my deepest gratitude to Prof. Koutsouleris for his unwavering support and guidance throughout the journey of completing this doctoral thesis. Additionally, I would like to thank Ariane, Esther, and Riya, who supervised me at various points. Their expertise, patience, and encouragement have been invaluable. I am also grateful to David for his assistance with data analysis and interpretation. His insights have greatly enriched the findings presented in this thesis.

Special thanks to my dearest Madalina and Elif for their constructive feedback, insightful discussions and motivation during my low phases. Thanks to my lovely colleagues John, Lisa, Clara W., Clara V., Alessa, Anne and Maureen, who provided constant support during times of frustration and gave valuable advice. Thanks to the entire NDA lab members for their support whenever needed.

I am most thankful to my mother, father, uncles, aunts, and cousins, as well as my best friends turned family Aishwarya, Rubanya and Sagufa, for their mental support and for bearing my late-night calls, never letting me feel far away. My dearest Ipsika, Soumya, Mahathi and Philipp, who were always there to handle frustrations and keep their house doors open for me, and specifically Philipp, Mahathi, Sarra, Claudi, Madalina, Elif, Adriana, my mini family in Munich, for their unconditional love, support and constant encouragement.

This thesis would not have been possible without the contributions of these individuals, and for that, I am truly grateful and feel blessed to have them in my life.

8. Affidavit

Affidavit

Khuntia, Adyasha Tejaswi

_____

Surname, first name

Nußbaumstrasse 7

_____

Street

80336, Munich, Germany

_____

Zip code, town, country

I hereby declare, that the submitted thesis entitled:

Multi-scale, multi-modal stratification and comorbidity analysis of patients with psychotic disorders

is my own work. I have only used the sources indicated and have not made unauthorised use of services of a third party. Where the work of others has been quoted or reproduced, the source is always given.

I further declare that the dissertation presented here has not been submitted in the same or similar form to any other institution for the purpose of obtaining an academic degree.

Munich, 11.03.2025 Adyasha Tejaswi Khuntia

_____ _____

place, date Signature doctoral candidate

9. Confirmation of congruency

Confirmation of congruency between printed and electronic version of

the doctoral thesis

Khuntia, Adyasha Tejaswi

_____

Surname, first name

Nußbaumstrasse 7

_____

Street

80336, Munich, Germany

_____

Zip code, town, country

I hereby declare, that the submitted thesis entitled:

Multi-scale, multi-modal stratification and comorbidity analysis of patients with psychotic disorders

is congruent with the printed version both in content and format.

Munich, 11.03.2025 Adyasha Tejaswi Khuntia

_____ _____

place, date Signature doctoral candidate

10. List of publications

1. Dwyer, D. B., Chand, G. B., Pigoni, A., Khuntia, A., Wen, J., Antoniades, M., Hwang, G., Erus, G., Doshi, J., Srinivasan, D., Varol, E., Kahn, R. S., Schnack, H. G., Meisenzahl, E., Wood, S. J., Zhuo, C., Sotiras, A., Shinohara, R. T., Shou, H., … Dazzan, P. (2023). Psychosis brain subtypes validated in first-episode cohorts and related to illness remission: Results from the PHENOM consortium. Molecular Psychiatry, 28(5), 2008–2017. https://doi.org/10.1038/s41380-023-02069-0
2. Schwarz, E., Alnæs, D., Andreassen, O. A., Cao, H., Chen, J., Degenhardt, F., Doncevic, D., Dwyer, D., Eils, R., Erdmann, J., Herrmann, C., Hofmann-Apitius, M., Kaufmann, T., Koutsouleris, N., Kodamullil, A. T., Khuntia, A., Mucha, S., Nöthen, M. M., Paul, R., … Meyer-Lindenberg, A. (2021). Identifying multimodal signatures underlying the somatic comorbidity of psychosis: The COMMITMENT roadmap. Molecular Psychiatry, 26(3), 722–724. https://doi.org/10.1038/s41380-020-00915-z
3. Khuntia, A. T., Popovic, D., Sarisik, E., Buciuman, M. O., Pedersen, M. L., Westlye, L. T., Andreassen, O., Meyer-Lindenberg, A., Kambeitz, J., Salokangas, R., Hietala, J., Bertolino, A., Borgwardt, S., Brambilla, P., Upthegrove, R., Wood, S., Lencer, R., Meisenzahl,
   E., … Wiegand, A, Koutsouleris, N. (2024). BMIgap: A new tool to quantify transdiagnostic brain signatures of current and future weight. (under revision in Nature Mental Health)
4. Khuntia, A., Buciuman, M.-O., Fanning, J., Stolicyn, A., Vetter, C., Armio, R.-L., From, T., Goffi, F., Hahn, L., Kaufmann, T., Laurikainen, H., Maggioni, E., Martinez-Zalacain, I., Ruef, A., Dong, M. S., Schwarz, E., Squarcina, L., Andreassen, O., Bellani, M., …
   Koutsouleris, N. (2025). Towards collaborative data science in mental health research: The ECNP neuroimaging network accessible data repository. Neuroscience Applied, 4, 105407. https://doi.org/10.1016/j.nsa.2024.105407
5. Sarisik, E., Popovic, D., Keeser, D., Khuntia, A., Schiltz, K., Falkai, P., Pogarell, O., & Koutsouleris, N. (2024). EEG-based Signatures of Schizophrenia, Depression, and Aberrant Aging: A Supervised Machine Learning Investigation. Schizophrenia Bulletin, sbae150. https://doi.org/10.1093/schbul/sbae150
6. Di Camillo, F., Grimaldi, D. A., Cattarinussi, G., Di Giorgio, A., Locatelli, C., Khuntia, A., Enrico, P., Brambilla, P., Koutsouleris, N., & Sambataro, F. (2024). Magnetic resonance imaging-based machine learning classification of schizophrenia spectrum disorders: A meta-analysis. Psychiatry and Clinical Neurosciences, 78(12), 732–743. https://doi.org/10.1111/pcn.13736
7. Madalina-Octavia Buciuman, Shalaila S. Haas, Linda A. Antonucci, Lana Kambeitz-Ilankovic, Elif Sarisik, Adyasha Khuntia, Anne Ruef, Stefan Borgwardt, Joseph Kambeitz, Christos Pantelis9, Rebekka Lencer, Alessandro Bertolino, Paolo Brambilla, Rachel

Upthegrove, …, Nikolaos Koutsouleris (2024). From Snapshots to Stable Outcomes: rs-fMRI-based Prognosis of Functioning inPatients with Psychosis Risk or Recent-Onset Depression. (under revision in Biological Psychiatry)